QC
807.5
.U6
A7
no.168

alyzed

Technical Memorandum ERL ARL-168

TRIAD: A PUFF-TRAJECTORY MODEL FOR REACTIVE GAS DISPERSION WITH APPLICATION TO UF_6 RELEASES INTO THE ATMOSPHERE

B. B. Hicks
K. S. Rao
R. J. Dobosy
R. P. Hosker, Jr.
J. A. Herwehe
W. R. Pendergrass

LIBRARY
MAY 24 1989
N.O.A.A.
U.S Dept of Commerce

Air Resources Laboratory
Silver Spring, Maryland
February 1989

noaa NATIONAL OCEANIC AND ATMOSPHERIC ADMINISTRATION / Environmental Research Laboratories

QC
807.5
.U6 A7
no. 168

NOAA Technical Memorandum ERL ARL-168

TRIAD: A PUFF-TRAJECTORY MODEL FOR REACTIVE GAS DISPERSION WITH APPLICATION TO UF_6 RELEASES INTO THE ATMOSPHERE

B.B. Hicks
K. S. Rao
Atmospheric Turbulence and Diffusion Division
Oak Ridge, Tennessee

R. J. Dobosy
J. A. Herwehe
Oak Ridge Associated Universities

R. P. Hosker, Jr.
W. R. Pendergrass
Atmospheric Turbulence and Diffusion Division

Air Resources Laboratory
Silver Spring, Maryland
February 1989

UNITED STATES
DEPARTMENT OF COMMERCE

Robert A. Mosbacher
Secretary

NATIONAL OCEANIC AND
ATMOSPHERIC ADMINISTRATION

William E. Evans
Under Secretary for Oceans
and Atmosphere/Administrator

Environmental Research
Laboratories

Joseph O. Fletcher
Director

LIBRARY
MAY 26 1989
N.O.A.A.
U.S. Dept. of Commerce

NOTICE

Mention of a commercial company or product does not constitute endorsement by NOAA/Environmental Research Laboratories. Use for publicity or advertising purposes of information from this publication concerning proprietary products or tests of such products is not authorized.

ATDL Contribution File No. 87/24

TABLE OF CONTENTS

LIST OF FIGURES v

LIST OF TABLES vi

ACKNOWLEDGEMENTS vii

ABSTRACT viii

EXECUTIVE SUMMARY 1

1. INTRODUCTION 3

2. BACKGROUND AND HISTORICAL DEVELOPMENT 4

2.1 THE EVOLUTION OF THE PLANETARY BOUNDARY LAYER 4
2.2 THE PLUME MODEL 7
2.3 MODELS FOR SITE ASSESSMENT 8
2.4 RECOMMENDATIONS CONCERNING DEVELOPMENT OF A PUFF MODEL 11

3. THEORY FOR REACTIVE GASES 13

4. THEORY FOR DENSE GASES 16

5. APPLICATION TO UF_6 20

6. COMPONENTS OF THE TRIAD MODEL 21

6.1 INITIAL PUFF SPECIFICATION 21
6.2 WIND FIELD INTERPOLATION 34
6.3 PUFF TRANSPORT AND DISPERSION 36

7. LIMITATIONS OF THE TRIAD MODEL 37

7.1 BUILDING WAKES 37
7.2 INCOMPLETE REACTIONS 37
7.3 HEAT OF REACTION AND PLUME RISE 38
7.4 MODEL EVALUATION DATA 39

REFERENCES 40

APPENDICES 42

A. USER'S GUIDE FOR TRIAD 2.0 42

SUMMARY 43

ACKNOWLEDGEMENTS 44

CONTENTS (continued)

SECTION I: INTRODUCTION 45

SECTION II: MODEL OVERVIEW 46

SECTION III: TECHNICAL DISCUSSION 49

SECTION IV: TRIAD COMPUTER PROGRAM 69

SECTION V: INPUT DATA PREPARATION 74

REFERENCES 93

B. TRIAD EXAMPLE PROBLEMS 95

C. PLUME RISE 121

REFERENCES 125

D. SETTLING AND DEPOSITION VELOCITIES 126

REFERENCES 128

E. GRAPHICS SOFTWARE 129

LIST OF FIGURES

Fig. No.		Page
1.	Isopleths showing mean maximum daytime mixed layer depths (m) across the continental U.S.A., for typical (a) winter and (b) summer conditions. The calculations are by Holzworth (1964), as reported by Slade (1968).	6
2.	The absolute humidity probability distribution at noon for Oak Ridge, Tennessee. Note that winter humidities rarely drop below 2 g/m^3, and summer humidities rarely exceed 20 g/m^3.	17
3.	As in Figure 2, but for midnight.	18
4.	Initial evidence for a humidity dependence of the exponential time scale of reaction of UF_6 released into air, as computed by the PLUME (turbulent mixing-limited reaction rate) model.	23
5.	Initial evidence of the dependence of the exponential time scale of reaction of UF_6 on the atmospheric stability class.	24
6.	Dependence of the time (to 90% completion) of reaction on atmospheric humidity, for a release rate of 1.47 kg/s of UF_6 vapor.	26
7.	Dependence of reaction time on atmospheric humidity and UF_6 release rate. The solid lines denote 100% UF_6 vapor, and the dashed lines denote a mixture of 60% vapor and 40% solid or liquid UF_6 at release.	27
8.	Correlation showing the variation of the reaction time with ambient humidity and the UF_6 release rate. The solid line gives the best-fit correlation given by Eq. (15) in the text. UF_6 release: Δ - 100% vapor; O - 60/40 vapor/solid or liquid mixture.	28
9.	Correlation showing the variation of the vertical dispersion parameter with ambient humidity and UF_6 release rate. The best-fit line is given by Eq. (16) in the text. This result is used to set the initial puff size in the TRIAD model.	29
10.	Correlation showing the variation of the lateral dispersion parameter with ambient humidity and UF_6 release rate. The best-fit line is given by Eq. (17) in the text. This result is used to set the initial puff size in the TRIAD model.	30
11.	Correlation showing the variation of the temperature rise (over the ambient) of the puff with ambient humidity and UF_6 release rate. The best-fit line is given by Eq. (18) in the text. Note that ΔT, which results from the heat of reaction, is nearly independent of the UF_6 release rate.	32

LIST OF TABLES

Table No.		Page
1.	Summary of significant model features.	2
2.	Desirable features of a second generation UF_6 dispersion model.	11
3.	Estimates of the near-source "exclusion zone" in which predictions by the TRIAD model are likely to be erroneous, due to the assumption that chemical reactions are completed. The values quoted are transit times, in seconds; estimates of the corresponding distance scales can be derived by taking the product of these values with the wind speed.	38

ACKNOWLEDGEMENTS

This report has been prepared for the U.S. Department of Energy (DOE) Oak Ridge Operations (ORO) with the active participation and collaboration of the U.S. Nuclear Regulatory Commission (NRC). This work was accomplished under interagency agreements among DOE, NRC, and the National Oceanic and Atmospheric Administration. The authors wish to thank James Behrend of DOE, David Sheffey and Michael Boyd of DOE/ORO, and William Crowley, Robert Just, and Reid Williams of the Martin Marietta Energy Systems (MMES) Division for providing the MMES's UF_6 dispersion model code (PLUME) and related documentation to ATDD, and for their guidance and advice during the course of this work. Mr. Williams was especially helpful in making repeated computer runs of the PLUME model and explaining the model formulations and the computational results. The wind field model is based on a technique refined by Frank Kornegay, also of MMES. Mary Rogers typed the final version of this report.

ABSTRACT

Chemical reactions between released pollutants and atmospheric constituents can influence atmospheric dispersion if the heats of reaction are such that buoyancy can be affected or mechanical turbulence damped. If the reaction is sufficiently exothermic, plume rise can be increased; if sufficiently endothermic, then plume rise can be suppressed. The model described here focuses on uranium hexafluoride, a common chemical in the nuclear industry, which reacts exothermically with atmospheric water vapor. The reaction can generate heat at a sufficient rate that turbulent mixing is enhanced considerably. The model is constructed to take the consequences of such chemical reactions into account by modifying the initial puff specification. A puff dispersion code is operated in conjunction with a wind field routine that accepts data from an array of towers (or a single tower, if that is all that is available), and interpolates wind field information as required. The puff module is based on the INPUFF-2 model developed by the Environmental Protection Agency. The three components (initial puff specification, wind field, and puff dispersion) of the model have been combined into a single code named TRIAD. This report outlines the theoretical basis for the chemical parameterizations, summarizes the results of tests conducted using a more sophisticated air chemistry model, discusses the capabilities and limitations of the TRIAD, and includes a detailed User's Guide to the current version of the TRIAD model.

EXECUTIVE SUMMARY

This report describes a numerical model designed to simulate the dispersion of gases that react exothermically with moisture in the atmosphere. Primary attention is directed to uranium hexafluoride (UF_6) and the products of its reactions with atmospheric water vapor (hydrogen fluoride and uranyl fluoride).

The goal is to provide an improved model for purposes of safety assessment associated with the possible release of UF_6 (and the products of its chemical reactions) from uranium processing facilities. Exothermic reactions of UF_6 with atmospheric water vapor can cause significant changes in dispersion, as was indicated in earlier developmental programs using a simple Gaussian plume routine as a dispersion framework. That earlier model (the PLUME model) was subject to all of the criticisms normally leveled at simple Gaussian plume schemes. In particular, light wind situations could not be addressed with confidence, and building and terrain effects were not considered. The present model is a step towards rectifying these problems, by combining a Gaussian puff model with an objective wind field scheme.

A summary of significant features of the present and previous models is presented in Table 1. It should be noted, however, that development still continues. Density effects at the source must be taken into account, and work must be completed on using a direction-dependent initial dispersion specification to account for local effects of arrays of buildings.

Work to date has concentrated on three major components:

PART A. Initial puff specification. Note that this does not include purely mechanical aspects of the release, but represents the specification of the initial puff characteristics as viewed by the atmospheric dispersion routines (i.e., the amount and composition of the released material, and the dynamic characteristics of its release into the atmosphere).

PART B. Puff dispersion module. This work has selected and modified an appropriate puff dispersion routine, and has coupled with it the chemical reaction schemes already developed as a component of earlier model studies based on a Gaussian plume approach. The final product presented here does not include explicit consideration of the density interface between a cloud of dense gas and the background atmosphere. This omission is anticipated to be a major source of error in application of the overall puff dispersion scheme that is developed in this program; it will be a subject for attention during later phases of this work.

PART C. Wind-field simulation. This component provides the vectorial flow fields necessary to drive the puff model developed in Part B. The intent is to provide the ability for using both postulated wind-field inputs and actual wind data, in an assimilative, interpolative mode so as to provide more detailed transport information.

The primary purpose has been to develop a simulation tool useful for both safety analysis and emergency preparedness applications. The model has been constructed with the intent to provide some capability to address the dispersion of other dense gas and reactive materials, as well as UF_6. This capability will be added as part of future (ongoing) work.

Because of the construction of the model, involving separate initialization, dispersion, and transport modules, the product is referred to as the "TRIAD" model.

Table 1. Summary of significant model features.

	PLUME model	TRIAD model
Wind speed range	$\geq$ 2 m/s	All speeds
Mean wind variability with time	Constant speed and direction	Updated at intervals specified by user
Mean wind variability in space	Constant speed and direction at single point	Interpolated from all available observation locations
Dispersion Computation	P-G scheme	On-site sigmas or P-G scheme
Chemical reaction	Detailed, fine time resolution	Integrated to completion of chemical reaction, based on theory and PLUME model
Initial plume rise	Detailed, fine time resolution	Based on a thermodynamic model, and standard plume rise formulations
Initial puff dimensions	Detailed, fine time resolution	Parameterizations based on theory and PLUME model
Initial dilution	None	Direction-dependent,* based on wind tunnel

*Feature not yet included.

1. INTRODUCTION

The wide variety of needs for numerical models of atmospheric dispersion imposes requirements for models of a wide range of complexities. In terms of incidents involving accidental releases of industrial gases, it is clear that simple models giving conservative estimates are most suitable for purposes of screening studies or real-time emergency response, whereas more sophisticated models can be used for assessing risk, for planning response strategies, or for evaluating the consequences of previous accidents. The range of modeling capabilities must also be adequate to encompass the spectrum of circumstances to be addressed, including terrain complexity, different meteorological conditions, and a variety of source configurations.

Impact assessment can perhaps be best accomplished using a probabilistic model in which extreme sophistication of the meteorological model is not expected or required, but a wide range of possible source configurations and meteorological conditions are sampled. The Calculation of Reactor Accident Consequences (CRAC) model (U.S. NRC, 1975) is an example of a probabilistic risk/impact assessment model.

An analogy can be found between the models classified by some of the dispersion modeling community (including NRC) as Class A and Class B models, and models designed to answer questions of real-time emergency response and emergency preparedness. Class A models are simpler than Class B, and are more suited for real-time emergency response; some sophistication of the meteorological codes is sacrificed in favor of quick turn-around. A conscious decision is made to accept some level of uncertainty in the model answer in exchange for improved response time. Class B models are more complicated, and are intended for application in scenario planning and accident assessment. In this application, time constraints are not as important, and a sophisticated model may be applied to yield a more accurate and more defensible prediction of the potential consequences of a release. Class B models contain better descriptions of a wider range of contributing processes than do the simpler Class A models. However, it should be emphasized that a higher level of sophistication does not necessarily guarantee more accurate predictions in every circumstance; instead, the benefit of increased sophistication is in permitting a wider range of conditions of applicability to be addressed in a defensible manner, since more of the known physics of the atmosphere can be included in the model.

A characteristic feature of most class A and class B models used for dispersion prediction or assessment is that the codes are balanced syntheses of all the processes that are important over the time and space scales of interest. No particular process or set of processes receives more attention than is required in order to meet the goals that are set. An intermediate level of modeling is of special relevance in the context of this report: process-specific research models. Such models are not intended for routine use in studies of dispersion, but are instead designed to investigate specific mechanisms thought to influence dispersion in a particular process of interest. These models are intentionally unbalanced, in the sense that they emphasize details of specific processes to be investigated at the expense of other mechanisms. Models of this kind

are generally research models, used for assessing the role of particular mechanisms and for examining their interactions with other processes.

The model addressed in the present report is an intermediate step in the development of a dispersion routine for reactive, dense gases. The dispersing material of principal interest is uranium hexafluoride (UF_6) and the products of its reactions; UF_6 is one of the principal chemical agents used in uranium enrichment.

2. BACKGROUND AND HISTORICAL DEVELOPMENT

2.1 THE EVOLUTION OF THE PLANETARY BOUNDARY LAYER

The earth's atmosphere is characteristically stratified, with denser air below and less dense air above. It is only during the day when the surface is heated by solar radiation that the stratification is eroded and a near-surface convective layer develops. The popular perception of a well-mixed atmosphere near the surface is in fact an oversimplification. Over most land areas, the diurnal cycle of solar radiation causes a remarkably strong diurnal cycle in the mixing of the lower atmosphere.

A few hours before sunset, the surface starts to cool as it loses heat by radiation. As this cooling progresses, the atmosphere starts to revert to its normal state of stratification, and as time progresses, the stratification becomes stronger. Eventually, the lower atmosphere can become sufficiently stratified that layers can move nearly independently of layers immediately above and below them. Thin layers of polluted air can meander across large areas of the countryside, causing horizontal "spreading" while retaining the vertical integrity of individual layers. Above the lowest few tens of meters, the local velocity gradient is then largely independent of the height above the surface, and hence the wind speed will tend to vary linearly with altitude.

The atmospheric conditions observed near the surface can therefore be rather misleading. The usual impression is of light winds. However, the arguments above suggest that, because of the linear profile, the wind speed increases strongly as height increases. Over fairly flat land it is common to find a wind speed maximum, often in excess of 10 m/s, several hundred meters above the surface, caused by a combination of factors including synoptic variations and large scale terrain slope. This wind speed maximum (nocturnal jet) marks the top of the so-called nocturnal boundary layer.

The strength and altitude of this nocturnal jet vary with time. In general, the jet builds up as the night goes on, and can reach a sufficient strength to destroy by purely mechanical mixing the very stratification which generated it. An intermittency results, which is known to be characteristic of the nocturnal atmosphere in many circumstances.

Thus, the nocturnal boundary layer is characterized by a stably-stratified layer near the surface, in which velocities increase with height (often linearly), and which is penetrated by intermittent turbulence bursts. It was thought that the nocturnal atmosphere does not permit strong vertical dispersion of plumes that reside in it. It is now known,

however, that plumes aloft can be brought to the surface and mixed throughout the nocturnal boundary layer by the intermittent turbulence bursts.

The atmosphere near the surface is most strongly stable just before dawn. At this time, cooling has occurred throughout the night, and air near the surface is likely to be calm and near 100% relative humidity. Often dewfall occurs as a consequence. When the sun rises, the situation changes rapidly. Solar heating of the surface soon causes convection as a direct consequence of the buoyancy of heated air.

However, deep convective mixing does not begin immediately at sunrise. There is a period after sunrise when the surface heating serves to erode the stable stratification that was generated overnight. Once this nocturnal stratification is destroyed, convection can play a very strong role. Starting usually a couple of hours after sunrise, convection rapidly increases in intensity and over the next few hours will thoroughly mix a layer of the lower atmosphere up to 1 to 1.5 km in depth. By mid afternoon, as the intensity of solar radiation striking the surface begins to decrease with time, the depth of the convectively mixed layer no longer continues to increase, and tends to reach a plateau which corresponds to the "depth of the mixed layer," as reported in standard meteorological literature.

A plume emitted into this strongly mixed atmosphere will be quickly dispersed in the vertical, at a rate which is clearly a strong function of the solar radiation striking the surface. This is the underlying basis for the use of radiation in indices of atmospheric stratification in dispersion models. Modern literature, however, makes use of more sophisticated parameterizations of the convective activity, largely based upon observations made in field experiments and laboratory models. The parameter that is most frequently discussed is the convective scaling velocity (w_*), an index of the strength of the convective cells and the velocity of the air moved by them.

In summary, we must consider two completely different situations for plumes released into the lower atmosphere, one for the nocturnal stratified regime and the other for the daytime convective regime. In the nighttime case, the plume could exist as a tightly confined entity, somewhat like a pencil, but perhaps spreading horizontally, until it is affected by nocturnal bursting events should they occur. A relatively slow vertical dispersion is the normal situation. An opposite situation exists in the daytime case, in which a plume emitted into the strongly mixed part of the lower atmosphere will become mixed rather quickly throughout the entire depth of the convective boundary layer.

The distance scales over which convective mixing occurs can be computed on the basis of the wind speed, the depth of the mixed layer at the time of interest, and the appropriate convective scaling velocity. Simple algebra leads to an expression for this distance, $x = hu/w_*$. Here, x is the distance, h is the depth of the mixed layer, w_* is the convective velocity, and u is the wind speed. Figure 1 illustrates the average maximum mixing layer depth for winter and summer conditions.

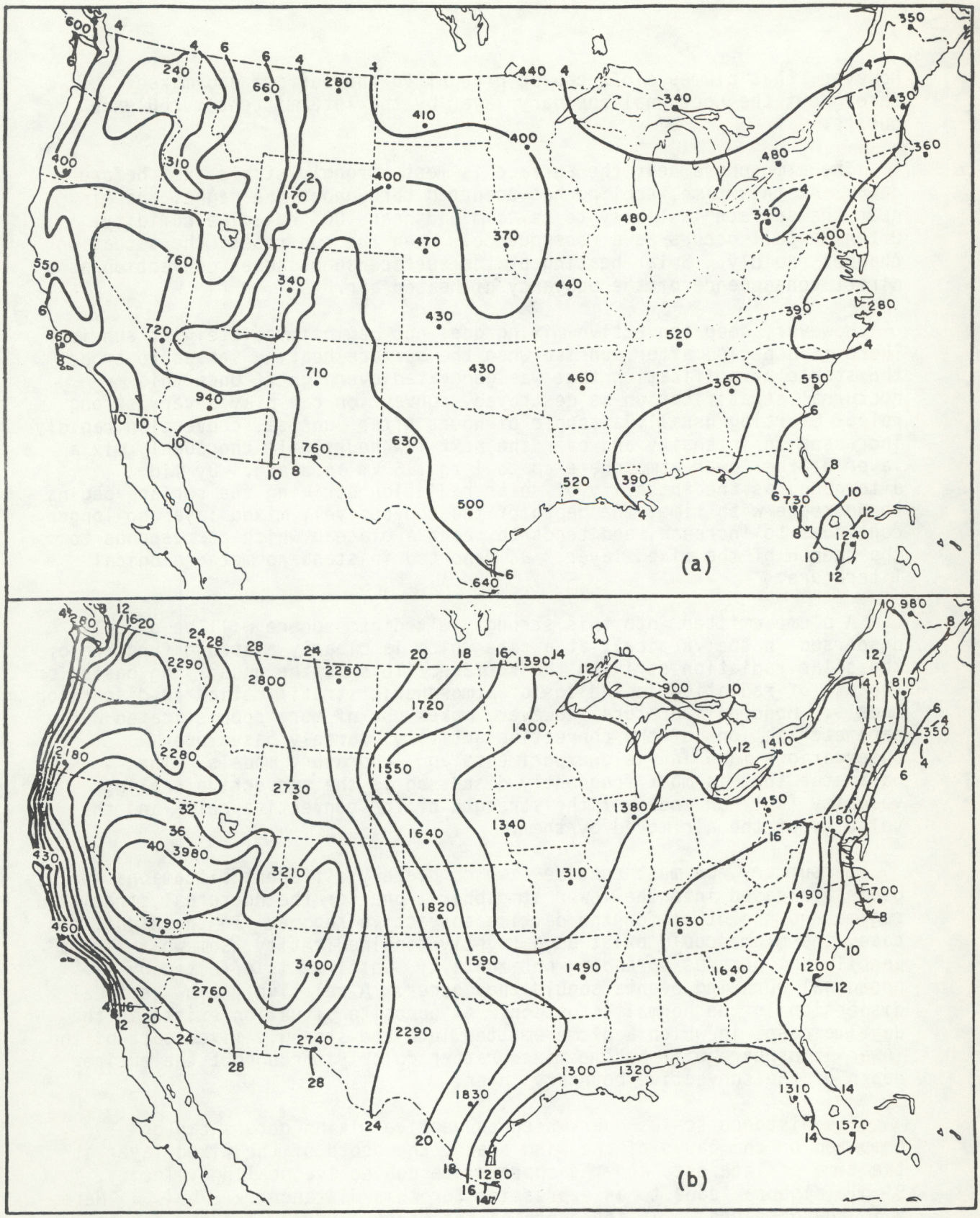

Figure 1. Isopleths showing the mean maximum daytime mixed layer depths (m) across the continental U.S.A., for typical (a) winter and (b) summer conditions. The calculations are by Holzworth (1964), as reported by Slade (1968).

The time evolution of the lower atmosphere defines an envelope in which vertical mixing occurs, marked by the depth to which daytime convection mixes the lower atmosphere. This envelope is known as the planetary boundary layer; i.e., that part of the atmosphere which is affected by contact with the surface of the planet over which it flows. The dominant feature of this contact is the heat exchange that occurs at the surface.

All of the above refers to situations in which it is the daytime heating which is important, not the topography. In complex terrain, nocturnal gravity flows can be strong; these flows will commonly override the relatively weak forces associated with the cooling that causes nocturnal jets to arise in simpler situations. Thus, nighttime flows in complex terrain are of special interest, and these are presently not well simulated in any kind of dispersion model. On the other hand, in daytime, heating of the surface causes buoyancy to mix fluids in the vertical. Thus, the influence of topography is somewhat reduced.

2.2 THE PLUME MODEL

Uranium hexafluoride, an important chemical in uranium enrichment processes, has certain properties that complicate its use, and cause considerable concern regarding the consequences of accidental releases. First, storage and handling conditions are such that it may be necessary to consider all of the solid, liquid, and gas phases if a release to the atmosphere occurs. Second, the gas is much denser than air, so that the assumptions of negligible density effects made in most trace-gas atmospheric dispersion routines may be violated. Third, UF_6 reacts exothermically with water. It has been postulated that chemical reactions between UF_6 and atmospheric water vapor are sufficiently exothermic to influence dispersion, so that standard dispersion models may again be inappropriate.

Researchers of Martin Marietta Energy Systems (MMES) at Oak Ridge, Tennessee, simulated UF_6 chemical reactions in a numerical model coupled to Gaussian plume dispersion (Just and Williams, 1986). This MMES Gaussian plume model (hereafter referred to as the PLUME model) was intended for use in safety assessment studies, and served as a convenient framework for developing relationships dealing with the exothermic nature of UF_6 atmospheric chemistry. However, the straight-line Gaussian plume dispersion used in the model has well-known shortcomings, identified by a review panel set up to comment on the application of the model to site assessments (Hicks et al., 1985).

In essence, straight-line Gaussian plume models are unable to produce acceptable results in light winds, and in cases where their assumption of straight-line, constant-velocity transport is violated. Gaussian plume models are most credible when results are taken as ensemble averages, over distances sufficiently short that the wind field may be considered uniform and stationary. In many instances, such conditions are satisfied. This is especially the case in assessment studies, in which long-term averaging is used to reduce the consequences of errors involved with any single release situation. However, Gaussian plume models are essentially inappropriate if

the terrain is not simple, if conditions are changing with time, if the distance of interest is greater than can be accommodated by the constant-velocity assumption, or if single events (e.g., individual accidents) are addressed.

Although the simplicity of the dispersion framework was seen as a severe limitation on the operational use of the overall model, the chemical aspects of the PLUME model are quite detailed and sophisticated. The PLUME model is therefore a valuable first-generation exploration of plume chemistry, in which other components of atmospheric dispersion are necessarily simplified.

Such an application follows the classical pattern for model development. Specific segments of the overall program are explored using models, which emphasize the segment of interest in particular detail, usually at the expense of simplification of other segments. For example, the details of dispersion are usually investigated in models of atmospheric turbulence that are far more detailed than any common risk assessment code. Likewise, the matters of dry deposition and wet deposition are investigated in specialized models whose conclusions are summarized into simplified "parameterizations" for more routine application in assessment models. In this case, the development work of the MMES researchers indicated that the exothermic reaction of emitted UF_6 with ambient water vapor could modify the behavior of a plume containing large amounts of UF_6 and its hydrolysis products.

We apply the results of this detailed chemistry analysis, summarizing and parameterizing the consequences of the atmospheric chemical reactions of UF_6 as computed by the more detailed model. The resulting simplified chemistry scheme is then combined with a more versatile dispersion scheme. It is important to note that much remains unknown about the behavior of UF_6 and its hydrolysis products in the atmosphere. A number of areas of uncertainty were summarized by Just and Williams (1986). Even under the most favorable circumstances, the chemical parameterizations developed here will be subject to those same uncertainties. Nevertheless, the intent is to develop a balanced operational model framework that represents, with equivalent detail, the known relevant physical and chemical processes.

2.3 MODELS FOR SITE ASSESSMENT

For assessment applications, it is normal to exercise a model many times to investigate what will happen over a wide range of hypothetical scenarios, none of which can usually be prejudged to be the most important. Results from such exercises must be coupled with the probability of occurrence of the scenarios (source conditions and meteorology) as well as the probability of higher or lower concentrations resulting from natural variability; this will be discussed in detail in the following sections. Thus, an assessment model must be both economical and rational, so that a wide variety of potential scenarios can be investigated without forfeiting defensibility of the overall scheme. In common with all straight-line Gaussian plume models, the first-generation UF_6 dispersion model is unable to treat some scenarios of potential importance.

It is fairly easy to construct a list of factors likely to be important in site assessment studies. These include:

a. Source configuration

Emission rate and duration
Exhaust speed and direction
Emission concentrations, temperatures, etc.
Initial dilution due to emission dynamics, building wakes, etc.
Physical height of emissions and plume rise
Ambient conditions (meteorology, terrain, etc.)

b. Transformation

Heats of reaction
Gas to particle conversion
Reactions with background constituents

c. Transport and dilution

Mean and turbulent wind fields (including terrain effects)
Plume entrainment
Ambient stratification
Mixing layer depth
Synoptic conditions
Elevations of receptors with respect to source

d. Deposition

Plume washout
Convective rainout
In-cloud or fog chemistry
Surface gas transfer
Particle deposition

These aspects are considered to varying degrees of sophistication in most modern assessment models, but the present application requires increased emphasis to be placed on particular features. It is in these particular areas where detailed process models are required, to explore the ways in which standard dispersion codes are deficient and to develop methods for improving them in a cost-effective manner. The features that appear to be important in the present context are as follows.

Exothermic chemistry: Chemical reactions may modify standard plume rise estimates and may influence dispersion rates.

Dilution: The importance of the chemistry will be determined by the amount of dilution of emissions and entrainment of ambient moisture immediately upon release. This raises questions concerning the dynamics of the release, the effects of the very large buildings characteristic of gaseous diffusion facilities, local terrain and vegetation, and the role of turbulence in modifying plume chemistry.

Topography: Especially important situations are likely to occur at night, when turbulent dilution will be minimal and when emissions will be carried by local flows steered by local terrain features. High humidity and even local fog, especially along waterways, is common under these conditions. Emissions which react exothermically when water vapor is present will often be meteorologically constrained at night to flow along the same routes as local rivers and streams. The combination might be of considerable importance.

Precipitation: The emissions are sufficiently reactive with water that scavenging by precipitation should be quite efficient, especially in the case of convective storms, which can cleanse large volumes of the planetary boundary layer and deposit the scavenged materials in relatively confined areas. The rates of removal will correspond to scavenging rates in the range 10^{-3} (for thunderstorms) to 10^{-5} (for wintertime light drizzle) per second, so that the corresponding horizontal distance scales of precipitation scavenging and wet deposition in the area of concern are likely to vary over several orders of magnitude, depending on the winds.

Fog and mist: If emissions take place into a very humid atmosphere, then nucleation must be expected, with consequent deposition by interception mechanisms. If ground fog already exists, then capture of material by hydrometeors is probable, and deposition is also likely to be substantially accelerated. Heat released by the chemical reactions would evaporate some of the existing water droplets and hence the plume rise assumptions might require suitable modification.

The three major sources of basic uncertainty in dispersion models are (1) the simplification of model physics, (2) errors associated with scenario assumptions, including model inputs, and (3) uncertainties introduced by natural atmospheric variability. Specific mechanisms in category (1) which are not well handled by a Gaussian plume model are the omission of terrain-related effects, the inability of the model to treat very light wind conditions, and the exclusion of ambient fogs and ground moisture (e.g., dew). Possible errors introduced in category (2) are more difficult to assess since they depend on how the model is applied. Some of them are related to the inadequacies in the model physics, such as the inability to treat calm or light wind conditions, and fog scenarios. Another is the specification of initial conditions corresponding to a possible tank rupture outdoors; this appears to be an obvious case where it is extremely difficult to guarantee conservative predictions. In category (3), we believe that neglect of inherent variability due to atmospheric turbulence will generally lead to nonconservatism in the peak exposure level predicted in a safety analysis. Natural atmospheric variability imposes a possibility, albeit small, of high surface concentrations under conditions in which the model might predict low average values. Many of these shortcomings were earlier identified by the developers of the Gaussian plume first-generation UF_6 model. The review panel (Hicks et al., 1985) recommended specific steps that should be taken to develop a second-generation computer model, by building upon the model already developed. In particular, the review panel recommended use of a puff model, to overcome problems associated with light winds and near-field dispersion.

2.4 RECOMMENDATIONS CONCERNING DEVELOPMENT OF A PUFF MODEL

The first-generation PLUME dispersion model provides the capability to investigate the influence of chemistry on atmospheric dispersion of a reactive heavy gas. Early work using this code demonstrated that dispersion is indeed affected by the exothermic chemistry. It was the present goal, therefore, to develop a model that does not have the meteorological limitations imposed by the straight-line Gaussian assumptions of the existing code, so as to provide a dispersion model for UF_6 and its reaction products better suited to site-specific safety analysis reports (SARs) and for emergency response planning. The review of the first-generation dispersion model recommended several key features for the revised model, as shown in Table 2.

Table 2. Desirable features of a second-generation UF_6 dispersion model. (Hicks et al., 1985)

a. A puff model is recommended to handle light winds and short-term releases. This was accomplished in the TRIAD model by incorporation of a modified form of the INPUFF-2 dispersion model.

b. Initial dilution of a puff should be handled using site-specific parameterizations. This was not accomplished in the initial TRIAD model, but will be a component of the second-generation form of TRIAD.

c. A consistent puff rise formulation should be developed. In the TRIAD model, the latest forms of the Briggs (1975) relationships were adopted.

d. Dispersion calculations should make use of on-site turbulence measurements or PBL similarity scaling relationships, rather than the usual Pasquill-Gifford schemes. This was accomplished in the TRIAD model.

e. Transport must be addressed, to account for terrain-induced effects (three-dimensional, and site-specific). Effects of terrain are included in TRIAD by calling on wind field observations from strategically-located towers.

f. A capacity to accept real-time data is desirable, to improve the model's applicability for real-time emergency response applications. Although not a major feature of TRIAD, such a facility is now available.

g. Atmospheric variability should be addressed by incorporating a model capability to estimate variances and peak-to-mean ratios. This step was not accomplished in TRIAD, in its present form.

h. Tests of model components should be conducted, using field, laboratory, and theoretical methods. Tests await the availability of suitable field data, not yet on hand.

For the dispersion of heavy reactive gases (e.g., UF_6), it is not immediately clear how best to select an optimal modeling approach. If emissions are expected to occur only over a short time (less than 15 minutes, say), then it is perhaps most appropriate to rely heavily on scenario planning as the optimal basis for emergency response. At the opposite end of the time and space spectrum of possible emergencies, extended releases affecting large areas require a large effort to address, especially in compiling the necessary data and coordinating wide-area response actions.

There are two possible ways to proceed:

1. Build upon an existing, tested, heavy gas puff dispersion model. Species-specific chemistry could then be added.

2. Improve the existing PLUME model by introducing a puff dispersion scheme. This will provide a model appropriate for "Class A" applications, but it will be specific for UF_6 and its products, and will lack the capability to account for the density interface problem. Extension to other dense gases could be difficult.

The preferred way to proceed is the first option. To handle dense reactive gases such as anhydrous HF and NH_3, it would be best to start with a dense-gas dispersion model and add the relevant chemistry. But practical requirements demanded a more immediate improvement to the PLUME model than this line of development would permit. In particular, immediate attention must be given to the treatment of light or variable winds and terrain effects, these being the major problems normally associated with straight-line Gaussian plume models.

Different models (and modeling approaches) require different input data. Probabilistic models require only limited meteorological input, often little more than meteorological observations from a single station collected over a fairly extensive time period; however, the level of confidence associated with the model results is correspondingly limited. Probabilistic models are not designed to address individual cases but to assess the consequences of hypothetical worst case scenarios. At the other extreme, real-time emergency response models often require an extensive network of meteorological instruments, providing information on actual wind fields for use in relatively simple dispersion schemes. This allows fast delivery of the desired concentration estimates, but the accuracy of these real-time models is directly coupled to the detail and accuracy of the input wind field data.

In general, the appropriate model complexity for any given application increases with the complexity of the circumstances, but must be limited by the execution time available to run the model. Considerable additional complexity can arise if the pollutant involved is dense, or if it reacts chemically after emission. The case of dense gas dispersion has received extensive attention, largely as a result of potential emergencies associated with the transport and storage of liquified gaseous fuels. In this case, the density interface between the gas and the atmosphere is a stabilizing influence, tending to isolate the underlying "bubble" of dense gas from the turbulence of the ambient atmosphere. The volume of dense gas

can then be free (if dense enough) to respond to its own dynamical forces, largely independent of the atmosphere passing over it. One consequence is that spreading may be rapid, but dilution may be slow.

Endothermic chemical reactions can make a pool of emitted trace gas act as if it were a genuine dense gas, even though quite dilute. On the other hand, exothermic chemical reactions will tend to increase plume rise and enhance vertical mixing between the trace gas and the ambient air.

The present purpose is to explore the options available to modelers faced with the need to consider the consequences of exothermic and endothermic reactions, and then to present the methods that have been developed in the work following development of the first-generation PLUME model. We start with consideration of the complexities arising as a consequence of chemical reactions between the material emitted and components of the air. Next, dense gas effects are discussed. Following these sections, we present the three-component "TRIAD" model, developed as an intermediate step towards a final product that answers the objections to the earlier model, as identified above in Table 2.

3. THEORY FOR REACTIVE GASES

Consider a trace gas released into the air and reacting with some atmospheric constituent, such as water vapor. The chemical reaction is then of the general type:

$$X_1 + H_2O \xrightarrow{k_c} X_2 + X_3 + J \qquad (1)$$

where species X_1 reacts with H_2O (in this example) with specific rate constant k_c (per second) to form species X_2 and X_3 and releasing thermal energy J (Joules per mole). If J is positive, then the reaction enhances turbulent mixing due to buoyancy. In this case, it is informative to consider the role of the additional thermal energy in relation to the structure and behavior of the ambient atmosphere.

In a convective atmosphere with sensible heat flux H at the surface, the rate of generation of turbulent kinetic energy (Joules/kg/sec) associated with the buoyancy is

$$J_b = (g\ H)/(\rho_o\ c_p\ \theta) \qquad (2)$$

where ρ_o is the air density, c_p is the specific heat of air at constant pressure, g is the acceleration due to gravity, and θ is average potential temperature (absolute). The corresponding mechanical turbulent energy production term is

$$J_m = u_*^2\ (du/dz) \qquad (3)$$

where u_* is the surface friction velocity ($-\rho_o\ u_*^2$ is the momentum flux to the surface) and du/dz is the local wind gradient at the height in question. The sign convention is that positive momentum and heat fluxes are directed away from the surface, and du/dz is positive when wind increases with height.

In classical micrometeorology, the importance of buoyancy relative to shear-produced turbulent kinetic energy is quantified by the flux Richardson number, $R_1 = - J_b/J_m$, expressed as follows:

$$\begin{aligned} R_1 &= - [(g\ H)/(\rho_o\ c_p\ \theta)]/[u_*^2\ (du/dz)] \\ &= - [(k\ z\ g\ H)/(\rho_o\ c_p\ \theta\ u_*^3)]/\phi_m \\ &= (z/L)/\phi_m\ . \end{aligned} \tag{4}$$

Here, standard micrometeorological relations have been invoked to relate the local wind gradient to the friction velocity u_*, height z, von Karman constant k, and the stability-dependent dimensionless wind shear ϕ_m. The quantity L is the Monin-Obukhov length scale of turbulence, initially derived from dimensional arguments. The flux Richardson number R_1 is thus an index of dynamic instability associated with buoyancy, much like the familiar index z/L.

It should be noted that the stability parameter R_1 can be expressed in terms of two time scales, T_m and T_b, such that $R_1 = (T_m/T_b)^2$, where

$$T_m = 1/(du/dz) \tag{5}$$

which is associated with the mechanical mixing process, and

$$T_b = [(g/\theta)\ |\ d\theta/dz\ |\ ]^{-1/2} \tag{6}$$

which is associated with the effects of buoyancy. The inverse of T_b is the familiar Brunt-Vaisala frequency, normally used to characterize the oscillation of a parcel of air displaced from its equilibrium height in stable stratification. Thus, in stable conditions, T_b corresponds to the period of a cyclic oscillation. In unstable conditions, which are of interest here, T_b corresponds to a relaxation time.

The influence of chemistry on turbulent production can be addressed by considering a second buoyancy term, similar to J_b, but representing the consequences of an exothermic reaction:

$$J_c = k_c\ J\ \rho_1/(M_1\ \rho_o) \tag{7}$$

where ρ_1 (kg/m^3) is the partial density of the species X_1 in air and M_1 (kg/mole) is the molecular weight of the species X_1.

It is then apparent that if the ratio

$$\begin{aligned} R_2 &= J_c/J_b \\ &= k_c\ J\ \rho_1\ c_p\ \theta/(H\ g\ M_1) \end{aligned} \tag{8}$$

is at least comparable to unity, then the reaction is sufficiently exothermic to modify buoyancy significantly, in unstable conditions.

In unstable stratification, an endothermic reaction will tend to reduce the rate of buoyant mixing. In general, therefore, a modified index

of the net effective instability can be postulated:

$$R_3 = - (J_b + J_c)/J_m \qquad (9)$$

where J_c is positive for an exothermic reaction (positive J), and negative for an endothermic reaction. By analogy with Eq. (6), we can define a time scale associated with the heat of chemical reaction, as follows:

$$T_c = [J_c /(k\ u_*\ z)]^{-1/2}$$

$$= [(k_c\ J\ \rho_1)/(\rho_o\ M_1\ k\ u_*\ z)]^{-1/2} . \qquad (10)$$

It should be noted that Eq. (9) can be expressed as $R_3 = T_m^2\ [(T_b)^{-2} - (T_c)^{-2}\ ]$. Though this modified stability parameter has been developed here for unstable conditions, its generality is not so constrained. Just as z/L and R_1 are stability indices that extend across the range of stable and unstable stratification, so does R_3 provide a mechanism for modifying such standard quantities in the cases of exothermic and endothermic chemical reactions.

A scrutiny of the relations involving J reveals a few hidden difficulties. In particular, the chemical reaction rate k_c is not usually a constant, but depends on variables which might include temperature, pressure, and solar radiation. Furthermore, the reaction may be equivalent to a gas-phase titration, in which the reaction is controlled by the rate of delivery of one gaseous reactant or the other. Thus, from the present viewpoint the specification of k_c is far from trivial.

Examination of equations (8) and (9) reveals several intriguing conclusions:

(a) Plume rise enhancement/suppression

The practical effect of the release of heat of reaction is likely to be greatest in near-neutral conditions (when the surface heat flux H is small). The diurnal variation of H is large, with H typically varying from -10 to -20 W/m^2 at night to more than 200 W/m^2 at midday. The influence of J_c is therefore likely to be greatest near dawn and dusk, and (to a lesser extent) at night.

(b) Mechanical mixing with the ambient air

The suppression of dilution by an endothermic reaction is a strong function of the friction velocity, suggesting an inverse cubic dependence on wind speed. When terrain-constrained flow channeling effects (e.g., nocturnal flows over slopes) are present, the ambient wind direction also influences the mechanical mixing at the interface; the highest entrainment (dilution) rates are expected when the ambient wind opposes the denser near-surface flow.

The roughness of the surrounding surface is important, insofar as it controls the friction velocity u_* in given wind speed conditions. Minimum boundary-layer dilution rates will occur in light winds, over smooth flat terrain.

(c) The role of the reaction rate

The reaction rate constant enters as a first-order factor in both Eqs.(8) and (9). The appropriate reaction rate is the effective value in the conditions of interest, which will generally be less than the rate based on chemical considerations alone. Rapid chemical reaction quickly consumes the material available in the surrounding volume, and the rate of resupply of reactants becomes the controlling factor. Thus, if the rate k_c in Eqs. (8) and (9) is based on chemistry alone, then the properties J_b and J_m become indices of the potential importance of the heat of reaction, generally overestimating its actual importance in any specific instance.

(d) The importance of fogs

It has been suggested (Hicks et al., 1985) that the presence of liquid water in the air (as suspended drops: fog or cloud) will have a substantial effect on the exothermic chemistry and its consequences. In concept, it has been proposed that the heat released by the chemical reaction will be used to evaporate the water droplets.

Figures 2 and 3 show frequency distributions of absolute humidity at Oak Ridge, TN, for noon and midnight respectively. The consequences of frequent high humidities in summer and low humidities in winter are clearly evident. Comparison of Figures 2 and 3 reveals only small day/night differences; however, seasonal effects are great.

In general, the liquid water content of a fog rarely exceeds 1% of the total atmospheric water content. If the total water content is 20 g/m^3, then the liquid water partial density is not likely to be more than 0.2 g/m^3, and the quantity of heat needed to evaporate this is about 500 $Joules/m^3$. In comparison, the exothermic heat of reaction that would be released if all of the water were consumed in reaction with UF_6 would be about 30,000 $Joules/m^3$ (the heat of reaction is about 58,600 Joules/gm-mole, and the reaction of one mole of UF_6 would consume nearly all of the water in two cubic meters of air, in this example).

It is clear in this instance that the heat produced by the exothermic UF_6 reaction involving the water in the air greatly exceeds the heat needed to evaporate any liquid water that might be present. Consideration of other examples shows that this is always the case; in general, too little of the total water content of the air is present in liquid form. For this reason, the presence of fog has not been considered as a special case in the modeling development presented here.

4. THEORY FOR DENSE GASES

There has been extensive development of specialized models to predict dispersion from releases of heavier-than-air vapors and gases. None of this work handles plume rise in a manner suitable for the present application, but some of the more recent developments may provide a satisfactory framework for initiating new development. For example, some models are capable of handling moderate terrain complexity, and most of the more recent simulations avoid the need to use Pasquill-Gifford stability classification schemes for estimating dispersion.

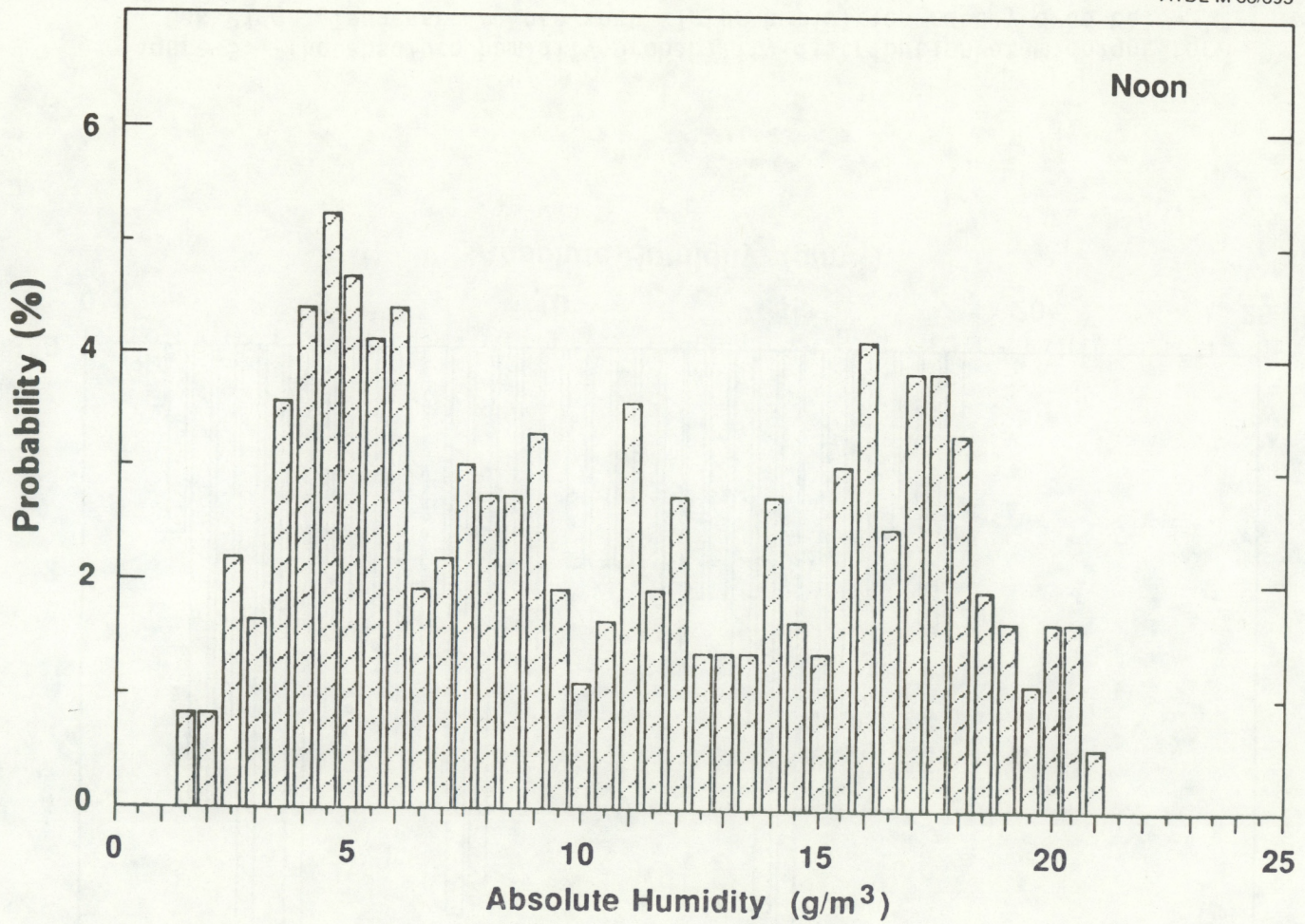

Figure 2. The absolute humidity probability distribution at noon for Oak Ridge, Tennessee. Note that winter humidities rarely drop below 2 g/m^3, and summer humidities rarely exceed 20 g/m^3.

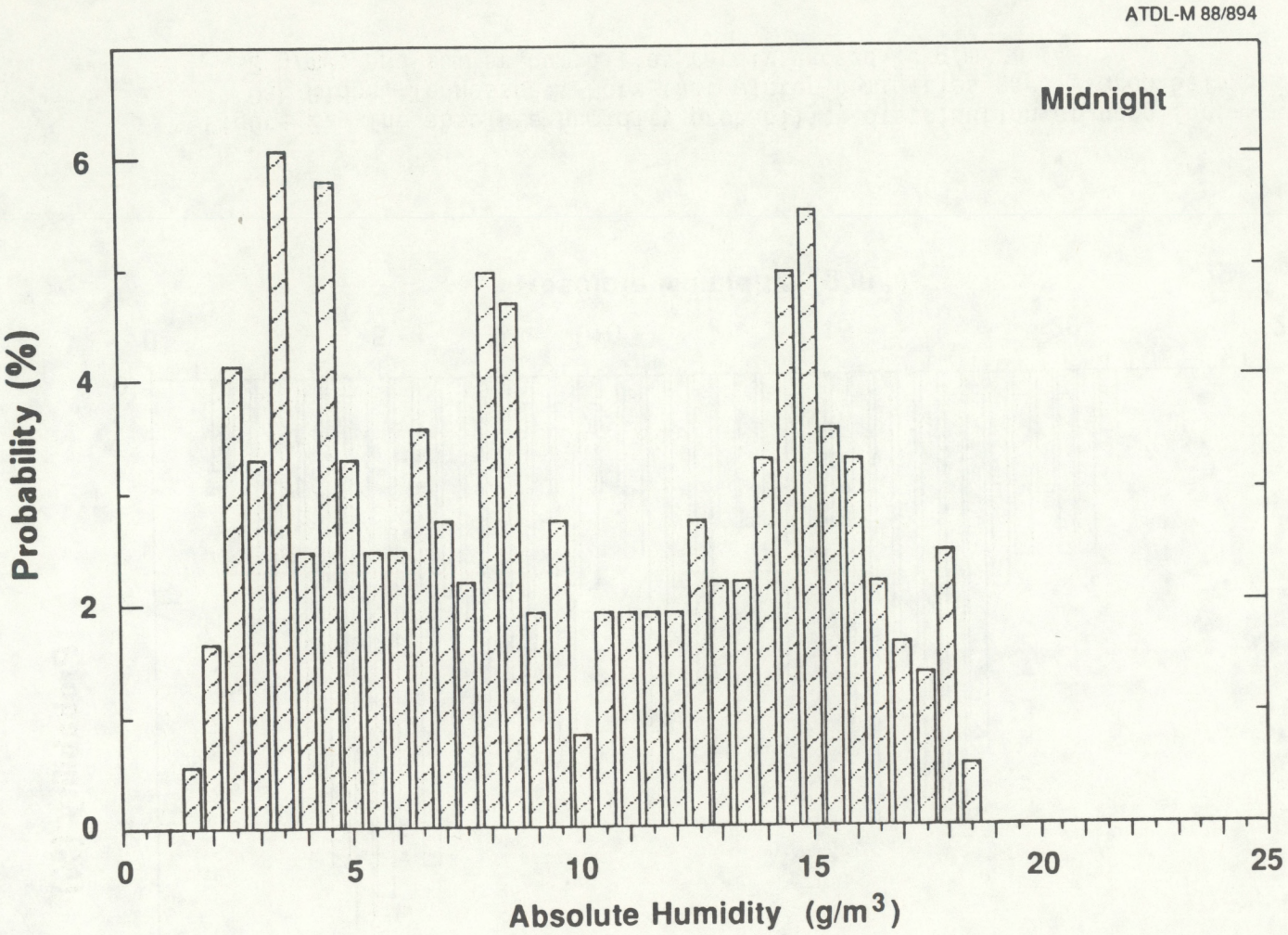

Figure 3. The absolute humidity probability distribution at midnight for Oak Ridge, Tennessee. Note that winter humidities rarely drop below 2 g/m^3, and summer humidities rarely exceed 20 g/m^3.

Much of the earliest dense gas model development was driven by the need to address problems perceived with the transportation, storage, and handling of liquified natural gas (LNG). This area of research was of special interest during the late 1960's and 1970's. The first models were modifications of simple Gaussian dispersion codes, but as development proceeded, more complicated methods were found necessary to represent the features of heavy-gas dispersion in a manner that was both conceptually acceptable and in accordance with field experiments.

The focus on LNG led to a strong emphasis on flammability and phase changes. The models are therefore not directly applicable to the case of UF_6 releases. However, the detailed dispersion codes developed for application to dense gas releases in a more general sense are far more applicable, provided adequate chemistry can be incorporated in them.

Both steady-state and fluctuating plume models were developed, with approximately equal emphasis on the development of puff models. The most modern developments are solutions of relationships that account for such controlling factors as gravitational spreading, heat exchange with the surface, entrainment, and terrain effects. Much of the related work has appeared in reports not yet available in the open literature. A bibliography on this topic can be found in Hicks et al. (1985).

Equations (8) and (9) provide a basis for "screening" chemical reactions for potential concerns related to modification of atmospheric mixing. Consideration of dense-gas effects can be included in the same general framework. In this case, consideration of relevant time scales provides useful physical insight. At a density interface, with more dense gas (density ρ_1) underlying less dense gas (ρ_o), the restoring force (per unit volume) associated with the displacement of a unit volume of denser fluid into the (upper) less-dense medium is

$$F = g\,(\rho_1 - \rho_o) \tag{11}$$

A time scale (T_d) associated with relaxation of the displaced parcel in the less dense medium is then

$$T_d = [(\rho_1/\rho_o - 1)(\theta/g)/\,|\,(d\theta/dz)\,|\,]^{1/2} \tag{12}$$

This is analogous to the time scales associated with restoration of a displaced air parcel in ambient stratification, presented earlier. A suitably modified form of the stability index which includes the effects of density gradients might then be constructed as

$$R_4 = T_m^2\,(T_b^{-2} + T_d^{-2}) \tag{13}$$

where T_m and T_b have already been defined (see Eqs. (5) and (6)).

Inspection of this further modification is not especially revealing, since it is no more than a restatement of the observation that local density variations must be used to adjust the ambient potential temperature gradient when calculating the local stability index. Such matters have been treated extensively elsewhere (e.g., Havens and Spicer, 1985). Stability indices R_2, R_3, and R_4 (given by Eqs. 8, 9, and 13) are useful

for screening the relative importance of chemistry and density effects in modifying the atmospheric turbulence and dispersion of reactive and/or dense gases.

5. APPLICATION TO UF_6

The need to consider the special characteristics of reactive gases in dispersion models leads immediately to two fundamental questions:

(a) Is the reaction completed fast enough that the consequences can be accommodated in the source term of a relatively standard dispersion code, or in its first time step?

(b) Does the reaction cause the dynamic behavior of the atmosphere to be modified?

The answers to these questions will determine the complexity of the model which must then be used. In some instances, such as when a reaction is strongly exothermic yet quite slow, a complicated model is likely to be required in all situations, and rapid computation (as required for real-time emergency response) may not be possible. An objective approach in less stringent conditions is to use a detailed simulation of the chemistry to derive parameterized models of the effects of reaction rates and exothermicity for a range of natural conditions. If the results of these explorations are satisfactory, then simpler models can be designed retaining acceptable levels of generality and applicability.

This general philosophy has been tested in the development of the model presented here. Upon release into the atmosphere, UF_6 reacts exothermically with water vapor, generating particulate uranyl fluoride (UO_2F_2) and gaseous hydrogen fluoride (HF). The amount of heat released and the rapidity of the reaction are clearly dependent on ambient absolute humidity. In this instance, scaling properties such as those discussed in Section 3 need to be supplemented since factors not included in the development of these scales might be critical. The treatment of this problem for the TRIAD model is discussed in the next section.

The chemical reaction is as follows:

$$UF_6 + 2H_2O \longrightarrow UO_2F_2 + 4HF + J \qquad (14)$$

The heat release rate J is a function of temperature and pressure but, for typical conditions involving gaseous UF_6 and water vapor, J is about 58,600 Joules/gm-mole of H_2O based on chemical considerations alone.

At room temperature, UF_6 is a white volatile solid which forms transparent crystals which sublime under atmospheric pressure. At higher pressures, they melt to form a clear, colorless, mobile liquid of high density (3.6 g/cm^3). The sublimation point is about 56.6 C and despite the high molecular weight (352.025 g/mole) of UF_6, the properties of its vapor closely approximate those of an ideal gas. The triple point of UF_6 is 64.1 C (at 114 cm Hg pressure). UF_6 is a highly reactive substance which reacts chemically with water, ether, and alcohol, forming soluble

reaction products. It reacts with most organic compounds and many metals. It does not react with oxygen, nitrogen, or dry air.

Anhydrous uranyl fluoride is a pale-yellow solid (density=6.4 g/cm^3) that decomposes without melting above 267 C. It is soluble in water and tends to form hydrates which are unstable above 100 C. UO_2F_2 at low temperatures is very hygroscopic. Its molecular weight is 308.025 g/mole.

Anhydrous hydrogen fluoride is a chemical widely used as a catalyst by oil refineries and as raw material by refrigerant manufacturers. It is a clear, colorless, hygroscopic liquid (density=1.0 g/cm^3) that vaporizes readily when exposed to the atmosphere to produce corrosive fumes with an intolerable, pungent odor. It boils at 20 C to form a colorless vapor. In both the liquid and gaseous states, anhydrous HF is believed to exist mostly as a polymer, though at high temperatures and low pressures the average molecular weight of anhydrous HF (20.008 g/mole) approaches that of the monomer. HF strongly interacts with available moisture resulting in a lowering of the pure component vapor pressures. A nonideal mixture is formed which is in equilibrium with the vapor phase.

Gaseous UF_6, when released in the atmosphere, reacts rapidly with the ambient moisture to form HF gas, and particulate UO_2F_2 which tends to settle on surfaces. The corrosive properties of UF_6 and HF are such that exposure to a severe release can result in skin burns and temporary lung impairment. The inhalation of fumes from very large releases for more than a few breaths may result in temporary lung impairment quite soon after the exposure and, in some instances, mild but repairable kidney damage within a few days. HF is considered life-threatening after 30 min of exposure in concentrations as low as 20 ppm. Water-soluble uranium compounds such as UO_2F_2, like most heavy metal compounds, are toxic to the kidneys when inhaled or ingested in large quantities. For uranium of uranium-235 enrichment less than 10%, the chemical toxicity is more important than the radiotoxicity.

The UO_2F_2 and HF which form quickly during a release of UF_6 in the atmosphere result in a readily visible white cloud. A concentration of 1 mg of UO_2F_2 per cubic meter of air is visible and the cloud from large releases may obscure vision.

6. COMPONENTS OF THE TRIAD MODEL

Three separate but closely interacting activities were combined to produce the so-called TRIAD model for the dispersion of UF_6 and its reaction products. These three sub-projects addressed problems of (a) initial puff specification, (b) wind field interpolation, and (c) puff transport and dispersion.

6.1 INITIAL PUFF SPECIFICATION

Dispersion models typically use averaging-time periods of the order of five to sixty minutes. There is no fixed criterion that determines the precise (or optimum) length of the dispersion time step; rather, it is

governed by the conditions under which the dispersion model is meant to operate. If the intent is to make use of measured wind field information, as in the present case, and if the winds are likely to vary rapidly with time, then clearly a short dispersion time step is indicated. The design of the present TRIAD model is predicated on the assumption that a five to fifteen minute time step will be employed, providing the capacity for wind fields to be updated every five to fifteen minutes.

A sophisticated numerical model of UF_6 reactions in air (the PLUME model) was developed earlier (Just and Williams, 1986). This includes a detailed description of the turbulent resupply of reactants as material is consumed (Varma, 1982), and provides a convenient tool for investigating the rapidity of UF_6 reactions in air. This model was exercised repeatedly to test the validity of the theoretical predictions developed above. The model was run assuming a 300 second duration vertical or horizontal release of either 100% vapor, or a 60/40 mixture of vapor/liquid or vapor/solid UF_6 at a height of 5 m, with an exit velocity of 9 m/s. The meteorological conditions were D stability, 6 m/s wind velocity, 20 C temperature, and relative humidity ranging from 5% to 90%. In addition, model outputs corresponding to several large cylinder release cases from past studies were examined.

These data were then supplemented with a series of simulations using the PLUME model for two different emission rates (0.37 kg/s and 20.05 kg/s of pure 100% vapor UF_6). Such parameters as the ambient temperature, plume temperature, specific humidity, ambient wind speed, stability class, puff release duration (also averaging time), and instantaneous versus turbulent-mixing-limited reaction of UF_6 with H_2O, were varied in these runs. Most of these simulations used the following base case conditions: ambient temperature = 20 C, plume temperature = 57 C, ambient wind speed = 6 m/s at 2 m AGL, neutral stability (class D), and plume exit velocity of 9 m/s. These input conditions were selected to ensure that the performance of the PLUME model was not limited by overly difficult assumptions about the prevailing conditions.

Figures 4 and 5 illustrate the results. Figure 4 shows the time required for the reaction to be (1-1/e) complete (the "exponential reaction time") as a function of ambient mixing ratio (grams of water vapor per kilogram of dry air). In Figure 4 the reaction time is seen to be short in comparison to the meteorological time step used in puff-dispersion models (typically about five to fifteen minutes). Figure 5 illustrates the changes in reaction time with atmospheric stability class. There is little need to consider background atmospheric stability as a controlling factor since, for even the most stable case considered, the reaction appears to be completed in 30 seconds. Hence, in this particular case it appears adequate to assimilate the chemistry and its consequences in the first time period of a standard puff model, and to use the more detailed chemical model to develop the appropriate parameterizations. This is true whether the model assumes an instantaneous reaction upon entrainment of water vapor, or allows additional time for mixing within the plume.

The theoretical discussion presented earlier indicates that both the UF_6 mass release rate and the water vapor content of the air are critical controlling variables. In particular, the theory indicates that absolute

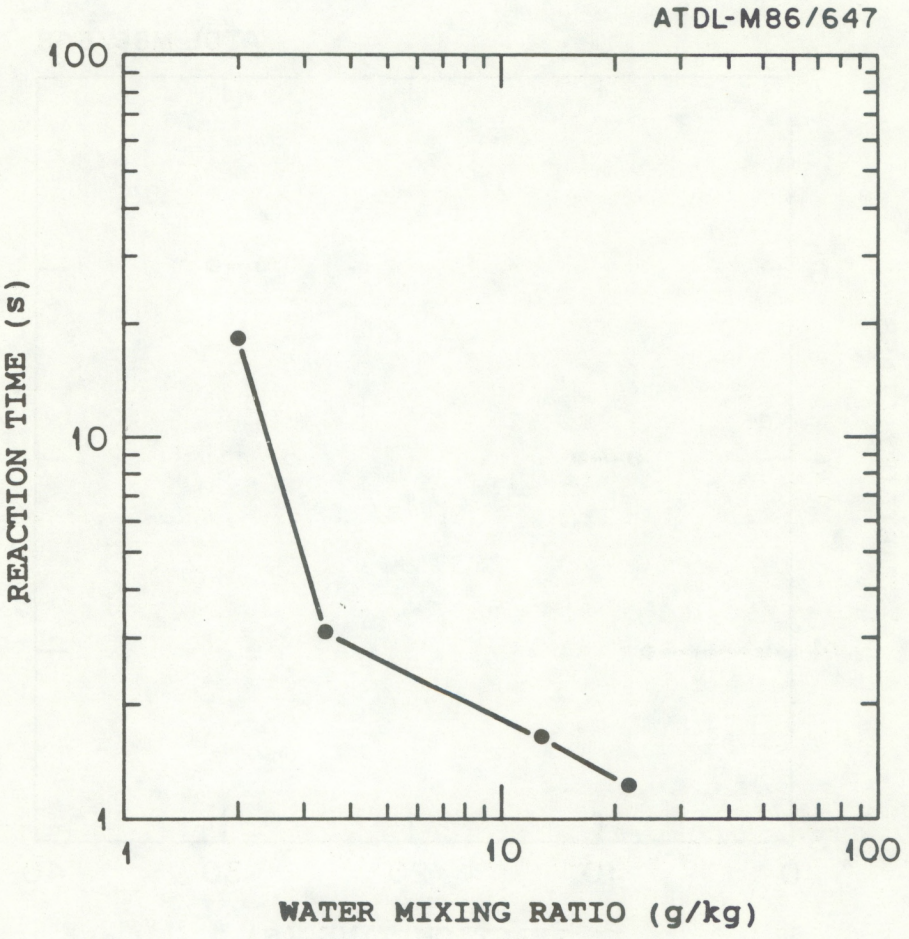

Figure 4. Initial evidence for a humidity dependence of the exponential time scale of reaction of UF_6 released into air, as computed by the PLUME (turbulent mixing limited reaction rate) model.

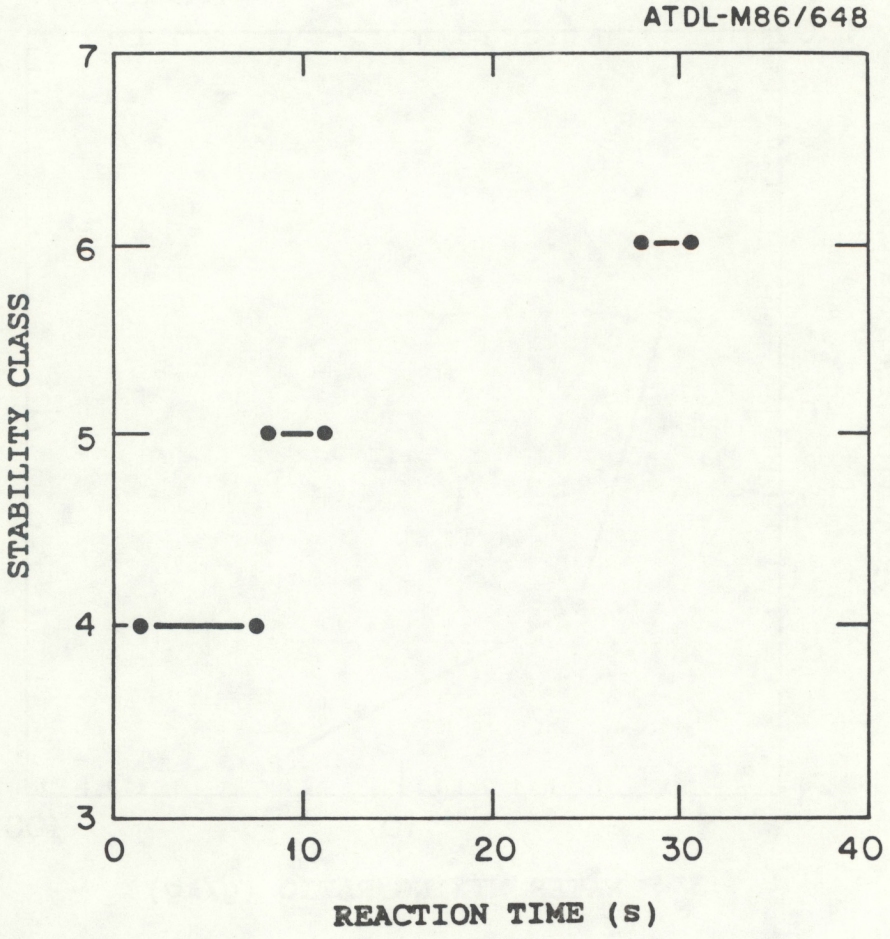

Figure 5. Initial evidence of the dependence of the exponential time scale of reaction of UF_6 on the atmospheric stability class. Note that 4 = Pasquill stability class D, 5 = E, and 6 = F.

humidity (expressed in units of mass of water per unit volume of air) is one of the critical variables. This and other predictions of the theory have been tested using the results from the PLUME model. The consequences of this testing program will be discussed below.

Figure 6 summarizes the results of a series of tests using the PLUME model, with a constant source term (a mass rate of 1.47 kg/s of UF_6). The line drawn through the data points shows that the time of reaction varies inversely as absolute humidity (grams of water vapor per cubic meter of air), with an exponent of about -1/2.

The question then arises as to the role of the emission rate (mass of UF_6 per unit time) on the reaction time. Total reaction time for larger releases will be governed by the entrainment of ambient air into the puff, the primary mechanism by which atmospheric reactants are supplied to the pollutant cloud. Figure 7 presents a series of tests made with different release rates ranging from 0.37 to 20.1 kg/s of gaseous UF_6, as a function of absolute humidity. The best-fit lines through the results show nearly the same slope, but are displaced upwards as the release rate increases. Figure 8 summarizes the results of all these tests. This plot, which collapses the nearly parallel lines shown in Figure 7 into a single line, shows the relationship between reaction time t_{90} (the time in seconds to 90% completion of reaction), absolute humidity E (g/m^3), and the UF_6 release rate $\dot{Q}$ (kg/s). The modeled releases included 100% UF_6 vapor as well as 60% vapor and 40% solid or liquid UF_6 as shown in Figure 8. The scatter in this plot is due to vertical versus horizontal emission orientation, and due to raising the absolute humidity to an approximate power of 0.4. The best-fit correlation can be written as

$$t_{90} = a \dot{Q}^{b} E^{-n} \qquad (15)$$

where a = 0.81 ± 4.8% and b = 0.57 ± 5.2%, with a correlation coefficient r = 0.96 when n is assigned a nominal value of 0.4 (n varied from 0.38 to 0.43 over the range of release rates used here).

Figures 9 and 10 show similarly-derived correlations for the dispersion parameters, σ_z and σ_y, in relation to the UF_6 release rate and the absolute humidity. These plots give the relations for the enhancement of the puff initial size due to the exothermic reaction of UF_6, as follows:

$$\sigma_z = a_1 \dot{Q}^{b_1} E^{-n_1} \qquad (16)$$

$$\sigma_y = a_2 \dot{Q}^{b_2} E^{-n_2} \qquad (17)$$

where σ_z and σ_y are in meters, a_1 = 0.51 ± 1.4%, b_1 = 0.55 ± 1.5%, and a_2 = 1.26 ± 1.8%, b_2 = 0.48 ± 3.0%, with correlation coefficients $r_1 = r_2$ = 0.99 when n_1 and n_2 are assigned a nominal value of 0.5. Hence, both the vertical and the lateral dispersion parameters are taken to be proportional to the square root of the UF_6 release rate, and the inverse square root of the absolute humidity.

In order to assess the ability of the parameterized relationships to address questions of initialization of puff routines, we must take into

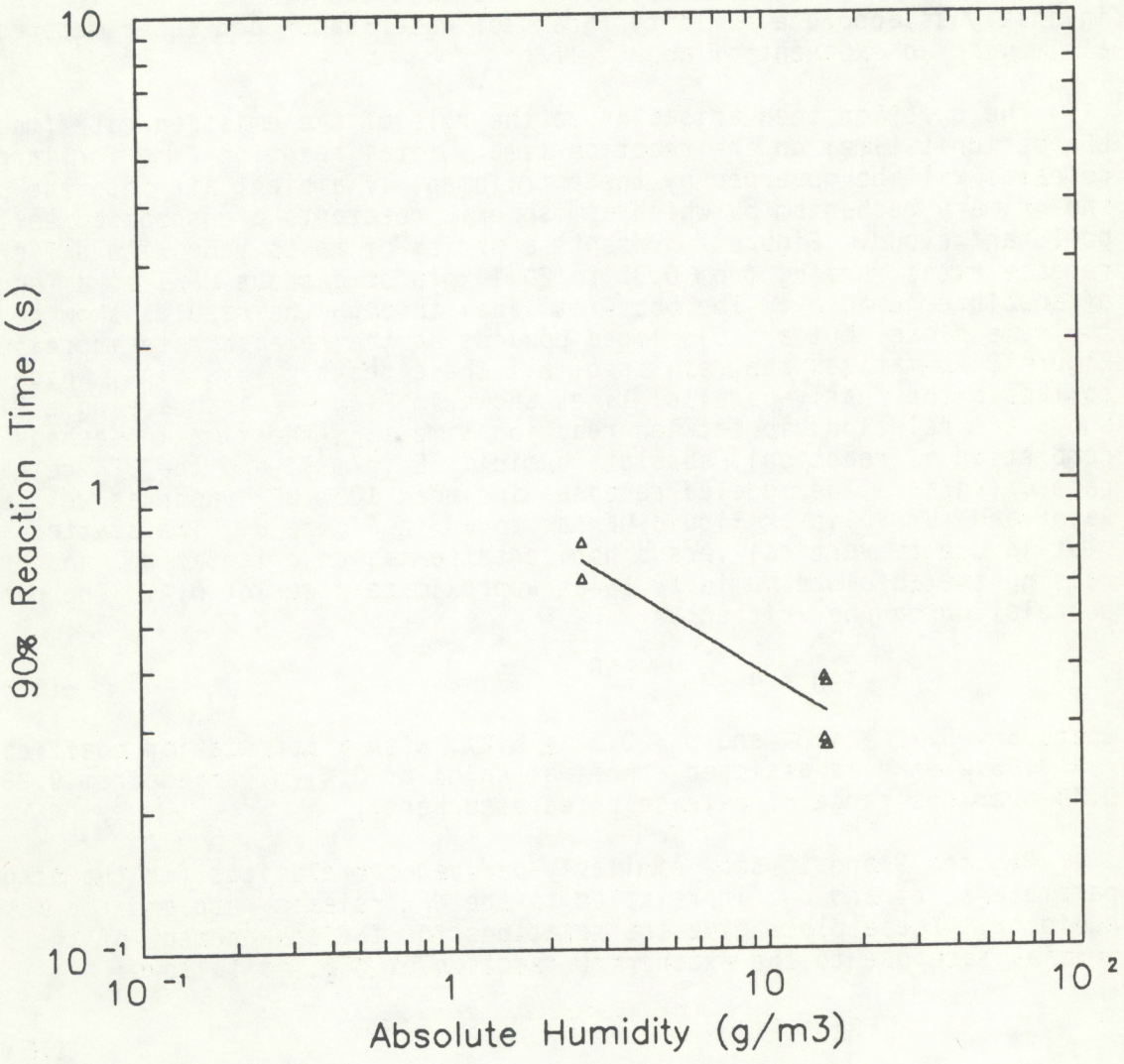

Figure 6. Dependence of the time (to 90% completion) of reaction on atmospheric absolute humidity, for a release rate of 1.47 kg/s of UF_6 vapor.

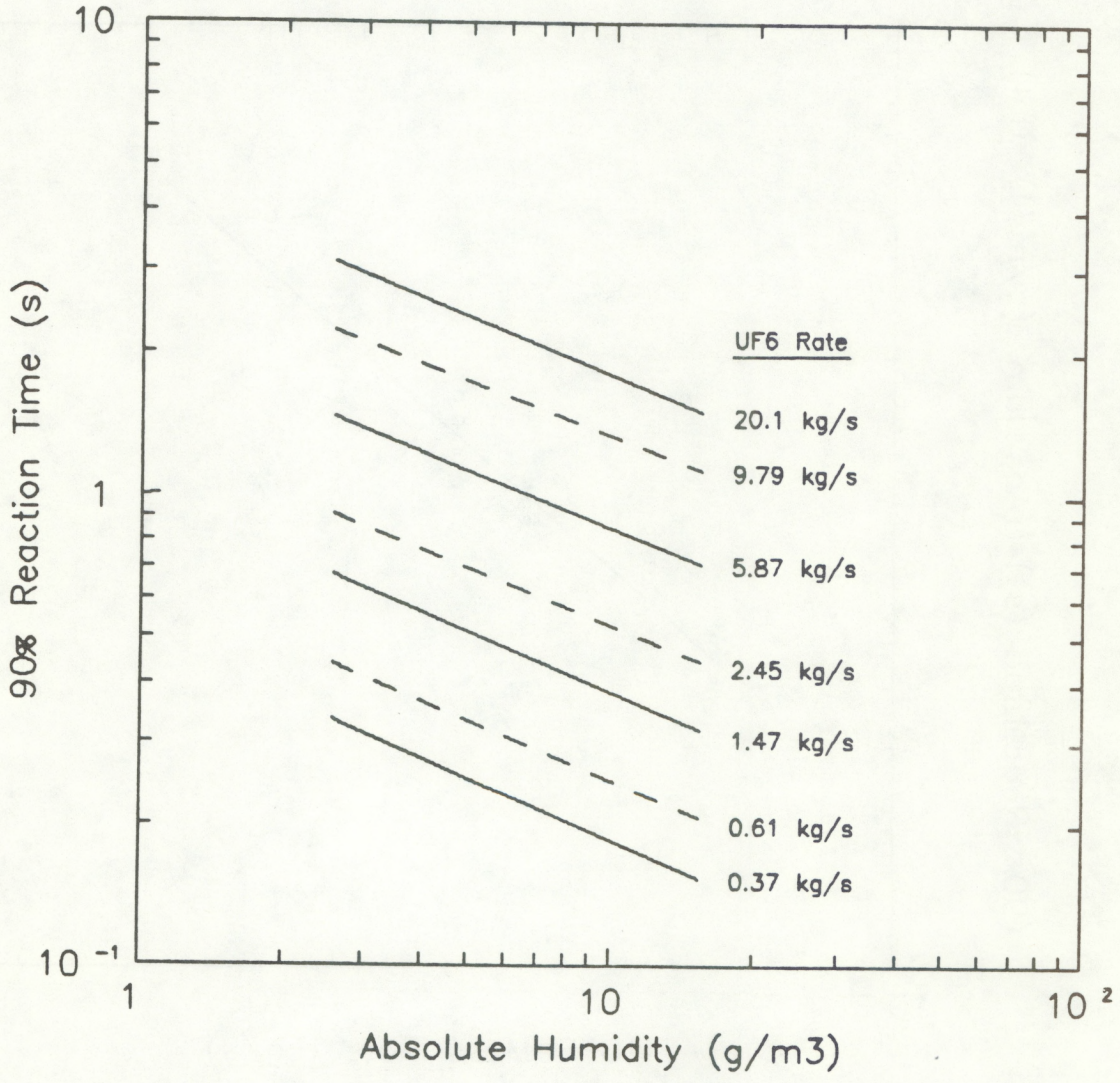

Figure 7. Dependence of reaction time on atmospheric humidity and UF_6 release rate. The solid lines denote 100% UF_6 vapor, and the dashed lines denote a mixture of 60% vapor and 40% solid or liquid UF_6 at release.

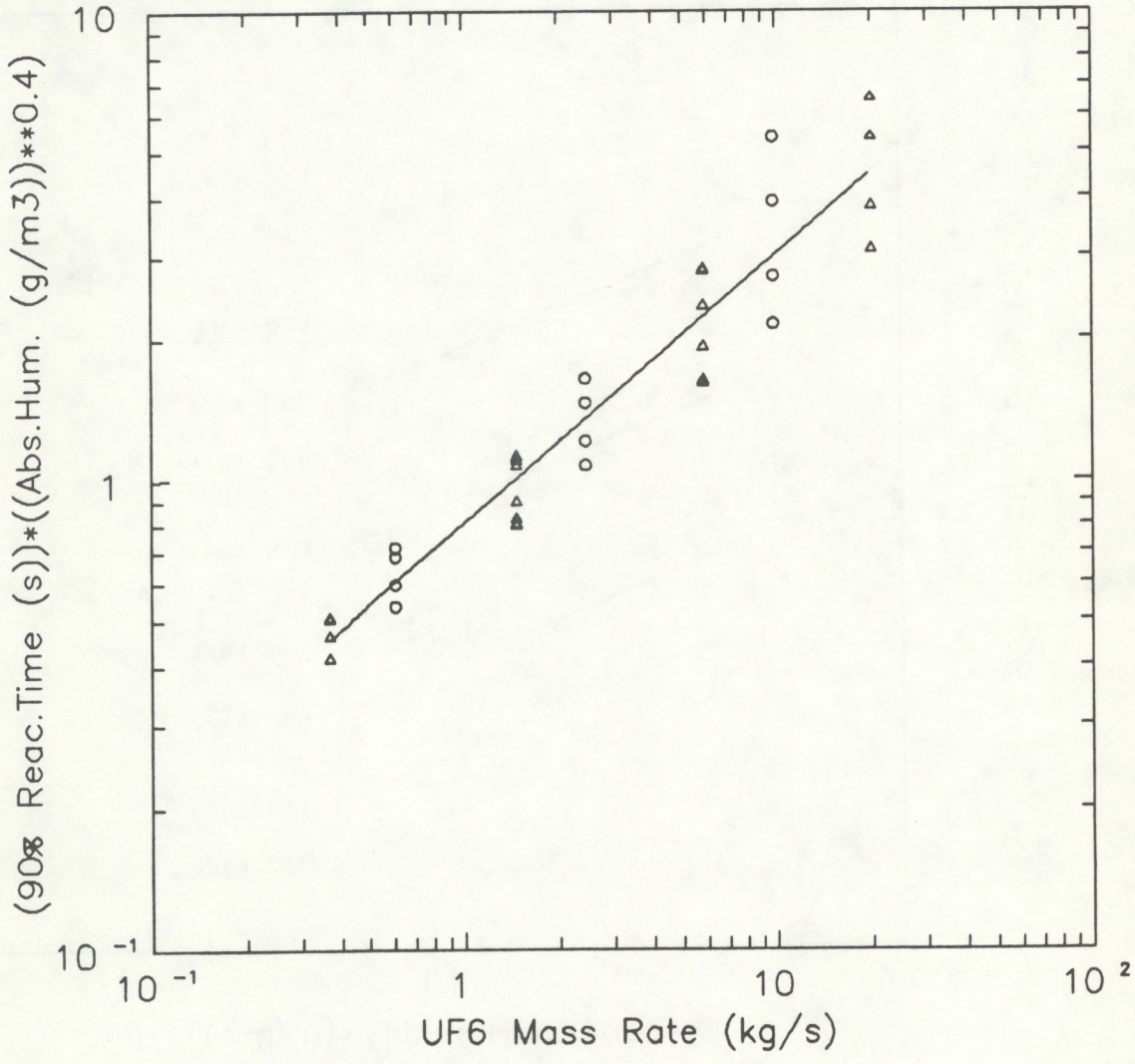

Figure 8. Correlation showing the variation of the reaction time with ambient humidity and the UF_6 release rate. The solid line gives the best-fit correlation given by Eq. (15) in the text. UF_6 release: Δ - 100% vapor; o - 60/40 vapor/solid or liquid mixture.

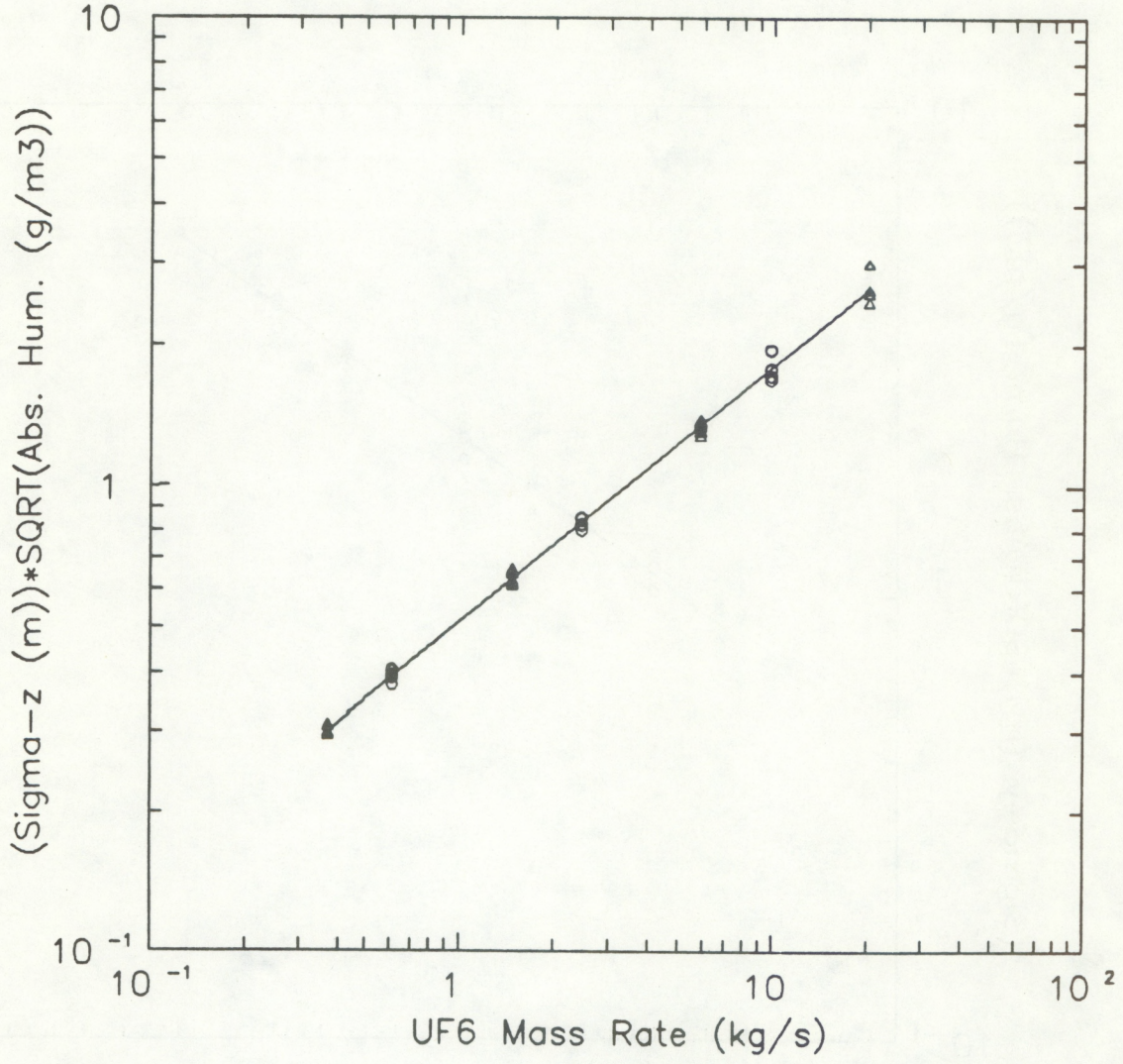

Figure 9. Correlation showing the variation of the vertical dispersion parameter with ambient humidity and UF_6 release rate. The best-fit line is given by Eq. (16) in the text. This result is used to set the initial puff size in the TRIAD model.

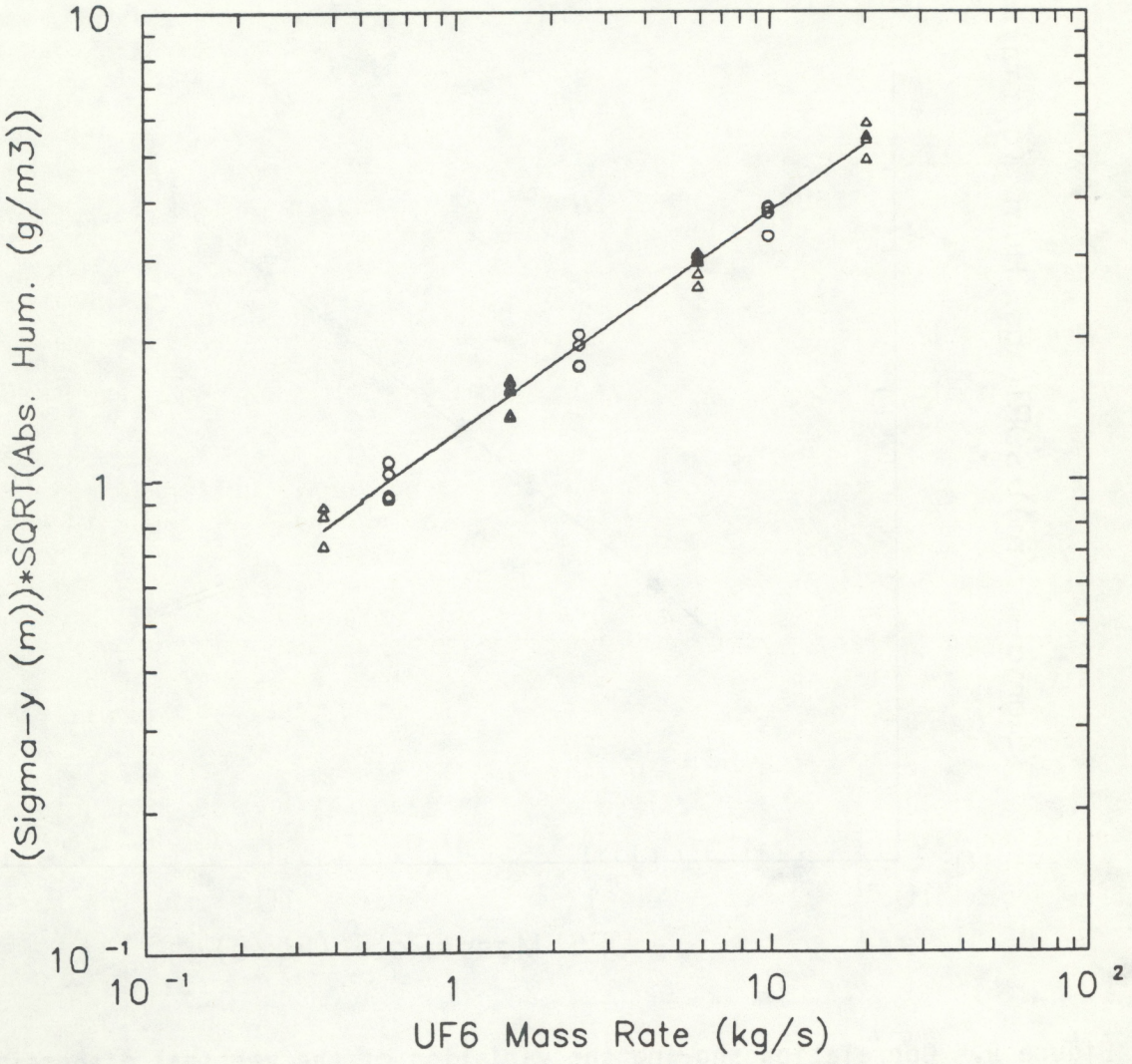

Figure 10. Correlation showing the variation of the lateral dispersion parameter with ambient humidity and UF_6 release rate. The best-fit time is given by Eq. (17) in the text. This result is used to set the initial puff size in the TRIAD model.

account the conditions under which the models must be run. As mentioned, the wind field update time step of the puff model will be 5 to 15 minutes, and puffs are assumed to be released every 10 to 60 seconds. These factors impose constraints on the interpretion of Figure 8. Absolute humidities are typically 10 to 20 g/m^3 in summer, and 2 to 10 g/m^3 in winter (as illustrated in Figures 2 and 3). The model time step, puff release frequency, and typical humidities enable bands to be specified on Figure 8 which can then be used to identify circumstances where the PLUME model predictions (with the sophisticated chemistry model) will provide results that are compatible with the application of the TRIAD model (which uses simple parameterizations partially based on that chemistry model). The largest UF_6 release rate of about 20 kg/s used in deriving the initial-puff parameterizations should impose no significant constraint on the potential applications of the TRIAD model.

Formulation of Plume Rise

Classical expressions describing plume rise in terms of external parameters and emission quantities describe averages, not single events. They should therefore be used cautiously. Typical plume and puff dispersion models include parameterizations of rise terms that are now well accepted. In all cases, the assumption is that the material released to the atmosphere has an initial exit velocity, and differs in temperature from the ambient conditions. These characteristics lead to a momentum and/or buoyant plume rise.

In the case of UF_6, there are two factors that must be considered. First, there is rise occurring due to the puff's initial buoyancy and/or momentum. Once the exothermic reaction is completed, the remaining material has a temperature excess relative to the surrounding atmosphere, which causes additional buoyant puff rise. Consideration of plume rise is therefore split in the present approach, between that which occurs due to initial conditions and that which results from a temperature elevation of the puff due to the heat of reaction. The first is contained within the puff model itself, while the second is part of the puff initialization.

Figure 11 shows the correlation with absolute humidity and mass emission rate for the temperature increase of the puff due to the exothermic reaction of UF_6. The temperature rise increases linearly with the absolute humidity, but is nearly independent of the UF_6 release rate. The best-fit correlation is given by

$$\Delta T \cong 2.0 \quad E, \tag{18}$$

where ΔT is in degrees C (or K). This equation, however, is not very useful in estimating the enhancement of the puff buoyancy flux unless we can also specify the associated mass flux. It is difficult to calculate the latter accurately, because it is a function of puff speed, size, and entrainment, among other factors. Therefore, an alternate approach has been developed, as outlined below, for estimating the enhancement of the initial puff buoyancy flux by the exothermic reaction. This derivation is based on the assumption that the UF_6 vapor in the initial puff reacts completely with the ambient water vapor during the time of the puff release, typically about 10 to 60 sec.

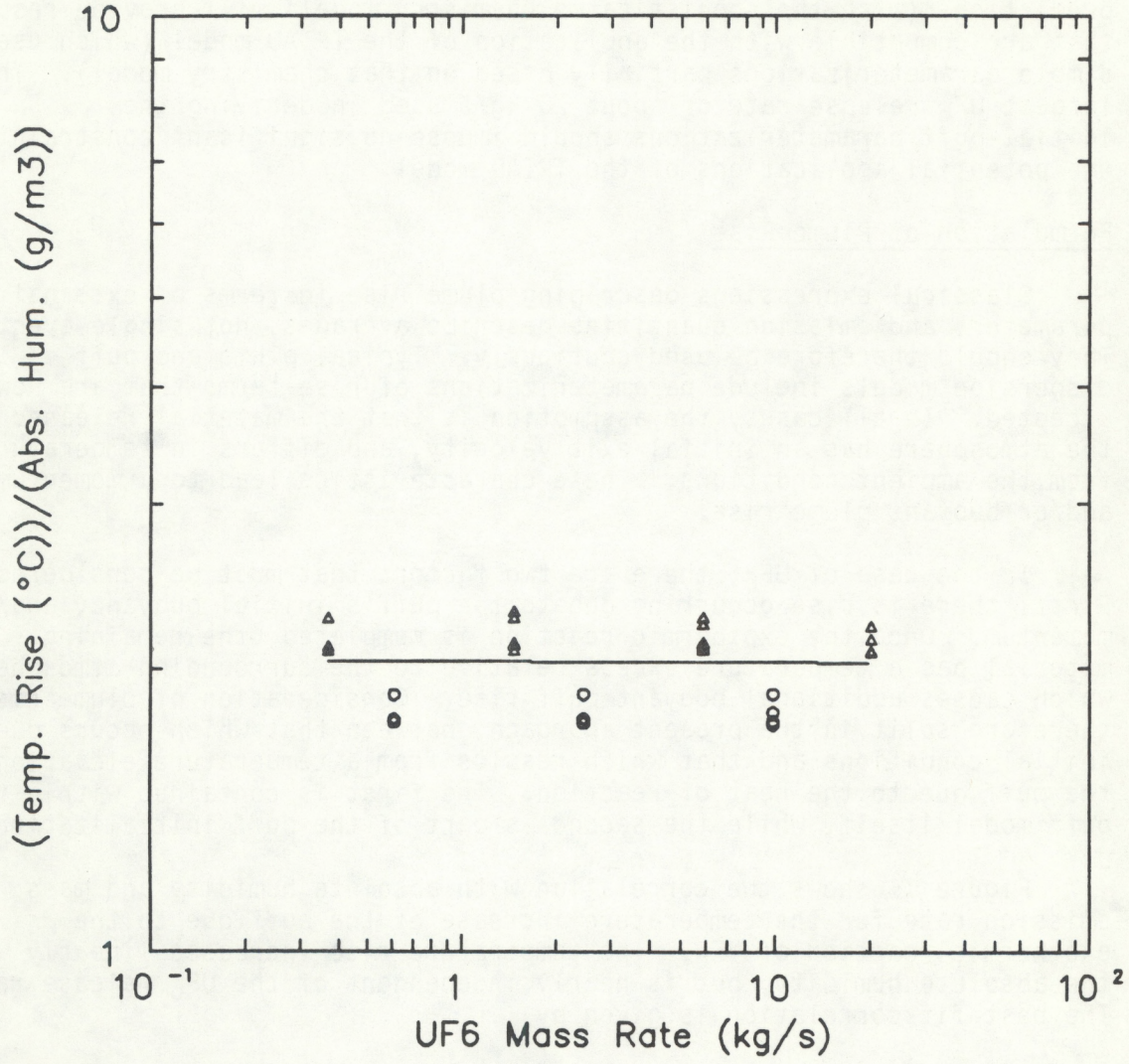

Figure 11. Correlation showing the variation of the temperature rise (over the ambient) of the puff with ambient humidity and UF_6 release rate. The best-fit line is given by Eq. (18) in the text. Note that ΔT, which results from the heat of reaction, is nearly independent of the UF_6 release rate.

The exothermic reaction of gaseous UF_6 with ambient water vapor is described by Eq. (14). This equation states that 1 mole of UF_6 requires 2 moles of H_2O for complete reaction. If a puff with Q grams of UF_6 was released into an ambient atmosphere with specific humidity q (g of water vapor per g of moist air), then the constituents of the puff for complete reaction are as follows:

Constituent	Number of moles	Partial mass
UF_6	$n_u = Q/M_u$	$m_u = Q$
H_2O	$n_v = 2\, n_u$	$m_v = n_v\, M_v$ (19)
Dry air	$n_d = 2\, n_u \frac{M_v}{M_d} \frac{(1-q)}{q}$	$m_d = n_d\, M_d$

The UF_6 vapor, water vapor, and dry air can be treated as ideal gases. The density ρ_p of the puff comprised of this mixture of ideal gases is given by

$$\frac{p}{\rho_p} m = R^* T_p [n_u + n_v + n_d] \tag{20}$$

where p is the pressure, T_p is the temperature, R^* is the universal gas constant, and

$$m = m_u + m_v + m_d \tag{21}$$

is the total mass. Using relations (19) and (21) in (20), we obtain

$$\rho_p T_p = \frac{p}{R_d} \frac{\left[2 + \frac{M_u}{M_v} q\right]}{\left[3 \frac{M_d}{M_v} q + 2 (1-q)\right]}$$

where $R_d = R^*/M_d$ is the gas constant for dry air. Substituting the molecular weights $M_u = 352.025$ gm, $M_v = 18$ gm, and $M_d = 28.964$ gm, this equation reduces to

$$\rho_p T_p = \frac{p}{R_d} \frac{(2 + 19.56\, q)}{(2 + 2.83\, q)} \tag{22}$$

The buoyancy flux (due to the heat of reaction) to be used in the plume-rise equations is given by

$$F = \frac{1}{\pi} \frac{g}{T_p} \frac{Q_H}{\rho_p c_p} \tag{23}$$

where the heat release rate Q_H during the reaction is estimated as follows.

The exothermic heat of reaction in Eq. (14) is

$$J = 58600 \text{ Joules/gm-mole of } H_2O \text{ .}$$

In a complete reaction of Q grams of UF_6 over a puff-release time period t_s (typically 10 to 60 sec), the heat release rate is given by

$$Q_H = n_v J/t_s = \frac{2Q}{M_u}\frac{J}{t_s}$$

$$\cong 333 \times 10^3 \dot{Q} \text{ Joules/sec} \cong 80 \times 10^3 \dot{Q} \text{ cal/sec} \qquad (24)$$

where $\dot{Q} = (Q/t_s) \times 10^{-3}$ is the UF_6 release rate (kg/s). Combining Eqs. (22) to (24) now yields the buoyancy flux F (m^4/s^3) to be used in plume-rise calculations as follows:

$$F = \frac{1}{\pi}\frac{g}{p}\frac{R_d(2 + 2.83\ q)}{c_p(2 + 19.56q)} 80 \times 10^{-2} \dot{Q}$$

$$= \frac{2.988}{p}\frac{(2+2.83\ q)}{(2+19.56\ q)}\frac{Q}{t_s} \times 10^3 \text{ .} \qquad (25)$$

Here p is the ambient pressure in millibars, g = 9.81 m/s^2 is the gravitational acceleration, c_p = 0.24 cal/g/K is the specific heat of air at constant pressure, R_d = 287.05 $m^2/s^2/K$, and q (g/g) is the ambient specific humidity. Equation (25) is used in the TRIAD model to estimate the buoyancy flux enhancement due to the complete exothermic reaction of the UF_6 in the puff with ambient water vapor.

6.2 WIND FIELD INTERPOLATION

At the user's option, the TRIAD model may use wind data, variable in both time and space, from a meteorological grid. This option requires measured winds from multiple anemometer sites. The algorithm interpolating these measured winds to the meteorological grid was adapted from MESOI-2, a puff-dispersion program of the Nuclear Regulatory Commission (Ramsdell et al., 1983). If wind data are only available from a single point, winds are then assumed to be horizontally homogeneous, though they may vary from one meteorological period to another.

The algorithm in the wind-field module works as follows. Wind data from several sites are adjusted to a standard elevation by a stability-dependent power-law relation applied to the speed. The direction is unchanged by the adjustment. The adjusted winds are then converted to eastward and northward components ($\bar{u}$,$\bar{v}$), and interpolated to a rectangular grid. Interpolation is by a weighted average, with the weights given by

inverse squared distance, a commonly-applied operational interpolation scheme. The mathematical form, taking wind-component $\bar{u}$ as an example, is:

$$\bar{u}_{ij} = \sum_{k=1}^{N} (\bar{u}_k / r_{kij}^2) / \sum_{k=1}^{N} (1/r_{kij}^2) \qquad (26)$$

where $\bar{u}_{ij}$ is the interpolated wind at grid-point (i,j), $\bar{u}_k$ is the measured value at site k, r_{kij} is the distance from grid point (i,j) to measurement site k, and N is the number of measurement sites. Far away from all measurement sites, the interpolated wind approaches the vector average of all observations. Upon close approach to an individual measurement site, all other data rapidly lose influence due to the weighting scheme. A comparison of several interpolation methods including inverse-squared-distance weighting is given by Goodin et al. (1979).

The current version of the wind-field module does not explicitly treat terrain effects. To do so in a simple scheme of this type requires the specification of a large number of parameters to locate the terrain, and to indicate whether flow goes over or around obstacles. Since values of such parameters can not be objectively determined, a network of carefully-placed meteorological towers adequate to represent the wind field in complex terrain is essential. The influence of the terrain is thus reflected in the wind observations. Variable elevations of the anemometer sites (with respect to a constant reference level) are taken into account in the power-law extrapolation of the wind speed. In addition, gross differences in elevations between sources and receptors in complex terrain are taken into account in estimating the concentrations (see Appendix A).

Meteorological Grid Structure

The meteorological grid is rectangular, oriented north-south (y) and east-west (x). The grid spacing in the x-direction may differ from that in the y-direction. The grid may have an unequal number of grid cells in the x- and y-directions up to a total of 100 cells, typically covering a physical region of radius 5 to 10 km. A larger grid may be provided by adjusting the array sizes. The default of 100 points was chosen in TRIAD to control run time and storage requirements.

Operating Considerations

The standard elevation to which measured winds are adjusted before interpolation is set at the beginning of the run to be 10 m above the ground level at the anemometer site located on the highest ground. This avoids the problem of interpolating winds to points below the local ground level at any of the anemometers. Winds are further adjusted from the standard elevation to the effective puff height by the same power law in order to compute the puff transport.

There is a radius of influence beyond which wind data are ignored in computing interpolated winds at a given grid point. However, at least three (if available) and no more than ten wind sites are used regardless of distance. The square of the radius of influence is defined as five times

the product of the x- and y- grid spacing. Wind data from sites more than one radius of influence beyond the outermost points of the meteorological grid are ignored by the interpolation program, both for the actual interpolation and for the computation of the standard elevation defined in the previous paragraph. The meteorological grid should be chosen to include as many wind sites as possible, especially in the generally downwind direction. Winds interpolated to a fine grid may differ from those at the corresponding locations in a coarse grid because the fine grid may not include all of the wind measurements included in the coarse grid.

Puffs located within the meteorological grid boundary are carried by the wind at the nearest meteorological grid point with no further interpolation. Puffs outside of the meteorological grid are still carried by the wind at the nearest grid point, however distant. Clearly, it is risky to rely on puff positions more than one-half grid interval beyond the outermost meteorological grid points. A warning message is provided for such puffs. More information on the operation of the wind module and its design are given in Appendix A.

6.3 PUFF TRANSPORT AND DISPERSION

As part of the work undertaken under Phase I of this program, several puff models developed in the context of air pollution and trace gas dispersion were reviewed, and an optimal puff model was selected. The integrated puff model, INPUFF-2, developed by Petersen and Lavdas (1986) for the U.S. Environmental Protection Agency, is capable of addressing the accidental release of a substance over a short time period, or of modeling the typical continuous plume from a stack. The implied modeling scale is from tens of meters to tens of kilometers.

INPUFF-2 incorporates state-of-the-art parameterizations for dispersion, dry deposition, and sedimentation of particulate matter. The model has the capability to include on-site turbulence schemes, source updates, and multiple stationary or moving point sources. Many technical and output options are available to increase the model's flexibility and range of applications. These include the user-supplied plume rise schemes, dispersion parameters, and wind field. Additional options were added by ATDD to account for differences in ground elevations of sources and receptors. This feature, in conjunction with the objective interpolation of wind data from multiple towers, gives the capability to consider terrain effects. Output concentrations at up to 100 receptors can be estimated in any user-specified units. All of these features make it easy to adapt the model to a given application. Details of the INPUFF-2 model can be found in Appendix A.

Petersen (1986) evaluated the INPUFF-2 model using the MATS data base. Rao et al. (1988) adapted this model for complex terrain and successfully simulated ASCOT tracer data in the nocturnal drainage flow in a deep mountain valley in western Colorado.

7. LIMITATIONS OF THE TRIAD MODEL

7.1 BUILDING WAKES

As described in this report, the TRIAD model fails to take into account the effects of building wakes. These effects are necessarily such that additional dilution will occur, on the average, downwind of buildings that modify flow fields. On the other hand, local hot spots can most certainly occur, and these will not be predicted or described by any modeling capacity that omits consideration of the detailed configuration of the structures in the area of the release.

Hosker and Pendergrass (1984) reviewed the role of building wakes in dispersing pollutants released into the atmosphere near buildings. In subsequent work, Pendergrass and Hosker (1985) conducted a series of tests in a large wind tunnel to demonstrate the extent of plume modification caused by large buildings, such as those typical of uranium processing facilities. Their conclusion was that the role of the buildings was roughly equivalent to a shifting of the source location.

In the initial coding of the TRIAD model, no allowance was made for effects of building wakes. In consequence, the near-field predictions of the model are likely to be overestimates, by an amount that may be as high as a factor of two. The zone of influence of very large squat buildings such as those at gaseous diffusion plants is likely to extend downwind to a distance corresponding to about two to four building heights, i.e., about 40 to 80 m, depending on wind direction. Results from the present code should not be applied within the region of influence of buildings.

7.2 INCOMPLETE REACTIONS

A further complication arises as a consequence of the parameterization of the atmospheric chemical reactions, as used in the TRIAD model. In the near field, before reactions are fully completed, the released material will not follow precisely the path attributed to it by the TRIAD model. The reason is clear; the model assumes the chemistry is completed, whereas in reality the chemistry is not completed until a significant time has elapsed after the release. Figure 8 has already described the time to reaction completion on the basis of the controlling external parameters -- specific humidity and UF_6 release rate. If these controlling parameters are known, then the time to chemical reaction completion is specified. Table 3 shows this as a "transit time" for several UF_6 release rates and absolute humidities. This time can then be used in conjunction with the wind speed to specify the horizontal dimension of the second exclusion zone, within which the results of the TRIAD computations should be considered with considerable caution.

The distance scales derived using Table 3 will normally range from several meters to several tens of meters. In most circumstances, this distance is much smaller than the "exclusion zone" appropriate on the basis of building wake effects. In essence, it appears that the consequences of building wakes will dominate the effects of incomplete chemistry in the near field.

Table 3. Estimates of the near-source "exclusion zone" in which predictions by the TRIAD model are likely to be erroneous, due to the assumption that chemical reactions are completed. The values quoted are transit times, in seconds; estimates of the corresponding distance scales can be derived by multiplying these values with the wind speed.

Humidity (g/m^3)	2	5	10	20
UF_6 Release Rate (kg/s)				
0.5	0.41	0.28	0.21	0.16
1	0.61	0.42	0.32	0.24
2	0.93	0.64	0.49	0.37
5	1.61	1.14	0.85	0.64
10	2.44	1.69	1.28	0.97
20	3.70	2.56	1.95	1.47

7.3 HEAT OF REACTION AND PLUME RISE

In the parameterization of the exothermic heat of reaction (Section 6.1), it is assumed that the UF_6 vapor contained in the initial puff reacts completely with the ambient water vapor over the time of duration of the puff release (t_s), which is typically about 10 to 60 sec. This assumption is consistent with the PLUME model results shown in Figure 8 which suggest that, for typical humidities and release rates of up to 20 kg/s, the reaction will be completed within 10 sec. However, since the heat release rate and initial buoyancy flux are inversely proportional to t_s (see Eqs. 24 and 25), there is an uncertainty of up to a factor of six in their estimated values. This leads to an uncertainty of about a factor of 3 to 4 in the maximum plume rise (see Appendix C) estimates.

There are two ways to reduce this uncertainty. First, one can use a puff release time step of 30 sec for t_s. This would be a good compromise between having enough puffs in the model grid to simulate the transport, and reducing the uncertainty in plume rise estimates. Second, one can set t_s = c.10 sec in Eq. (25) where c is a constant to be specified by the user. By varying the value of c from 1 to 6, the user can calculate the range in plume rise and concentration estimates for a given set of ambient and release conditions. Ideally, the value of c should be determined by comparing the plume rise estimates with suitable data.

The plume rise due to the heat of reaction is expected to be partly compensated by the dense gas effects which are not considered in the TRIAD model. This justifies the use of a reaction completion time greater than 10 sec, as suggested above.

7.4 MODEL EVALUATION DATA

The predictions of even a good air quality model may have considerable uncertainty due to errors in input data (e.g., source description) and the stochastic variability of the atmosphere. Therefore, it is desirable to test and evaluate the TRIAD model with UF_6 dispersion data from full scale field experiments. However, such data are presently not available. There are three reasons for this: First, accidental releases are unplanned by nature and, therefore, such data tend to be rather qualitative and unreliable for model evaluation. Second, the toxic and corrosive nature of UF_6 and its reaction products discouraged experiments with large-scale releases in the open atmosphere. Third, detailed data sets from field experiments involving hazardous materials are often regarded as proprietary (in case of private companies) or confidential (in case of government research organizations).

There are several known accidents involving either UF_6 or HF. In January 1986, a 14-ton cylinder containing UF_6 ruptured while being heated in a steam chest at the Sequoyah Fuels Facility of the Kerr-McGee Plant in Oklahoma, causing one fatality and several injuries. Much of the facility and some offsite areas were contaminated. Though the plant workers used water hoses with fog nozzles in an attempt to suppress the emission, the airborne release continued for approximately 40 minutes. In October, 1987, about 6000 gallons of hydrofluoric acid were released over a period of a few hours after a crane at the Marathon Petroleum Refinery in Texas accidentally dropped a piece of equipment onto a pipeline containing the HF. Firefighters attempted to saturate the cloud with water sprays, but the toxic cloud that formed forced the evacuation of about 4,000 people, several hundred of whom were hospitalized. Neither of these releases provided sufficiently detailed meteorological and concentration data to test models such as TRIAD.

In the summer of 1986, AMOCO and the Lawrence Livermore National Laboratory conducted a series of anhydrous hydrofluoric acid spill experiments at the DOE's Frenchman Flats Test Site northwest of Las Vegas, Nevada. These so-called "Goldfish" dispersion experiments (Blewitt et al., 1987) consisted of six tests, four with spills of about 4 m^3 (1000 gal) and two of about 2 m^3 (500 gal) of HF at rates varying from 30 to 500 gal/min under varying meteorological conditions. The liquid HF was released suddenly through an orifice at the end of a horizontal pipe pointed downwind. Under the release conditions (40 C temperature and 115 psi pressure), approximately 20% of HF was expected to flash to vapor, and the remaining 80% to remain as liquid droplets. One of the major findings of the Goldfish tests was that all of the material released, both vapor and liquid aerosol, was transported downwind as a heavy cloud. The first three tests were designed to obtain data on source characteristics and dispersion, and the last three were designed to evaluate the effectiveness of various water spray curtains in knocking down the HF vapor. An extensive instrument array was deployed with rows of gas sensors at 300 m, 1000 m and 3000 m. Detailed data from the Goldfish and other recent field experiments (Koopman et al., 1988), when they become available, should be useful in the evaluation and refinement of dispersion models.

REFERENCES

Blewitt, D. N., J. F. Yohn, R. P. Koopman, and T. C. Brown, 1987: Conduct of anhydrous hydrofluoric acid spill experiments. AIChE International Conference on Vapor Cloud Modeling, Boston, MA. Nov. 2-4.

Briggs, G. A., 1975: Plume rise predictions. In: Lectures on Air Pollution and Environmental Impact Analysis, D. A. Haugen, ed., Am. Meteorol. Soc., Boston, MA. pp. 59-111.

Havens, J. A., and T. O. Spicer, 1985: Development of an Atmospheric Dispersion Model for Heavier-Than-Air Gas Mixtures, Vol. I. Final Report, Contract DT-CG-23-80-C-20029, U.S. Coast Guard. Available from NTIS, Report number GRI-85/0133, PB85-228633.

Hicks, B. B., W. S. Lewellen, and J. C. Weil, 1985: Review comments: Atmospheric components of the Oak Ridge UF_6 dispersion model. ATDD Contribution No. 85/11, NOAA, Oak Ridge, TN, 38 pp.

Holzworth, G. C., 1964: Estimates of the mean maximum mixing depth in the contiguous United States, Monthly Weather Rev. 92, 235-242.

Hosker, R. P., Jr., and W. R. Pendergrass, 1984: Flow and Dispersion near Clusters of Buildings, U.S. NRC NUREG/CR-4133, 96 pp. Also available as NOAA Technical Memorandum ERL-ARL-153, 95 pp.

Goodin, W. R., G. J. McRae, and J. H. Seinfeld, 1979: A comparison of interpolation methods for sparse data: application to wind and concentration fields. J. Appl. Meteor. 18, 761-771.

Just, R. A., and W. R. Williams, 1986: A Computer Program for Simulating the Atmospheric Dispersion of UF_6 and Other Reactive Gases Having Positive, Neutral, or Negative Buoyancy. Martin Marietta Energy Systems, Inc., Engineering Document No. K/D-5694. Oak Ridge, TN.

Koopman, R. P., D. L. Ermak, and S. T. Chan, 1988: A review of recent work in atmospheric dispersion of large spills. AIChE Hazardous Materials Spills Conference, Chicago, IL, May 16-19.

Pendergrass, W. R., and R. P. Hosker, Jr., 1985: Portsmouth Gaseous Diffusion Plant Purge Stack Plume Study -- Interim Report. NOAA/ATDD Contribution Number 85/31, NOAA, Oak Ridge, TN, 70 pp.

Petersen, W. B., and L. G. Lavdas, 1986: INPUFF 2.0 - A Multiple Source Gaussian Plume Dispersion Algorithm. EPA/600/8-86-011, U.S. Environmental Protection Agency, Research Triangle Park, NC, 105 pp.

Petersen, W. B., 1986: A demonstration of INPUFF with the MATS data base. Atmos. Environ. 20, 1341-1346.

Ramsdell, J. V., G. F. Athey, and C. S. Glantz, 1983: MESOI Version 2.0: An Interactive Mesoscale Lagrangian Puff Dispersion Model with Deposition and Decay. NUREG/CR-3344 (PNL-4753), U.S. Nuclear Regulatory Commision, Washington, DC.

Rao, K. S., R. M. Eckman, and R. P. Hosker, 1988: Simulation of tracer concentration data in the Brush Creek drainage flow using an integrated puff model. J. Appl. Meteor. (in press).

Slade, D. H., 1968: Meteorology and Atomic Energy, U.S. Atomic Energy Commission Publication TID-24190, 445 pp.

U.S. Nuclear Regulatory Commission, 1975: Reactor Safety Study, Appendix VI: Calculation of Reactor Accident Consequences. WASH-1400, NUREG 75/014.

Varma, A. K., 1982: Development of Models for the Analysis of Atmospheric Releases of Pressurized Uranium Hexafluoride. ARAP Report No. 482, Aeronautical Research Associates of Princeton, Inc., Princeton, NJ.

APPENDIX A

USER'S GUIDE FOR

TRIAD 2.0 : A PUFF-TRAJECTORY MODEL

FOR DISPERSION OF GASEOUS UF_6 REACTION PRODUCTS

by

K. Shankar Rao
Atmospheric Turbulence and Diffusion Division
National Oceanic and Atmospheric Administration
P.O. Box 2456, Oak Ridge, TN 37831

SUMMARY

The TRIAD computer code is designed to simulate the atmospheric dispersion of reactive gases, such as uranium hexafluoride and its reaction products, released from semi-instantaneous or continuous point sources into a spatially and temporally variable wind field. The TRIAD model combines three distinct components: initial puff specification, wind field interpolation, and puff dispersion.

In TRIAD, the effects of the exothermic heat of fast reaction of UF_6 (with atmospheric water vapor) on the initial size and buoyancy of the puff are specified by parameterizations derived from theory and verified by the PLUME model (Just and Williams, 1986). The objective wind interpolation scheme, adapted from the MESOI-2 model (Ramsdell et al., 1983), assimilates wind observations from several locations to produce a variable wind field to transport the puffs. In default mode, when only one meteorological tower is available, TRIAD assumes a spatially homogeneous wind field. The puff dispersion routine is based on the Gaussian integrated puff model, INPUFF-2, developed for the U.S. EPA (Petersen and Lavdas, 1986). TRIAD can estimate concentrations due to one or more sources at up to 100 receptors.

TRIAD utilizes three distinct Gaussian puff dispersion algorithms. For short travel-time dispersion, the user has the option of using either the Pasquill-Gifford (P-G) dispersion curves (Turner, 1970) or the on-site scheme (Irwin, 1983) based on turbulence data. The third dispersion algorithm is used for long travel times when the growth of the puff is assumed to be proportional to the square root of travel time. The rise of puffs due to initial buoyancy or momentum is estimated using Briggs'(1975) equations. Removal by dry deposition or gravitational settling is incorporated through the concentration algorithms developed by Rao (1982). The user has the option to provide his or her own subroutines for dispersion and plume rise. The code includes many other technical and output options that can be specified by the user in the input to the model.

This User's Guide to TRIAD discusses the concentration algorithms, computational techniques, capabilities, assumptions, and limitations of the model. The input data are listed and discussed. The use of TRIAD is illustrated in Appendix B with examples, input and output listings, and plots. The plume rise formulations are given in Appendix C, and the specification of deposition and settling velocities is discussed in Appendix D. A software plotting package is provided in Appendix E to display the wind field and puff trajectories for each simulation period.

ACKNOWLEDGEMENTS

This User's Guide to TRIAD 2.0 is partly based on an adaptation of the INPUFF 2.0 User's Guide prepared by W. B. Petersen and L. G. Lavdas (1986) for the U.S. Environmental Protection Agency. Several figures included here are reproduced from their report. The author expresses his appreciation to Mr. William Petersen of EPA for providing the INPUFF-2 computer program and User's Guide before their formal release to the public. Thanks are due to R. J. Dobosy and J. A. Herwehe of ATDD for their efforts in the development of the TRIAD computer program. Mary Rogers prepared the final copy of this report including expert typing of the equations.

SECTION I

INTRODUCTION

TRIAD is a Gaussian integrated puff model with a wide range of applications. The modeling scale may range from tens of meters to tens of kilometers. The model is capable of addressing the accidental release of a reactive substance over several minutes, or of modeling a typical non-reactive continuous plume from a stack. It can simulate moving point sources as well as stationary sources. TRIAD (version 2.0) is designed to optionally account for the parameterized effects of the exothermic fast reaction of gaseous uranium hexafluoride with atmospheric water vapor. In principle, other reactive substances also can be modeled in a similar fashion, if suitable parameterizations are available.

Computations in TRIAD can be made for multiple point sources at up to 100 receptor locations. In practice, however, the number of receptor locations should be kept to a minimum to avoid excessive run time. TRIAD is primarily designed to model a single event during which one meteorological transition period may occur, such as going from afternoon to evening conditions. Up to 144 separate meteorological periods of the same length may be used to characterize the meteorology during the event; this provides a time resolution that ranges from a few minutes to an hour. The user has the option of specifying the wind field for each meteorological period, observed at multiple stations (for interpolation by the model), or allowing the model to default to a homogeneous wind field.

Three dispersion algorithms are used within TRIAD for dispersion downwind of the source. The user may select the Pasquill-Gifford (P-G) scheme (Turner, 1970) or the on-site scheme (Irwin, 1983) for short travel time dispersion. The on-site scheme, which requires observations of the variances of the vertical and lateral wind velocity components, is a synthesis of work performed by Draxler (1976) and Cramer (1976). The long travel time scheme is the third dispersion algorithm, in which the growth of the puff becomes proportional to the square root of time. Optionally, the user can incorporate his or her own subroutine for estimating atmospheric dispersion.

TRIAD utilizes the deposition algorithms developed by Rao (1982). In the limit when pollutant settling and dry deposition velocities are zero, these expressions reduce to the familiar Gaussian puff-diffusion concentration algorithms.

This User's Guide gives the concentration algorithms, computational techniques, capabilities, assumptions, and limitations of the TRIAD model. The input data set is described and the data parameters are discussed.

SECTION II

MODEL OVERVIEW

TRIAD is capable of addressing the accidental release of a substance over a short time period, or of modeling the typical continuous plume from a stack. The implied modeling scale is from tens of meters to tens of kilometers. For a reactive substance, the consequences of an exothermic fast chemical reaction can be included in the initial puff specification. TRIAD (version 2.0) presently incorporates such parameterizations for UF_6. The three basic components of this model are as follows:

- Puff transport and dispersion based on INPUFF-2 model developed by Peterson and Lavdas (1986)
- Objective wind interpolation scheme based on MESOI-2 model developed by Ramsdell et al. (1983)
- Initial puff specification for UF_6, partly based on MMES plume/chemistry model developed by Just and Williams (1986)

The model has the capabilities to address the following:

- Single or multiple sources
- Stationary or moving point sources
- Temporally-variable source characteristics
- Wind speed extrapolation to effective release height
- Up to a maximum of 100 receptors
- Differences in ground elevations of source(s) and receptors
- Temporally and spatially variable wind field
- Objective interpolation of wind data from multiple towers
- Wind speed adjustment for different tower heights and elevations
- Calm or light wind conditions
- Some consideration of terrain effects through the wind field
- On-site or standard Pasquill-Gifford dispersion schemes

In order to increase its flexibility and range of application, TRIAD 2.0 allows the user to include the following technical options:

- Effects of fast exothermic chemical reactions
- Stack-tip downwash
- Buoyancy-induced dispersion
- Dry deposition and gravitational settling
- Source updates
- User-supplied dispersion parameters
- User-supplied plume rise schemes
- User-supplied wind field
- User-specified concentration units
- Intermediate concentration output
- Puff information output
- Output files for graphics display and model evaluation

TRIAD requires input data on user options, grid dimensions, sources, meteorology, receptors, and time scales. These data are specified on ten required and five optional card types as summarized below:

Card type	Input Data	Comments
1	Title of the run	Used for I/O identification
2	User options	Technical and I/O options are selected on this card
2A	Concentration units	Optional, if other than g/m^3
3	Model grid	Origin and size of model region
4	No. of meteor. periods, sources, and receptors	Total number (of each) in this run and length of each meteor. period
5	Receptor locations	Coordinates of each receptor are given on a separate card
5A	Format for winds	Optional, to write interpolated meteor. data on Unit 21
5B	Meteorological grid	Optional; information on meteor. grid, and anemometer sites
5C	Anemometer locations	Optional; coordinates, elevation, and ID of each meteor. station are given on a separate card
5D	Wind data	Optional; observed wind speed and direction at all met. stations for each sampling period are given
6	Physical processes	Technical options are selected
7	Time scales	Puff release and concentration averaging time scales, and nominal anemometer height are specified
8	Meteorology for source	Meteor. and dispersion parameters for each met. period are listed on a separate card
9	Source location, etc.	Source coordinates, update info., and deposition parameters are given
10	Source characteristics	Emission parameters are specified

Note that all optional card-types are denoted by a letter suffix. Cards 8 to 10 are within the source-loop and are repeated for each source in the simulation. Details of the input data preparation, units, and format requirements are given elsewhere in this Appendix.

For ease of reference, TRIAD prints out and briefly explains all I/O control parameters and technical options used in a run. Input data for meteorological conditions and sources are also listed. For each sampling period, calculated values of surface concentrations are printed at all of the receptors. At the end, the output lists the concentrations averaged over all of the sampling periods. TRIAD output also permits the following three file options:

(a) The interpolated U and V components of the optional gridded wind field are stored on Unit 21 according to the format specified by the user. This can be used with the graphics software (provided in Appendix E) to plot the transport wind field for each sampling period.

(b) The puff coordinates, sizes, and intermediate concentrations etc., are optionally stored on Unit 22. After the run, these data can be used with the graphics software included in Appendix E to plot the puff trajectory for each sampling period. The sequential plots of the wind fields and the corresponding puff trajectories can be used together to examine the plume path and the transport simulations. (See the illustrated examples in Appendix B).

(c) Unit 25 optionally stores the concentrations for all sampling periods in the run at each receptor. This format (which can be easily modified by the user if necessary) is most suitable for model evaluation, statistical analysis, and time-series and contour plots of concentrations, using the software packages readily available at most computer centers.

Every dispersion model is limited by the assumptions used to predict the atmospheric concentrations. Although TRIAD, which is based on Gaussian puff concepts, has several advantages over its continuous plume counterparts, it still has several key limitations, as listed below:

Wind direction is assumed constant with height
Puff transport is by winds at effective release height only
(This may be in error if strong subsidence occurs)
No explicit treatment of chemical reactions (only
parameterized effects are included)
No direct consideration of complex terrain effects (except
as reflected in the variable wind field data, and
adjustments for differences in elevations between
the source(s) and the receptors)
No consideration of building wake or cavity effects

The limitations of TRIAD are discussed along with the assumptions, as appropriate, in various sections of this report.

SECTION III

TECHNICAL DISCUSSION

The inclusion of the parameterized effects of fast chemical reactions in TRIAD has been discussed in the main report. This section gives the technical details of the puff dispersion model, INPUFF-2, developed by Petersen and Lavdas (1986), which is incorporated with several modifications in TRIAD.

GAUSSIAN PUFF METHODOLOGY

A graphical representation of the puff transport is given in Fig. A-1. Puffs A, B, and C represent the location of three emitted puffs at time t_3. Here puff A (the puff with the longest trajectory) was first exposed to east-southeast winds, followed by slightly stronger winds from the south and then the south-southeast. Puff B was released at the time the winds shifted from east-southeast to south. Puff C was released when winds were from the south-southeast. The stability conditions may vary from one time step to the next, although this feature is not illustrated in the figure, (i.e., the rate of puff growth is constant over the entire interval). INPUFF (and hence TRIAD) assumes $\sigma_x = \sigma_y$; thus puffs remain circular throughout their lifetime.

In Gaussian-puff algorithms, source emissions are treated as a series of puffs emitted into the atmosphere. Constant conditions of wind and atmospheric stability are assumed during a time step. The diffusion parameters are functions of travel time. During each time step, the puff centers are determined by the trajectory and the in-puff distributions are assumed to be Gaussian. Thus, each puff has a center and a volume which are determined separately by the mean wind, atmospheric stability, and travel time.

The concentration, C, of a pollutant at (x,y,z) from an instantaneous puff release having mass Q at an effective emission height, H, is given by the equation:

$$C(x,y,z,H) = \frac{Q}{(2\pi)^{3/2}\sigma_x\sigma_y\sigma_z} \exp\left[\frac{-1}{2}\left(\frac{x-ut}{\sigma_x}\right)^2\right] \exp\left[-\frac{1}{2}\left(\frac{y}{\sigma_y}\right)^2\right]$$

$$\left\{ \exp\left[\frac{-1}{2}\left(\frac{z+H}{\sigma_z}\right)^2\right] + \exp\left[\frac{-1}{2}\left(\frac{z-H}{\sigma_z}\right)^2\right] \right\} \quad \text{(A-1)}$$

Since each puff is free to move in response to changing wind speed, u, and is not constrained to a single centerline, the diffusion parameters are given as functions of travel time, t, rather than of downwind distance.

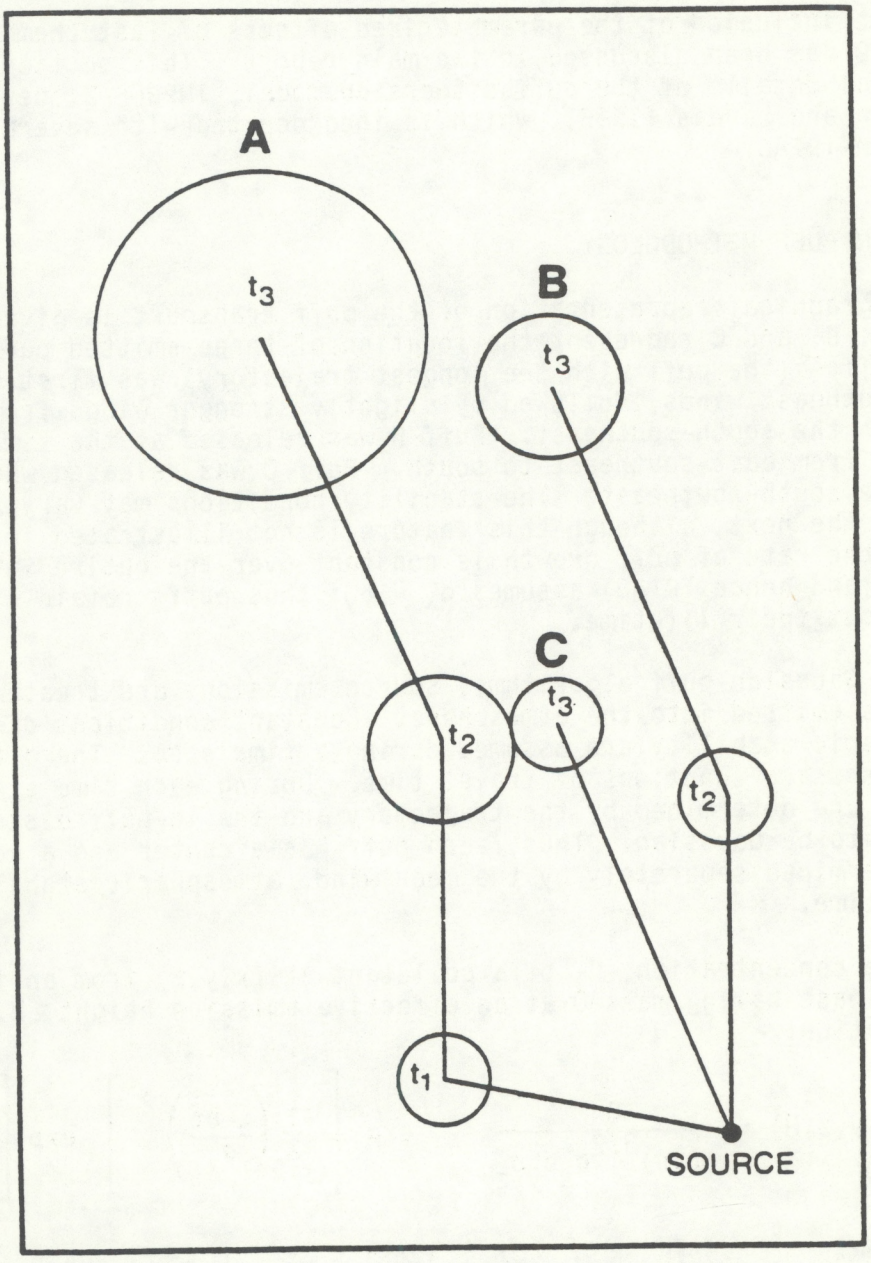

Figure A-1. Gaussian puff model.

Following the puff and assuming $\sigma_x = \sigma_y = \sigma_r$, where $r^2 = (x-ut)^2 + y^2$, the puff equation can be rewritten as follows:

$$C(r,z,H) = \frac{Q}{(2\pi)^{3/2}\sigma_r^2\,\sigma_z} \exp\left[\frac{-1}{2}\left(\frac{r}{\sigma_r}\right)^2\right]$$

$$\left\{\exp\left[\frac{-1}{2}\left(\frac{z+H}{\sigma_z}\right)^2\right] + \exp\left[\frac{-1}{2}\left(\frac{z-H}{\sigma_z}\right)^2\right]\right\} \qquad \text{(A-2)}$$

When σ_z becomes larger than 80% of the mixed layer depth, L, the puff is assumed to be well mixed and the concentration equation is expressed as

$$C(r,z,H) = \frac{Q}{2\pi\sigma_r^2 L} \exp\left[\frac{-1}{2}\left(\frac{r}{\sigma_r}\right)^2\right] \quad \text{for } \sigma_z > 0.8\ L \qquad \text{(A-3)}$$

The contributions from all the puffs are summed at each receptor after each time step.

Although a Gaussian-puff model, such as INPUFF-2 and TRIAD, is useful for estimating pollution dispersion under unsteady and nonuniform flow, it has several limitations:

(1) Pollution dispersion within the puff is assumed to be Gaussian, and meteorological conditions within a time step are assumed to be spatially and temporally uniform. These assumptions may cause significant errors in estimating concentrations, especially at long travel distances.

(2) The diffused material is assumed to be stable over a long period of time. Chemical reactions are not explicitly treated during transport.

(3) Data for puff diffusion are sparse and there is no readily-available ordering of the sigma curves by stability; therefore, many Gaussian-puff models use plume sigmas. However, similarity theory for puff diffusion (Batchelor, 1953) suggests that there is a region in which puff growth is greater than plume growth. For downwind distances where travel time is larger than sampling time, the use of plume sigmas in a puff model may be inappropriate. However, as long as the variations in meteorological conditions are not simulated to any finer resolution than 3 to 10 minute periods, the use of plume-type characterization of dispersion may still be reasonable.

(4) Plume diffusion formulas apply to continuous plumes, where the sampling time is long compared to the travel time from source to receptor. Since INPUFF and TRIAD use plume-derived sigmas, one would expect that the concentration estimates from INPUFF or TRIAD would yield the best agreement with observations if the travel time was short compared to the averaging time of the concentration estimates. Since this condition does not hold, the model estimates are more appropriately viewed as the average of many

realizations of the same experiment; this recognizes that any given experiment may differ greatly from the average obtained over many experiments.

(5) Given the complex nature of the wind field, sampling the flow so that it can be completely defined from a mathematical point of view is impossible. There can be many solutions which could stem from one initial state, while satisfying most other requirements.

A major difference between Gaussian-plume models and INPUFF or TRIAD is that INPUFF and TRIAD can account for changing meteorological conditions, whereas typical Gaussian-plume models assume spatial and temporal uniformity in the meteorology. Perhaps even more important, INPUFF and TRIAD can handle light or calm wind conditions and can partly account for terrain effects by using observed wind fields. This is not the case with straight-line Gaussian plume models, which only use the winds at the source and exhibit a singularity for zero wind speed.

PLUME RISE

Plume rise from point sources is calculated using the formulations of Briggs (1969, 1971, 1973, 1975). Although plume rise is usually dominated by buoyancy, plume rise due to momentum is also considered. Stack-tip downwash (optional) can be considered, following Briggs (1973). Use of this option primarily affects computations from stacks having small ratios of exit velocity to wind speed. Building downwash and gradual plume rise are not treated by INPUFF or TRIAD. Only the final rise equations are summarized below. The reader is referred to Appendix C for details on the plume rise formulations and the crossover techniques between momentum and buoyancy.

For unstable or neutral atmospheric conditions, the downwind distance of final plume rise is

$$x_f = 3.5\ x^*,$$

where

$$x^* = 14\ F^{5/8} \qquad \text{for } F < 55\ m^4/s^3.$$

and

$$x^* = 34\ F^{2/5} \qquad \text{for } F \geq 55\ m^4/s^3.$$

The effective plume height under these conditions is

$$H = h' + [1.6\ F^{1/3}\ (3.5x^*)^{2/3}]/u(h) \qquad \text{(A-4)}$$

For stable atmospheric conditions, the downwind distance of final plume rise is

$$x_f = 0.0020715\ u(h)\ s^{-1/2}$$

where

$$s = g\ (\partial\theta/\partial z)/T.$$

The effective plume height is given for windy conditions by

$$H = h' + 2.6\ \{F/[u(h)s]\}^{1/3} \qquad \text{(A-5)}$$

and for near-calm conditions by

$$H = h' + 4\ F^{1/4} s^{-3/8} \qquad \text{(A-6)}$$

The lower of the two values obtained from Eqs. (A-5) and (A-6) is taken as the final plume height under stable conditions. Definitions and units of variables mentioned in this section are summarized in Table A-1.

Table A-1. Definition of variables used in plume rise equations.

Symbol	Definition	Units
F	Buoyancy flux parameter	m^4/s^3
g	Acceleration due to gravity	m/s^2
H	Effective height of plume	m
h'	Stack height adjusted for stack downwash	m
s	Stability parameter	s^{-2}
T	Ambient air temperature	K
θ	Potential temperature	K
u(h)	Wind speed at stack top	m/s
x_f	Distance to final rise	m
x*	Distance at which atmospheric turbulence begins to dominate entrainment	m

DISPERSION ALGORITHMS

Three dispersion algorithms are used within INPUFF (and hence TRIAD) for dispersion downwind of the source:

P-G scheme as discussed by Turner (1970)
On-site scheme formulated by Irwin (1983)
Long travel time scheme.

The user has the option of choosing either the P-G or the on-site algorithm

(for short travel-time dispersion) and specifying when the long travel-time dispersion parameters are to be utilized. Optionally, a user-supplied subroutine can be used to estimate dispersion.

Dispersion downwind of a source, as characterized by the P-G scheme, is a function of stability class and downwind distance. Stability categories are commonly specified in terms of wind speed and solar radiation. The on-site dispersion algorithms, which characterize dispersion as a function of travel time, require specification of standard deviations of the vertical and lateral wind directions. The third dispersion scheme is used, in combination with the other two, for long travel times in which the growth of the puff is proportional to the square root of time.

The primary purpose of the integrated puff model is to simulate a continuous or semi-continuous plume for varying meteorological conditions. The vertical and lateral dispersion parameters for continuous plume dispersion models are used in INPUFF and TRIAD. Under steady and spatially uniform meteorological conditions, the output concentrations of INPUFF should, all other factors such as plume rise being equal, approximate the results calculated by a Gaussian-plume model.

INPUFF and TRIAD include three dispersion regimes to account for initial dispersion, short travel-time dispersion, and long travel-time dispersion.

Initial Dispersion

The finite size of the release at the source is modeled by specifying the initial horizontal and vertical dispersion parameters, σ_{ro} and σ_{zo}. (The increase in these parameters due to the exothermic heat released by the near-instantaneous reaction of UF_6 with atmospheric water vapor is also considered here, as discussed in Section 6). For tall stacks, these parameters generally have little influence on downwind concentrations. However, if the source is large or close to the ground, then its initial size is important in determining ground level concentrations near the source. For a source near the ground, the initial horizontal dispersion can be calculated by dividing the horizontal dimension of the source by 4.3, and the initial vertical dispersion parameter is derived by dividing the height of the source by 2.15. This method of accounting for the initial size of a release near ground level gives reasonable concentration estimates at downwind distances greater than about five times the initial horizontal dimension of the source.

Buoyancy-Induced Dispersion

The buoyancy-induced dispersion feature is offered because emitted plumes undergo a certain amount of growth during the plume rise phase, due to the turbulence associated with the buoyant conditions of plume release and the turbulent entrainment of ambient air. Pasquill (1976) suggests that this induced dispersion, σ_{zb}, can be approximated by $\Delta H/3.5$, and the effective dispersion can be determined by adding variances, i.e.,

$$\sigma_{ze} = (\sigma_z^2 + \sigma_{zb}^2)^{1/2}$$

where σ_{ze} is the effective dispersion and σ_z is the dispersion due to ambient turbulence. At the distance of final rise and beyond, σ_{zb} becomes a constant using the value of ΔH at final rise. At distances closer to the source, the ΔH used to determine σ_{zb} is determined using gradual rise equations.

Since in the initial growth phases of the release the plume is nearly symmetrical about its centerline, buoyancy-induced dispersion in the horizontal direction is assumed equal to that in the vertical, i.e., $\sigma_{rb} = \Delta H/3.5$. This expression is combined with that for dispersion due to ambient turbulence in the same manner as shown above for the vertical.

In general, buoyancy-induced dispersion will have little effect upon maximum concentrations unless the stack height is small compared to the plume rise. Also, it is most effective in simulating concentrations near plume centerline close to the source, where treating the emission as a point source confines the plume to a volume much smaller than the actual plume. It should be clarified here that the buoyancy-induced dispersion close to the source is calculated in INPUFF and TRIAD, using gradual rise equations, even though the latter equations are not being used to determine the effective plume height.

Short Travel Time Dispersion

Dispersion downwind of the source can be characterized by the P-G scheme, which is a function of stability class and downwind distance, or by the on-site scheme, which is a function of travel time.

Pasquill-Gifford Scheme

The P-G sigma values applicable to areas characterized as rural are used in the model. However, for neutral atmospheric conditions two dispersion curves as suggested by Pasquill (1961) are incorporated into the model. Dispersion curves D1 and D2 are appropriate for adiabatic and subadiabatic conditions, respectively. The D2 curve is used in Turner (1970) for neutral conditions. From a practical point of view, since temperature soundings may not be available, we refer to the D1 and D2 curves as D-day and D-night. P-G stability classes are specified by numerical values in the puff model. Stability classes A through D-day are designated as 1-4, and classes D-night through F are designated as 5-7.

On-site Meteorology Scheme

The sigma curves of the P-G scheme above are based on data from releases near ground level in short-range dispersion studies. However, the P-G curves have also been applied to elevated releases over long range in violation of the conditions of their derivation. INPUFF and TRIAD provide an option of using on-site meteorological data, where available, for a more defensible estimate of dispersion. This scheme is a result of the recommendations of the American Meteorological Society's workshop on stability classification schemes and sigma curves (Hanna et al., 1977).

Irwin (1983) proposed characterizing σ_y and σ_z in a manner similar to Cramer (1976) and Draxler (1976). The standard deviation of the crosswind concentration distribution, σ_y, is

$$\sigma_y = \sigma_v \, t \, f_y \qquad \text{(A-7)}$$

where σ_v is the standard deviation of the horizontal crosswind component of the wind velocity, t is the travel time of the pollutant, and f_y is a nondimensional function of travel time. The standard deviation of the vertical concentration distribution, σ_z, for an elevated source, when σ_z is less than the source height, is

$$\sigma_z = \sigma_w \, t \, f_z \qquad \text{(A-8)}$$

where σ_w is the standard deviation of the vertical component of the wind velocity, and f_z is a nondimensional function, primarily dependent upon travel time. The nondimensional functions f_y and f_z are given by Irwin (1983) as

$$f_y = 1 \,/[1 + 0.9(t/1000)^{1/2}] \qquad \text{(A-9)}$$

$$f_z = 1 \qquad \text{for unstable conditions}$$

and

$$f_z = 1 \,/[1 + 0.9(t/50)^{1/2}] \qquad \text{for stable conditions} \qquad \text{(A-10)}$$

Besides the P-G stability class, the scheme requires σ_v and σ_w, which are assumed to be typical of conditions at final plume height. For small angles, $\sigma_v = \sigma_\theta . u$ and $\sigma_w = \sigma_\phi . u$ where u is the wind speed at measurement height and σ_θ and σ_ϕ are the standard deviations of the horizontal and vertical wind angles, respectively. The puff model requires σ_θ and σ_ϕ as data input and computes σ_v and σ_w.

Some guidance for specifying σ_θ and σ_ϕ for dispersion over flat terrain can be found in the literature (see, e.g., Gifford, 1976, and Hanna et al., 1982). These values (generally taken to be hourly averages at 10 m height), based on the Pasquill stability classes A to F, can be given as follows:

		σ_θ (deg)	σ_ϕ (deg)
Very unstable	A	25	10
Moderately unstable	B	20	8
Slightly unstable	C	15	6.5
Neutral (day)	DD	10	5.5
Neutral (night)	DN	10	4.5
Slightly stable	E	5	2.5
Moderately stable	F	2.5	1

It should be emphasized that these values (especially σ_ϕ) are only approximate, and this system should not be considered perfect. In complex terrain, σ_θ values in stable conditions are known to be much larger than those given above (see, e.g., Panofsky and Dutton, 1984); for light winds (less than 1.5 m/s) at night, σ_θ shows large variability due to plume meander resulting from large eddies. For shorter meteorological averaging periods (5 to 15 min), part of this meander may be reflected in the meaured wind field. For distances greater than 10 km, and effective release heights of above 100 m, the values given above may not be appropriate. For these reasons, direct on-site turbulence measurements and their theoretical extrapolations are recommended for most real-world applications.

Long Travel Time Dispersion

It is desirable that the dispersion parameters used in INPUFF (and TRIAD) satisfy the diffusion theory developed by Taylor (1921). Taylor showed that for an ensemble average of particle displacement during stationary and homogeneous conditions, the dispersion parameters can be written as,

$$\sigma_y^2 = 2\overline{v'^2} \int_0^{T_d} \int_0^t R(\tau)d\tau dt, \qquad \text{(A-11)}$$

where $R(\tau)$ is the Lagrangian autocorrelation, $\overline{v'^2}$ is the variance of the lateral component of the wind velocity fluctuation, and T_d is the diffusion time. In an analogous equation for vertical diffusion, $\overline{w'^2}$ is used instead of $\overline{v'^2}$. The autocorrelation starts at 1 and approaches 0 for large diffusion time. Therefore, from Eq.(A-11), while the growth of the puff is linear with time near the source, the growth becomes proportional to the square root of time at large distances. In the model, after the puff has attained a specified horizontal dimension, the algorithm automatically goes to a long travel time growth rate proportional to the square root of time. The size of the puff at that time, SYMAX, is specified by the user. For example, the user may decide that when σ_r for the puff is greater than 1000 meters, the long travel time dispersion parameters should be utilized. A very large SYMAX value causes the long travel time dispersion option to be bypassed.

MIXING HEIGHT

Depending on the stack height, plume rise, and height of the mixing layer, the puffs can be above or below the mixed depth layer, L. If the puffs are above L, then there are two cases that govern their growth. Initially the puffs are allowed to grow as for P-G stability class F, or if the on-site scheme is used, the puffs are restricted to a vertical growth rate characterized by $\sigma_w = 0.01$/sec. After the puffs attain a given size of σ_r (not actual puff size) specified by the user, the horizontal growth is proportional to $t^{1/2}$.

When the puffs are below L, then there are four cases that must be considered. Cases one and two describe puffs which are not well mixed vertically and whose growth rates are characterized either by the short travel time sigmas or by $t^{1/2}$. Cases three and four describe puffs that are well mixed vertically and whose growth for σ_r is either for short travel times or according to $t^{1/2}$. During the modeling simulation, every puff is given a "key" to indicate whether it is above or below L and whether its growth rate is characterized by the short-travel-time sigmas or by $t^{1/2}$.

In the modeling design, puffs are allowed to change their dispersion keys. When the height of L becomes greater than the puff height, the puffs are allowed to grow at the rate characterized by surface measurements. Normally this is a neutral or unstable situation. This transition period is likely to occur in the morning hours. In the afternoon, despite the decay of active mixing, a puff remains well mixed through the maximum mixing lid as shown in Fig. A-2. The maximum height of L is stored for each puff and is never allowed to decrease. This method assures that concentration does not increase with downwind distance or travel time in violation of physical laws.

ATMOSPHERIC STABILITY

As discussed earlier, short travel time dispersion can be characterized by two schemes, the P-G scheme and the on-site scheme. The P-G scheme uses the empirical P-G curves and a stability classification to estimate dispersion coefficients (Turner, 1970), whereas the on-site scheme relates diffusion directly to turbulence. If on-site meteorological data are not available, only the widely used P-G scheme can be adopted. If on-site meteorological data are available, and reliable, either scheme can be used, although the on-site scheme is recommended on scientific grounds.

INPUFF's on-site scheme adopts Irwin's algorithms (1983) in characterizing σ_y and σ_z. This scheme requires information on the standard deviations of horizontal (σ_θ) and vertical (σ_ϕ) wind direction fluctuations and wind speed at measurement height. Stability is classified as stable or unstable using the near-surface data for temperature difference, Richardson number, or an appropriate stability parameter.

GRAVITATIONAL SETTLING AND DRY DEPOSITION

Rao (1982) gave analytical solutions of a gradient-transfer model for atmospheric concentrations of a gaseous or suspended particulate pollutant, incorporating dry deposition and gravitational settling of pollutants from a plume. These solutions treat pollutant removal processes in a physically realistic manner and are subject to the same basic assumptions and limitations associated with Gaussian plume-type models. His equations for deposition and settling were incorporated in several EPA air quality models including PAL-DS (Rao and Snodgrass, 1982). The equations used in INPUFF are the same as those used in PAL-DS, except in INPUFF they are cast in terms of travel time instead of wind speed and downwind distance. The reader is referred to Rao's (1982) report for a comprehensive review of plume deposition models and details of derivation of the concentration

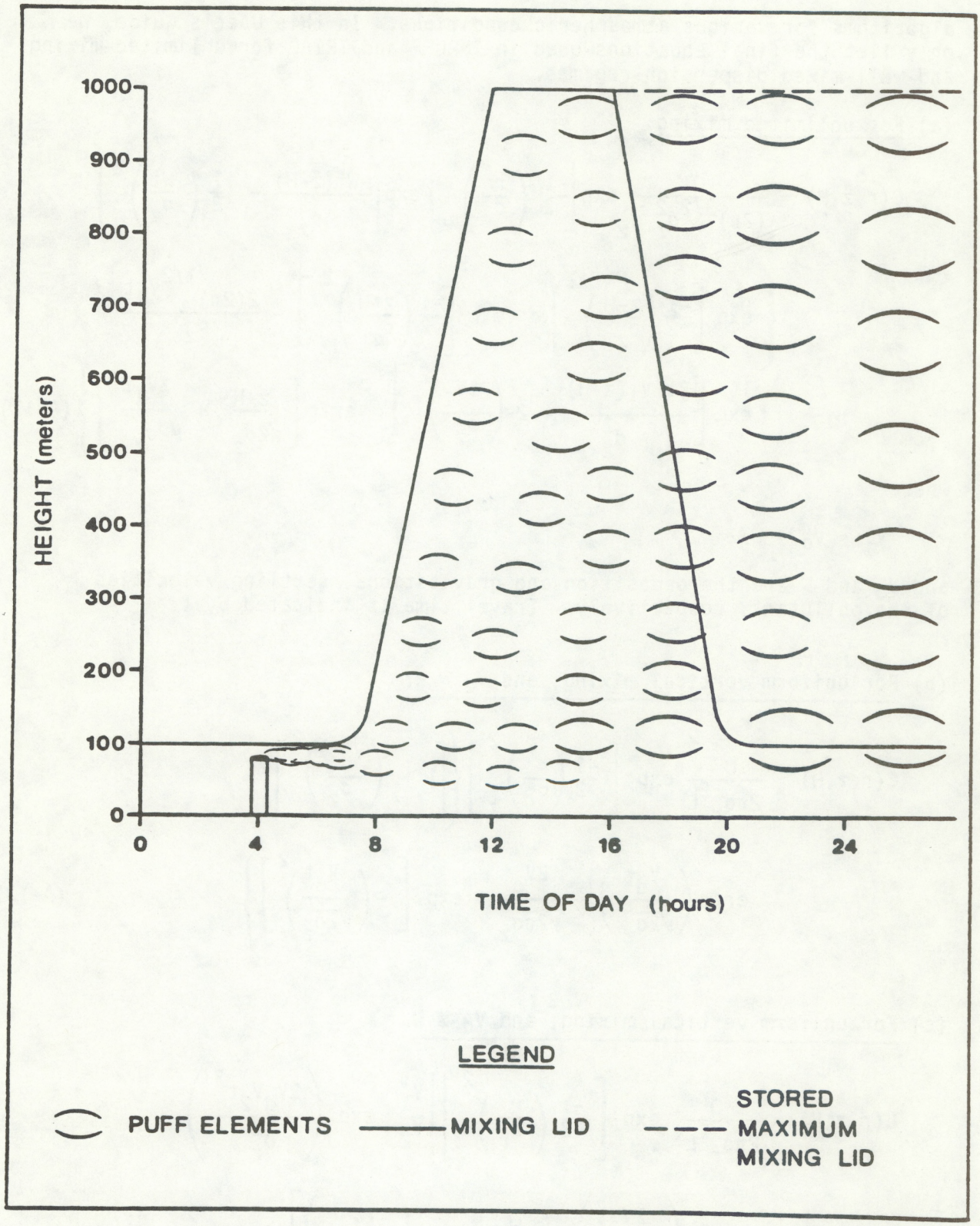

Figure A-2. Effect of variable mixing height on puff dispersion.

algorithms for various atmospheric conditions. In this User's Guide, we only list the final equations used in INPUFF and TRIAD for unlimited-mixing and well-mixed dispersion regimes.

(a) For unlimited mixing:

$$C(r,z,H) = \frac{Q}{(2\pi)^{3/2}\sigma_r^2\,\sigma_z}\exp\left[\frac{-1}{2}\left(\frac{r}{\sigma_r}\right)^2\right]\exp\left[\frac{-Wt(z-H)}{\sigma_z^2} - \frac{1}{2}\left(\frac{Wt}{\sigma_z}\right)^2\right]$$

$$\left\{\exp\left[\frac{-1}{2}\left(\frac{z-H}{\sigma_z}\right)^2\right] + \exp\left[\frac{-1}{2}\left(\frac{z+H}{\sigma_z}\right)^2\right] - \frac{2(2\pi)^{1/2}V_1 t}{\sigma_z}\right.$$

$$\left.\exp\left[\frac{2t\,V_1(z+H)}{\sigma_z^2} + 2\left(\frac{tV_1}{\sigma_z}\right)^2\right]\ \operatorname{erfc}\left[\frac{z+H}{\sqrt{2}\sigma_z} + \frac{2V_1 t}{\sqrt{2}\sigma_z}\right]\right\} \quad \text{(A-12)}$$

where

$$V_1 = V_d - W/2$$

and V_d and W are the deposition and gravitational settling velocities of the pollutant, respectively. Travel time is indicated by t.

(b) For uniform vertical mixing, and $V_d = W$:

$$C(r,z,H) = \frac{Q}{2\pi\sigma_r^2 L}\exp\left[\frac{-1}{2}\left(\frac{r}{\sigma_r}\right)^2\right]\left\{\left[1 + \left(\frac{V_d t}{\sigma_z}\right)^2\right]\right.$$

$$\left.\operatorname{erfc}\left(\frac{V_d t}{\sqrt{2}\sigma_z}\right) - \frac{2V_d t}{\sqrt{2\pi}\sigma_z}\exp\left[-\left(\frac{V_d t}{\sqrt{2}\sigma_z}\right)^2\right]\right\} \quad \text{(A-13)}$$

(c) For uniform vertical mixing, and $V_d \neq W$.

$$C(r,z,H) = \frac{Q}{2\pi\sigma_r^2 L}\exp\left[\frac{-1}{2}\left(\frac{r}{\sigma_r}\right)^2\right]\left[\frac{V_1}{V_2}\exp\left(\frac{2V_d V_2 t^2}{\sigma_z^2}\right)\right.$$

$$\left.\operatorname{erfc}\left(\frac{2V_1 t}{\sqrt{2}\sigma_z}\right) - \frac{W}{2V_2}\operatorname{erfc}\left(\frac{Wt}{\sqrt{2}\sigma_z}\right)\right] \quad \text{(A-14)}$$

where $V_2 = V_d - W$.

The above equations reduce to the corresponding Gaussian puff equations without deposition when $V_d = 0$ and $W = 0$. Appendix D provides information on specifying the deposition and settling velocities.

WIND FIELD AND MODELING GRIDS

To use gridded wind data, INPUFF requires a meteorological preprocessor to compute wind speed and direction in each grid square. The wind interpolation routine incorporated in TRIAD is described in Section 6. The location, grid spacing, and overall size of the meteorological region must be defined in the input. The modeling region, also defined in the input, need not be the same as the meteorological region. If the meteorological region is smaller than the modeling region and the puffs travel outside of the meteorological region, then they are advected according to the wind speed and direction at the closest grid point. If the meteorological region is larger than the modeling region and the puffs travel outside the modeling region, they are eliminated from further consideration. The source must stay within the modeling region; otherwise, all puffs are eliminated.

To improve the spatial resolution of the concentrations, receptors in INPUFF are specified by the user. The resolution of the receptors can be more detailed than that of the meteorological grid. The receptors may be placed independent of the meteorological grid. Figure A-3 illustrates a possible arrangement of the modeling region, meteorological grid, and receptor locations. In this example, the receptors are concentrated along part of the puff trajectory with a spatial resolution twice as fine as the meteorological grid.

EXAMPLES OF MODEL CAPABILITIES

Three example problems given in the INPUFF-2 User's Guide are included here to illustrate different modeling scenarios and to demonstrate several unique features of INPUFF. For I/O listings of the first two example problems, the reader should consult the report by Petersen and Lavdas (1986).

(a) Example 1 -- Moving Source

This example uses a unique feature of INPUFF that allows the source to move at a constant speed and direction over a specified time. Figure A-4 shows the source path and receptor locations. The source is initially southwest of the receptors and travels due east at 2 m/s for twenty minutes, while remaining south of all receptors. Southerly winds at 3.5 m/s are observed and the atmosphere is slightly unstable (P-G class C). Twenty minutes into the simulation the source assumes a northeast heading at the same speed. Atmospheric conditions become neutral, (P-G class, D-day) wind speed increases to 4 m/s, and wind direction changes slightly from 180 to 170 deg. The stack parameters of the source are as follows:

Emission rate -- 600 g/s
Stack height -- 30 m

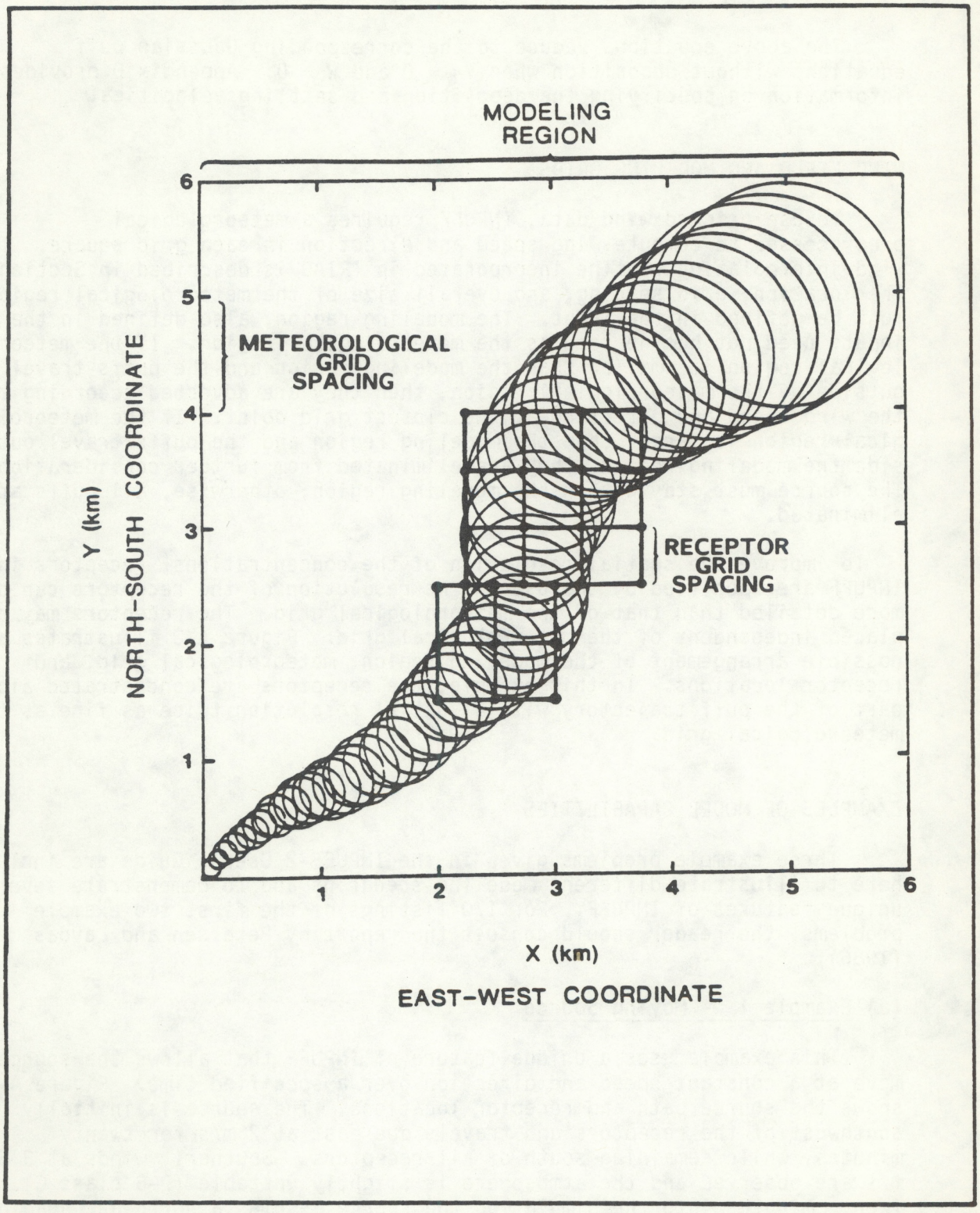

Figure A-3. A possible arrangement of modeling and receptor grids.

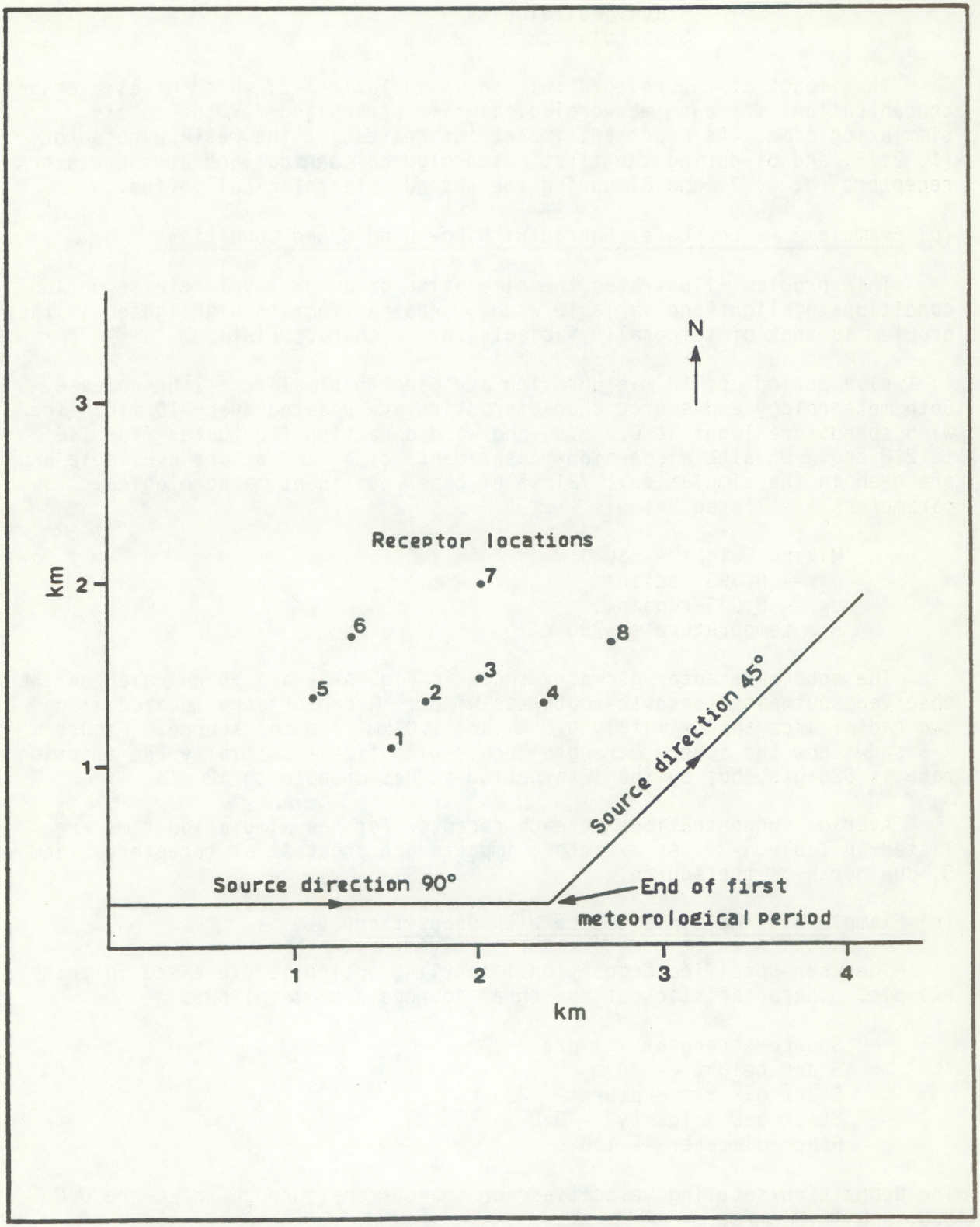

Figure A-4. Source path for example 1.

Stack gas temperature -- 390 K
Stack gas velocity -- 15 m/s
Stack diameter -- 2 m

The impact at the receptors is shown in Table A-2, which gives average concentrations for each meteorological time period and for the total simulation time. As expected, impact is greatest at the western receptors (1, 2, 5, and 6) during the first meteorological period, and at the eastern receptors (3, 4, 7, and 8) during the second meteorological period.

(b) Example 2 -- Low Level Source With Low Wind Speed Conditions

This problem illustrates the simulation of a low level release during conditions of light and variable winds. Another feature highlighted in the problem is that of temporally variable source characteristics.

Twelve periods of 10 min duration are used to simulate a 2 hr release. Both meteorology and source characteristics are updated every 10 min. The wind speeds are light at 0.5 m/s, and wind direction fluctuates from 145 to 210 deg. On-site dispersion measurements of σ_a and σ_e are available and are used in the simulation. Values of other pertinent meteorological parameters are listed below:

Mixing height -- 5000 m
σ_a -- 0.393 radians
σ_e -- 0.035 radians
Air temperature -- 290 K

The source-receptor geometry shown in Fig. A-5 was chosen based on the observed southeast to south-southwest winds. Receptors are located along two radial arcs approximately 0.5 km and 1.0 km from the source. Figure A-6 shows how the source strength decays with time. Initially the emission rate is 825 g/s, but by the 12th period it has dropped to 12 g/s.

Average concentrations at each receptor for the simulation time are listed in Table A-3. As expected, impacts are greatest at receptors 3 and 8, due north of the source.

(c) Example 3 -- Multiple Source With Deposition

The user-specified depositional settling option is exercised in this example. Characteristics of the three sources are as follows:

Source strength -- 1 g/s
Stack height -- 30 m
Stack gas temperature -- 293 K
Stack gas velocity -- 0.0
Stack diameter -- 1.0

The deposition/settling velocities for sources one through three are 0.0, 5.0, and 10.0 cm/s.

The hourly meteorological data remain the same through the run. Pasquill-Gifford sigma curves are used with stability class D-night

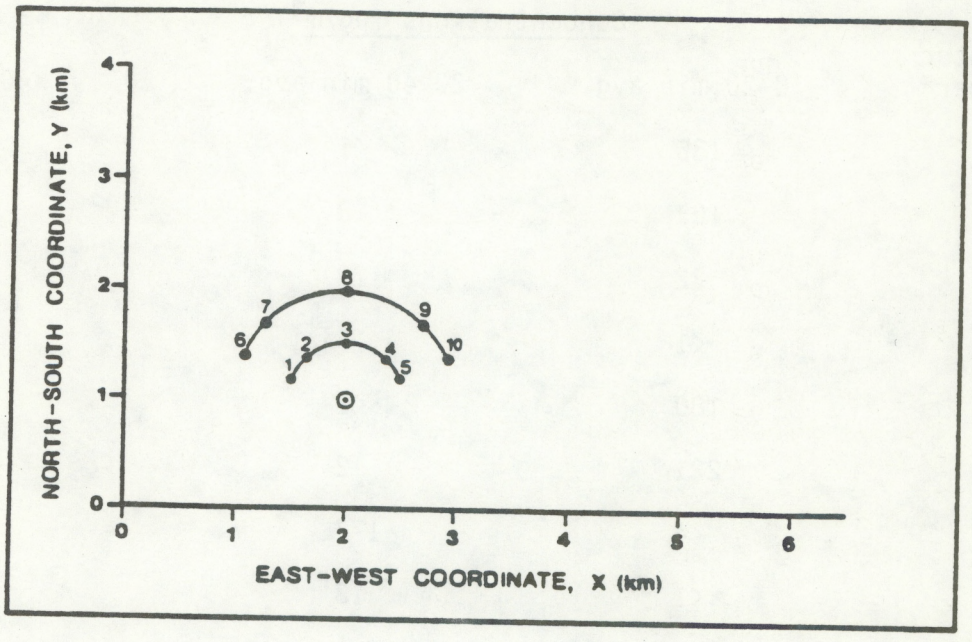

Figure A-5. Source-receptor geometry for example 2.

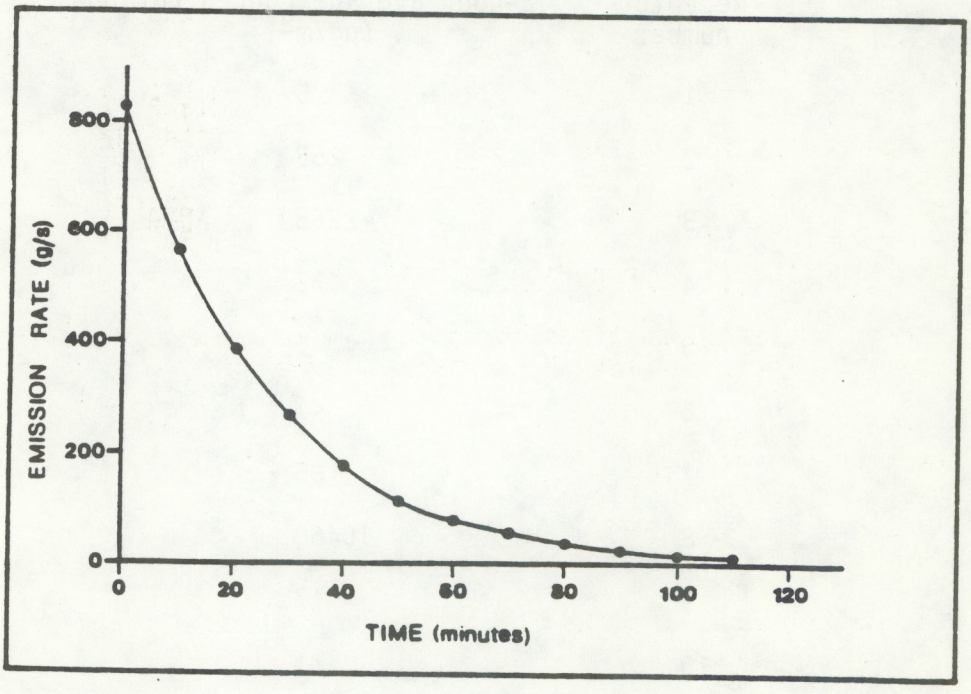

Figure A-6. Emission rate versus time plot for example 2.

Table A-2. Computed concentrations for example 1.

Receptor number	Concentrations ($\mu g/m^3$) 0-20 min avg.	20-40 min avg.	40 min avg.
1	135	<1	68
2	167	8	87
3	22	123	72
4	<1	13	7
5	180	<1	90
6	221	2	111
7	4	177	90
8	<1	13	6

Table A-3. Computed concentrations for example 2.

Receptor number	2-hour average concentrations ($\mu g/m^3$)
1	5
2	253
3	2268
4	132
5	1
6	<1
7	96
8	10460
9	17
10	<1

(KST=5). In effect the results are comparable to Figure 1 in Rao (1982). That figure has been reproduced here (see Fig. A-7) to demonstrate that INPUFF gives essentially the same result as PAL-DS for the same input conditions. The greatest differences occur for short travel distances, with excellent agreement between the two models for travel distances at and beyond the distance of maximum concentrations.

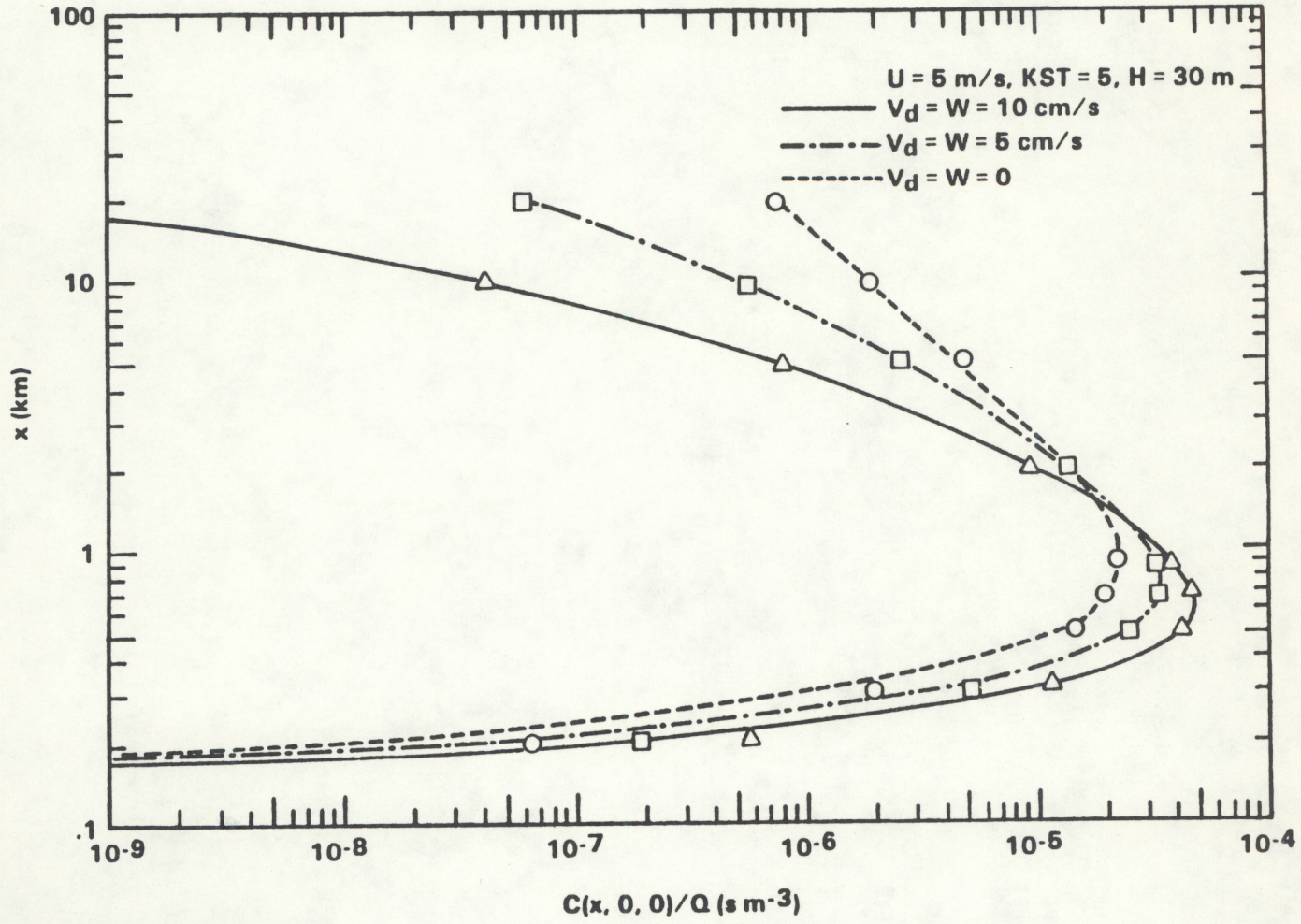

Figure A-7. Variation of plume-centerline surface concentration comparing INPUFF results with those of PAL-DS. INPUFF estimates are indicated by the symbols, PAL-DS by the curves.

SECTION IV

TRIAD COMPUTER PROGRAM

This section discusses the general framework of TRIAD to give the reader an overview of the computer program. The general flow and structure of TRIAD, and a brief description of each subroutine and function are included.

The following types of information are needed by the TRIAD model:

Options to be exercised during program execution
Simulation information and puff characteristics
Specifications of the modeling and meteorological grids
Anemometer locations and wind data
Source locations and characteristics
Receptor coordinates
Meteorological data.

TRIAD is a multiple source model that permits source characteristics to be updated at time steps evenly divisible into the meteorological period. The meteorology in the model can be specified by up to 144 equal length meteorological periods. Concentration estimates can be made for 100 locations.

PROGRAM STRUCTURE

Figure A-8 shows the structure of the subroutines and functions. TRIAD is the main routine that initializes the puffs and stores the appropriate data in common with the other subroutines. Subroutines that begin with the letter "R" read input data. A brief description of the main program, subroutines, and functions follows the figure. Table A-4 shows the input/output units used by TRIAD:

Table A-4. Input/output units.

Unit number	Mode	Contents
5	Input	Program control and input data
6 (IW)	Output	Output listing
21	Output	Output interpolated wind-field data (if used) for plots and analysis
22	Output	Output puff-trajectory and other data from main program for plots
25	Output	Output concentration data from main program for model evaluation, plots, and analysis.

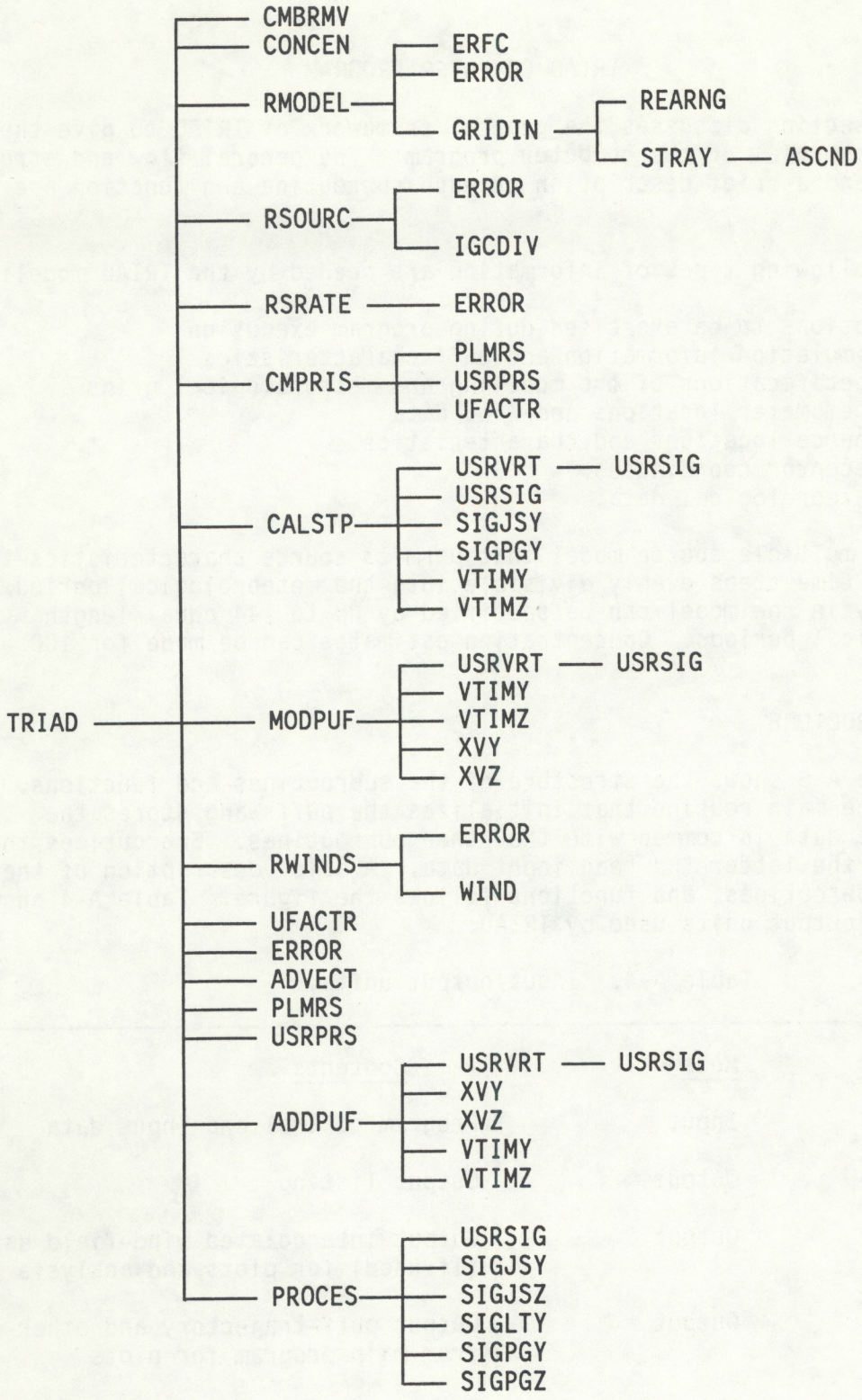

Figure A-8. Structure of TRIAD.

PROGRAM MODULES

TRIAD -- TRIAD is the main program that performs puff initialization. The following subroutines and functions are called by TRIAD: CMBRMV, CONCEN, RMODEL, RSOURC, RSRATE, CMPRIS, CALSTP, MODPUF, RWINDS, UFACTR, ERROR, ADVECT, PLMRS, USRPRS, ADDPUF, and PROCES. INPUFF prints out the input data and the concentration estimates at each receptor for each time period.

ADDPUF -- ADDPUF assigns most of the characteristics of a new puff. Subroutines USRVRT and USRSIG and functions XVY, XVZ, VTIMY, and VTIMZ are called by ADDPUF.

ADVECT -- This subroutine is called by TRIAD if the user-supplied wind feld option is exercised (i.e., LADT = TRUE). ADVECT computes the appropriate wind speed and direction for each puff.

ASCND -- This subroutine arranges meteorological stations in ascending order by distance from a given grid point. This is called by subroutine STRAY.

CALSTP -- This routine is called only if the input value for ISTEP is negative. The puff release rate and criteria for puff combination are determined in CALSTP. Subroutines USRVRT, and USRSIG and functions SIGJSY, SIGPGY, VTIMY, and XVY are called by CALSTP.

CMBRMV -- This subroutine combines and removes puffs.

CMPRIS -- This routine calculates the components of the wind and source motion (if source is moving). CMPRIS calls subroutines PLMRS, USRPRS, and function UFACTR.

CONCEN -- This subroutine is called by TRIAD and computes the concentration from each puff for each receptor location. The equations for deposition and gravitational settling are in this routine. CONCEN calls function ERFC.

EFRC -- This function calculates the complimentary error function of X, using rational Chebyshev approximations. It is called by CONCEN.

ERROR -- This routine produces error messages.

GRIDIN -- This routine is called by subroutine RMODEL if a user-supplied wind field is used (LADT=TRUE). It sets up meteorological grid and anemometer stations. GRIDIN calls subroutines REARNG and STRAY.

IGCDIV -- This function determines the greatest common divisor between two arguments. It is called by RSOURC subroutine.

MODPUF -- MODPUF updates KEYP values and virtual distances (times) as necessary for existing puffs. MODPUF calls subroutines USRVRT and USRSIG and functions VTIMY, VTIMZ, XVY, and XVZ.

PLMRS -- This routine calculates final plume rise using Briggs' equations.

PROCES -- Called directly by TRIAD, the major functions of PROCES are to determine which dispersion routine is called for each puff, assign dispersion keys (KEYP) for each puff, and account for the effect of the mixed depth layer for each puff. PROCES calls subroutine USRSIG, and functions SIGJSY, SIGJSZ, SIGLTY, SIGPGY, and SIGPGZ.

REARNG -- Called by subroutine GRIDIN, this routine checks and rearranges the set of active meteorological stations to be used in wind interpolation.

RMODEL -- This routine reads in all of the "one time only" input data and opens all external files. Subroutines GRIDIN and ERROR are called by RMODEL.

RSOURC -- This routine reads in source related input data. Subroutine ERROR and function IGCDIV are called by RSOURC.

RSRATE -- This routine reads in source emission rate and other related data that may vary during the course of a model run. RSRATE only calls subroutine ERROR.

RWINDS -- Subroutine RWINDS is called if LADT is true. Wind speed and direction are interpolated to each grid square RWINDS calls subroutine WIND and ERROR.

SIGJSY -- This function computes on-site σ_y based on travel time. It can be called by subroutines CALSTP and PROCES.

SIGJSZ -- This function computes on-site σ_z based on travel time. It can be called by subroutines CALSTP and PROCES.

SIGLTY -- σ_y for long travel time is computed in this function, called by subroutine PROCES. Growth is proportional to the square root of time.

SIGPGY -- This routine computes σ_y using the P-G curves. It can be called by subroutines CALSTP and PROCES.

SIGPGZ -- This routine computes σ_z using the P-G curves; it is called by PROCES.

STRAY -- This routine, called by GRIDIN, sets up the anemometer-station array for each meteorological grid point.

UFACTR -- This function computes the adjustment to the wind speed based on the stability-dependent power-law exponents.

USRPRS -- This is a user-supplied subroutine for plume rise.

USRSIG -- This is a user-supplied subroutine for dispersion parameters; it can be called by subroutines USRVRT and PROCES.

USRVRT -- The virtual times or distances for the user-supplied sigmas are computed by USRVRT. Subroutine USRSIG is called by USRVRT.

VTIMY -- This function calculates the virtual time, corresponding to the SIGJSY function.

VTIMZ -- This function calculates the virtual time, corresponding to the SIGJSZ function.

WIND -- This subroutine, called by RWINDS, decodes wind data elements into directions and speeds, and then interpolates to each meteorological grid point.

XVY -- This function calculates the virtual distance necessary to account for the initial crosswind dispersion using the P-G scheme.

XVZ -- This function calculates the virtual distance necessary to account for the initial vertical dispersion using the P-G scheme.

SECTION V

INPUT DATA PREPARATION

CARD INPUT SEQUENCE

There are ten card types that are read in TRIAD. Most of these are free format input, and two are alphanumeric. While the free format is very easy to use, care should be taken to ensure that every variable is given a value in the correct order. Each variable should be separated by a comma or blank space and should conform to the variable name type. Card-types 2A and 5A to 5D are optional, depending on the options exercised on card 2. Cards 1 through 5D are read in subroutine RMODEL. Cards 6 through 9 are read in subroutine RSOURC. And finally card 10 is read in subroutine RSRATE. A brief description of each input parameter is given in Table A-5 with the appropriate units. The metric system of units is used throughout the model. Thus horizontal coordinates of source and receptor locations are in kilometers, temperatures in degrees Kelvin, and emission rates in grams per second. Under the "Format" column of Table A-5, AN refers to alphanumeric, FF represents free format. Standard notation for real and integer variables are used. Logical and integer variables and units are indicated in the last column.

Table A-5. Card input sequence for TRIAD model.

Variable	Format	Description	Units/type
Card type 1: Title			
ALP	AN	72-character title to describe output.	--
Card Type 2: Options			
IW	FF	Unit number for write statements.	(integer)
LADT	FF	Does user supply a wind field?	(logical)
LP22	FF	Unit 22 output desired? (for puff-trajectory plots, etc.)	(logical)
KEYDSP	FF	Dispersion option KEYDSP = 1 For PG (distance dependent) sigma curves; KEYDSP = 2 For Irwin et al., (time dependent) sigma curves; KEYDSP = 3 For user specified	(integer)

Table A-5 (Continued)

Variable	Format	Description	Units/type
		distance-dependent sigma curves; KEYDSP = 4 For user-specified time-dependent sigma curves.	
SYMAX	FF	Maximum size of σ_y before going to SIGLTY function. If very large, then the use of SIGLTY is effectively prevented.	(m)
LPCC	FF	Option to print out puff information each ITIME.	(logical)
LPIC	FF	Option to print out intermediate concentrations.	(logical)
LCONV	FF	Option to convert concentration units from g/m^3 to other user-specified units.	(logical)
LP25	FF	Option to write predicted concentrations (for all sampling periods at each receptor) to a file on Unit 25.	(logical)

Card Type 2A: Concentration Units (Optional)

If LCONV is TRUE then read this card.

CONVF	FF	Conversion factor to user-specified concentration units (CUNITS) from g/m^3.	(CUNITS/g/m^3)
CUNITS	AN	30-character description of concentration units specified by the user.	--

Card Type 3: Model Grid

XGRDSW	FF	East-west coordinate of S.W. corner of model region.	(km)
YGRDSW	FF	North-south coordinate of S.W. corner of model region.	(km)
XSIZE	FF	East-west size of model region.	(km)
YSIZE	FF	North-south size of model region.	(km)

Table A-5 (Continued)

Variable	Format	Description	Units/type
Card Type 4: No. of Met. Periods, Sources, and Receptors			
NTIME	FF	Number of periods of simulation (No. of meteorological periods).	(integer)
ITIME	FF	Length of each meteorological period.	(seconds) (integer)
NSOURC	FF	Number of sources for this run.	(integer)
NREC	FF	Number of receptors.	(integer)
Card Type 5: Receptor Locations (Read NREC times)			
XREC	FF	X coordinate of receptor.	(km)
YREC	FF	Y coordinate of receptor.	(km)
ZREC	FF	Elevation of receptor above some constant reference level.	(m)
Four Optional Card Types Follow:			
Card Type 5A: Format for Winds (Optional)			
If LADT is TRUE then read this card.			
FRMATR	AN	User-specified format for optional gridded meteorological data stored on Unit 21. The format should be given within parentheses.	--
Card Type 5B: Meteorological Grid (Optional)			
If LADT is TRUE then read this card.			
XSWC	FF	East-west coordinate of grid point on S.W. corner of meteorological grid.	(km)
YSWC	FF	North-south coordinate of grid point on S.W. corner of meteorological grid.	(km)
NUMX	FF	Number of grid points in East-west direction at which wind is interpolated.	(integer)
NUMY	FF	Number of grid points in North-south direction at which wind is interpolated.	(integer)

Table A-5 (Continued)

Variable	Format	Description	Units/type
DGX	FF	East-west width of grid cell.	(km)
DGY	FF	North-south width of grid cell.	(km)
NUMSTA	FF	Number of anemometer sites for interpolation to the met. grid.	(integer)
Card Type 5C: Anemometer Locations (Optional)			
If LADT is TRUE then read this card. (Read NUMSTA times)			
XDIST	FF	East-West coordinate of anemometer site. (Same coordinate system as XSWC)	(km)
YDIST	FF	North-South coordinate of anemometer site. (Same coordinate system as YSWC)	(km)
ZDIST	FF	Height of anemometer above ground level.	(m)
ZGND	FF	Elevation of base of anemometer above some constant level to which receptor elevations are also referenced.	(m)
ISTAT	FF	Station status: 0 if data available, 1 if no data, 2 if data available but station is not on meteor. grid.	(integer)
NAMST	AN	A 4-character station identification.	--
Card Type 5D: Wind Data (Optional)			
If LADT is TRUE then read this card. (Read NTIME times)			
KYR	FF	Year in which anemometer data were taken.	(integer)
KDAY	FF	Day on which data were taken.	(integer)
KHR	FF	Hour in which wind measurement began.	(integer)
KMIN	FF	Minute at which wind measurement began.	(integer)
IDATA	FF	Wind data in six digits (DDDFFF) at NUMSTA stations. DDD: Direction from which wind blows. FFF: Wind speed multiplied by 10.	(integer) (degrees) (m/s)

Table A-5 (Continued)

Variable	Format	Description	Units/type
Card types 6 through 10 all occur under the control of a source loop and are executed NSOURC times:			
Card Type 6:	Physical Processes Options		
LSSH	FF	Stack downwash option.	(logical)
LBID	FF	Buoyancy-induced dispersion option.	(logical)
LDEPS	FF	Deposition and settling option.	(logical)
LUPLRS	FF	User plume-rise option.	(logical)
LCMBPF	FF	Does user want puff combinations? If so, the frequency of puff combinations is set automatically.	(logical)
LREACT	FF	Option to include dynamical effects of fast chemical reactions.	(logical)
Card Type 7:	Time Scales		
ISTEP	FF	Time between puff releases (used internally as MSTEP, in millisec). If ISTEP is negative, a value for MSTEP will be computed based on the stability class, wind speed, and minimum distance from source to receptor (CDIS). If positive, ISTEP must divide evenly into ITIME, ISUPDT, and ISAMPL.	(seconds)
ISAMPL	FF	Sampling time for concentrations (Used if LPIC is TRUE. Also used to assign value for ISTEP). ISAMPL must divide evenly into ITIME.	(seconds) (integer)
ISTRTC	FF	Time to start concentration calculations.	(seconds)
SDCMBN	FF	Fraction of crosswind dispersion for puff combination. If SDCMBN is negative and ISTEP is negative, SDCMBN is calculated based on MSTEP, relative speed of wind vs. source movement, and σ_y at the	--

Table A-5 (Continued)

Variable	Format	Description	Units/type
		closest receptor. If SDCMBN is negative and ISTEP is positive, SDCMBN is set to 1.0.	
ANHGT	FF	Anemometer height above the base of the source.	(m)

Card type 8 is within a meteorological period loop, which in turn is within the source loop. It is executed NTIME times for every source.

Card Type 8: Meteorology for source

WDIR	FF	Wind direction.	(degrees)
WSPD	FF	Wind speed.	(m/s)
HL	FF	Mixing height.	(m)
KST	FF	Pasquill stability class. 1=A, 2=B, 3=C, 4=D-Day, 5=D-Night, 6=E, 7=F.	(integer)
SGPH	FF	σ_ϕ, standard deviation of elevation angle.	(degrees)
SGTH	FF	σ_θ, standard deviation of azimuth angle.	(degrees)
TEMP	FF	Ambient air temperature.	(K)
RH	FF	Ambient air relative humidity.	(percent)
PRES	FF	Ambient air pressure.	(millibars)
CDIS	FF	Minimum distance source to receptor.	(km)

Card Type 9 is within the source loop only and is executed immediately after the met. data (card type 8) for the source have been read and checked.

Card Type 9: Source location, updates, and deposition

XSORC	FF	X Coordinate of source.	(km)
YSORC	FF	Y Coordinate of source.	(km)

Table A-5 (Continued)

Variable	Format	Description	Units/type
ZSORC	FF	Elevation of source above some constant level to which receptor elevations are also referenced.	(m)
NSRCDS	FF	Number of source emissions cards If ISUPDT is zero or negative, this should be 1, otherwise NTIME*ITIME should equal NSRCDS*ISUPDT.	(integer)
ISUPDT	FF	Time between source emissions updates (used internally as MSUPDT, in millisec.). If no updating, ISUPDT should be zero or negative or equal to NTIME*ITIME. If updating, ISTEP (if positive) must evenly divide into ISUPDT. Also, either ITIME must be a multiple of ISUPDT (but ITIME must be no more than 100 times ISUPDT), or ISUPDT must be a multiple of ITIME.	(seconds) (integer)
DV	FF	Deposition velocity.	(cm/s)
SVV	FF	Settling velocity.	(cm/s)

[Notes on DV and SVV:
Setting both DV=0. and SVV=0. is equivalent to a no-deposition case.
For deposition to occur, SVV should be less than or equal to DV.
For deposition of gases and very small particles, SVV=0.
For deposition of small particles, SVV is less than DV.
For deposition of medium and large particles, SVV=DV.
Re-entrainment of particles is implied if SVV is greater than DV.]

Card type 10 is effectively within a source emissions period loop, which in turn is within the source loop. It is executed NSRCDS times for each source. This is the last data type for unit 5.

Card Type 10: Source characteristics

QP	FF	Emission rate.	(g/s)
HPP	FF	Height of release.	(m)
TSP	FF	Stack gas temperature.	(K)
DP	FF	Stack diameter.	(m)

Table A-5 (Continued)

Variable	Format	Description	Units/type
VSP	FF	Stack gas velocity.	(m/s)
VFP	FF	Stack gas volume flow.	(m^3/s)
SYOP	FF	Initial sigma Y.	(m)
SZOP	FF	Initial sigma Z.	(m)
SDIR	FF	Source direction.	(degrees)
SSDP	FF	Source speed.	(m/s)

DISCUSSION OF INPUT PARAMETERS

Most of the input data are straightforward and typical of the kind of information required for Gaussian models. However, there are some input variables which are unique to this code and require additional explanation to ensure proper assignment of values.

Card 2

If KEYDSP is equal to 3 or 4, subroutine USRSIG must be included at the time the program is linked. This subroutine is provided so the user can incorporate his own characterization of dispersion. Dispersion can be characterized as a function of downwind distance or travel time. The appropriate value of KEYDSP (3 or 4) must be specified. A sample subroutine USRSIG is included in the code. The user's version must retain the same calling arguments.

SYMAX is the maximum size of σ_y for any puff before the program calls SIGLTY to compute the dispersion parameters. SYMAX can be assigned any size (in meters) depending on how soon the user wants the model to compute the dispersion parameters as a function of the square root of time. If it is desired not to call SIGLTY, then a very large value of SYMAX should be assigned.

Card 4

The data requested on card 4 give the program information regarding the modeling design. NTIME is the number of meteorological periods simulated in a run. ITIME is the time period associated with the meteorological data. For example, if the meteorological data are recorded in 20-minute averages and the user wants to make a 3-hour simulation, then NTIME = 9 and ITIME = 1200 seconds. Any number of sources may be simulated in a given execution of the model. However, run time is approximately proportional to the number of sources. The number of receptors, NREC, must not exceed 100.

Card 5

The coordinates of the receptor are specified on this card. Note that ZREC refers to the elevation of receptor above some constant reference level (e.g., mean sea level). In complex terrain, this information allows TRIAD to account for the differences in elevations of sources and receptors while computing the concentrations. In flat terrain, ZREC can be the height of the receptor above the ground.

Cards 5A and 5B

Cards 5A and 5B are read if LADT is TRUE. The information on card 5B defines the coordinates of the grid point on the SW corner of the meteorological grid and the size of each grid cell. There are a few restrictions associated with using gridded meteorological data. The source must stay within the defined region. The meteorological region defined on card 5B need not be the same as the modeling region defined on card 3, but it is best if the southwest corner of both have the same coordinates. If the meteorological region is smaller than the modeling region and the puffs travel outside of the meteorological region, then they will be advected according to the wind speed and direction at the closest grid location. If the meteorological region is larger than the modeling region and the puffs travel outside the modeling region, they will be eliminated from further consideration. Card 5A requires the user to input the format of the meteorological data file. This file, assigned to unit 21, is written by subroutine RWINDS according to the format specified by the user. If the the interpolated wind field option is exercised, then the meteorological data read on card 8 must be appropriate for the grid cell that contains the source. Card 8 must be supplied whether or not the wind field option is exercised.

Cards 5C and 5D

Cards 5C and 5D are read if LADT is TRUE. On cards of type 5C, the anemometer station coordinates including elevation above the constant reference level (which is used to specify receptor elevations on card 5) are given. There are NUMSTA cards of this type with NUMSTA $\leq$ 11. The elevation information is used in the model to ensure that observed winds are correctly extrapolated to the height appropriate to the puff-transport, while accounting for the differences in elevations of the anemometer sites in complex terrain. Card 5D lists the time of wind observation and the wind data. The latter consist of observed wind direction (from which the wind blows) in degrees with respect to North, and wind speed in m/s. The speed is multiplied by ten in order to include one significant decimal digit.

Card 6

An alternate plume rise algorithm can be utilized in TRIAD by setting LUPLRS to TRUE. The user may incorporate any plume rise algorithm appropriate to his modeling exercise. The subroutine name must remain USRPRS with the same calling arguments. Meteorology and source information are provided in common blocks. A sample plume rise program is provided in TRIAD to compute the plume rise from a forest fire.

For most applications LCMBPF should be TRUE. If it is false no puff combinations or removal will occur, resulting in excessive run time and possible program termination.

Card 7

The data requested on card 7 give the program additional information regarding the modeling design. ISTEP is the time interval between puff releases. If ISTEP is assigned a negative value the model computes ISTEP based on the stability class, wind speed, and minimum distance from source to receptor. The minimum value that can be assigned to ISTEP is 1 second. However, if ISTEP is negative the model may calculate a puff release rate faster than one every second. When assigning ISTEP for a moving source, be sure to take into account the path of the source when computing the minimum distance between source and receptor (CDIS), specified on card 8. ISTEP should always be divisible into ITIME, ISUPDT and ISAMPL, which is the time interval at which intermediate concentration values are printed out. ISUPDT is the time interval at which source characteristics are updated. For example, if ITIM = 1200 and ISAMPL = 300, then four 5-minute average concentration tables are printed (if LPIC = T) as well as the 20-minute average concentration table.

The next two input parameters, ISTRTC and SDCMBN, are used to reduce computing time. ISTRTC is the time when concentration calculations are to begin. For most cases ISTRTC is assigned a value of zero. However, if the minimum source-receptor distance is large and requires a substantial amount of travel time for the puffs to reach the receptor, a value for ISTRTC can be assigned which would advect the puffs downwind but would delay the concentration calculations until the current time equaled ISTRTC.

The parameter SDCMBN controls when puff combinations take place. Combinations occur only for adjacent puffs in the release sequence which have the same dispersion key. A puff can have one of six possible dispersion keys: (1) puff is below the mixing height and using short travel time dispersion; (2) puff is using long travel time dispersion; (3) puff is above the mixing height; (4) puff is well mixed and using either P-G or on-site dispersion; (5) puff is above the mixing height and using long travel time dispersion; and (6) puff is well mixed and using long travel time dispersion. For instance, suppose two puffs are adjacent in time and have identical dispersion keys. If SDCMBN is 1 then the puffs combine when their centers are within one σ_y of each other (σ_y of the younger puff is used for the test). If SDCMBN equals 2, then the puffs combine when their centers are within 2 σ_y of each other. A value of SDCMBN equal to 0 results in no puff combinations. SDCMBN can be assigned any value; however, in practice, SDCMBN equal to 1 is a reasonable value for puff combination. If SDCMBN is negative TRIAD will compute a value for SDCMBN.

The positions, displacements, and travel times of two puffs are combined based on the mass-weighted average. The puff sigmas are calculated according to the weighted geometric means. The mass is summed.

Card 8

With the exception of stability class (KST) the variables on this card are typical of many air quality models. TRIAD considers seven stability categories, including D-day and D-night. Thus stability classes A through D-day are specified by 1-4, and classes D-night through F are specified by 5-7, respectively.

Card 10

The input parameters NSRCDS and ISUPDT must be correctly specified. If no updates to the source characterization are desired, then ISUPDT should be zero or negative and NSRCDS should be assigned a value of one. If you would like to update some aspect of the source characterization, such as emission rate, then ISUPDT must be positive. If ISTEP is positive, ISUPDT should be specified such that ISTEP divides evenly into ISUPDT. In addition, ISUPDT must be a multiple of or must divide evenly into ITIME. The source can be updated up to 100 times during any meteorological period. For example, if ITIME is 3600 seconds and you want to update the source every five minutes, then NSRCDS=12 and ISUPDT=300. If there are three meteorological periods (NTIME=3), then NSRCDS=36 and ISUPDT remains the same.

WIND MODULE OPERATION AND DESIGN

The wind interpolation combines two tasks: relating the anemometer-site locations to the points on the meteorological grid, and interpolating the measured winds to this grid. The first task, including specification of the standard elevation to which the winds will be adjusted before interpolation, is done by subroutine GRIDIN called from subroutine RMODEL. This first task is done only once in any run. Subroutine GRIDIN calls three subsidiary routines:

REARNG to remove inactive anemometer sites from consideration.
STRAY to specify up to ten of the closest anemometer sites for each meteorological grid point.
ASCND to arrange the ten closest anemometer sites in order of increasing distance from the given grid point.

All necessary data are read in subroutine RMODEL. These data appear in the input set as card types 5A-5D.

The second task, including the adjustment of the wind speed to the standard elevation and the interpolation to the meteorological grid are done by subroutine WIND. WIND is called by subroutine RWINDS for each meteorological period for each source. Subroutine WIND also writes the interpolated wind components to Unit 21 for plotting and other post diagnoses. The format for writing on Unit 21 is specified as input on card type 5A. Experience indicates that at least two decimal places should be provided (e.g., 10F7.2).

Size parameters defining the meteorological grid include NUMX, NUMY, DGX, and DGY, which appear on card 5B. Two other parameters, XSWC AND YSWC, also given on card 5B, define the location of the meteorological grid with respect to the basic model grid. If these parameters are incorrectly specified, the puffs will travel in directions unrelated to the winds. These parameters are illustrated in Figure A-9. Note that XSWC and YSWC are the coordinates of the southwest data point of the meteorological grid.

The distinction between the computed standard elevation for the meteorological grid, HGTMET, and the anemometer height, ANHGT, specified on card type 7 must be recognized. HGTMET is computed once each run and used to adjust puff-transport winds to puff height. ANHGT is the height of the source anemometer above the source ground-level. This value, which may change from source to source, is used to adjust source winds to the physical stack height for computation of plume rise and aerodynamic downwash. ANHGT is not used for puff-transport winds if the meteorological grid option (LADT=.TRUE. of card type 2) is selected.

Figure A-10 shows a schematic diagram illustrating the various quantities used for the wind data interpolation and complex terrain adjustments in the TRIAD model. Receptor R_1 is below the plume and will get a low concentration. Receptor R_2, which is in the plume impact zone, will be exposed to a high concentration. Receptor R_3 is well above the plume and will have a low concentration. In TRIAD model, the plume height above the reference level remains constant after the maximum effective plume height (HE) is attained. The plume will not climb the hill and, unless the transport winds dictate it, the plume will not be deflected around the hill. The plume passes through the elevated terrain and will reappear on the other side. This limitation is a consequence of not specifying detailed three-dimensional terrain information in the model input, except for the isolated locations of the sources, receptors, and anemometers. Therefore, a network of meteorological towers, carefully located to depict the influence of complex terrain on the winds, is critical to the puff transport simulations in the TRIAD model.

The meteorological grid size and location may be adjusted for different wind regimes. Wind speeds and wind-data averaging period generally determine the grid spacings. Wind direction and the distribution of meteorological measurement sites determine the grid location with respect to the source.

In specifying a meteorological grid, one needs to consider the winds in the entire set of meteorological periods in a run since the grid cannot be changed during a run. A useful rule of thumb is to select a grid spacing such that the puffs travel about one grid interval per meteorological period at the typical wind speed of the entire simulation period. The length of a meteorological period is generally equal to the averaging time for the wind data, typically 15 to 60 min. There may be up to 144 meteorological periods in a full simulation period, but if the simulation period is very long, the winds may change sufficiently to render the meteorological grid inappropriate.

The primary output from the wind-field module is a set of wind components interpolated to the points of the meteorological grid.

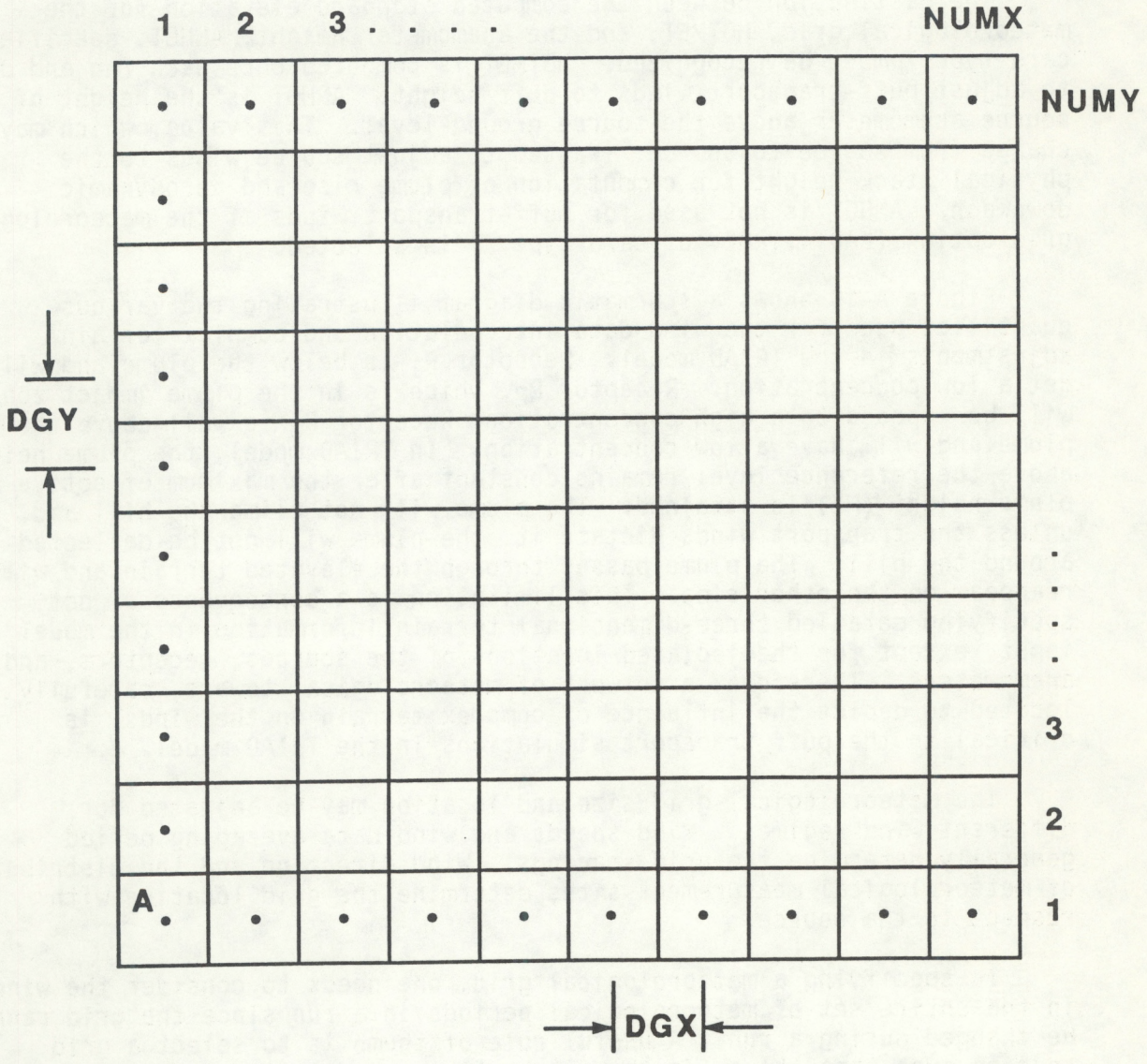

Figure A-9. Schematic representation of the meteorological grid used by TRIAD. Data are interpolated by the wind module to points centered in each grid square. The filled circles are a sample of these points. A puff having its center anywhere within a given grid square will be advected by the wind at the grid point in that square. The coordinates of grid point A are XSWC and YSWC, specified in Card Type 5B. Generally point A is taken to be at the origin of the model region, in which case XGRDSW=XSWC and YGRDSW=YSWC.

R_1, R_2, R_3---------- Receptors
M_1, M_2, M_3---------- Anemometers
HPP---------- Release (Stack) Height
HE---------- Effective Plume Height
HGTMET---------- Standard Elevation for the Meteorological Grid
ANHGT---------- Source Anemometer Height Above ZSORC
ZSORC---------- Stack Base Elevation
ZREC---------- Receptor Elevation
ZGND---------- Anemometer Base Elevation
ZDIST---------- Anemometer Height

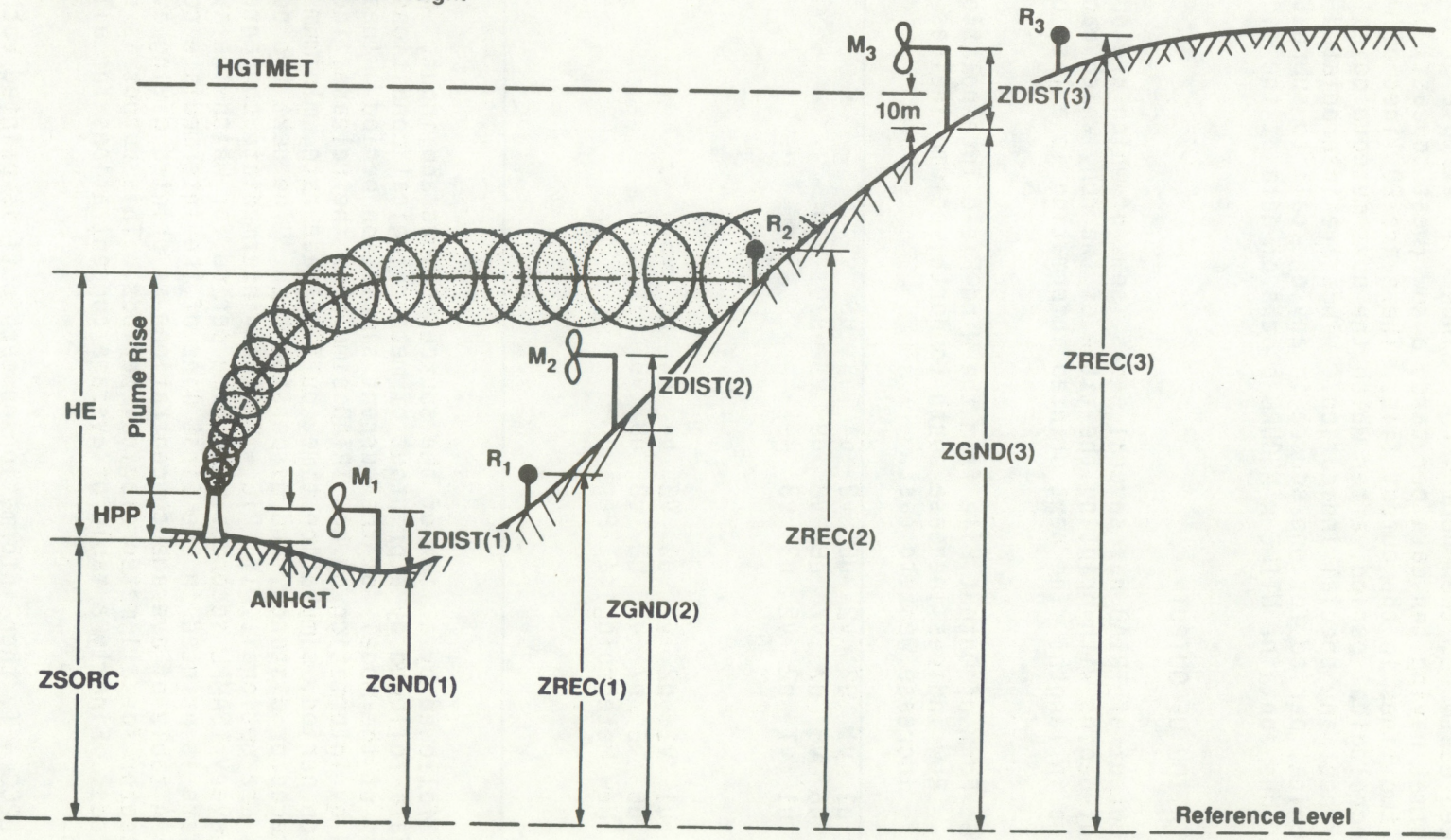

Figure A-10. Schematic diagram illustrating the various quantities used for wind data interpolation and terrain elevation adjustments in the TRIAD model.

The format is shown in Table A-6 for an example grid of 10 rows and 10 columns. The data start at the southwest corner of the meteorological grid and proceed eastward, then northward. Since this example grid is 10x10 and uses a format having ten data per card, a row (west to east) on the grid occupies two lines in the output file. There are 20 lines of wind data for each meteorological period, after which the next meteorological period begins without any special indication. Winds are interpolated from one meteorological period for one source in any one call to subroutine WIND. The file thus contains NTIME x NSOURC blocks of data at the end of the run.

INTERPRETATION OF OUTPUT

The output of TRIAD has several parts, some of which are optional. The output begins with printing the title of the run, which can be up to 80 characters in length. The next printed information is a list of model

Table A-6: Form of Output File from the Wind-Field Interpolation. Row indices increase south to north, column indices increase west to east.

Row 1:	u1	v1	u2	v2	u3	v3	u4	v4	u5	v5
	u6	v6	u7	v7	u8	v8	u9	v9	u10	v10
Row 2:	u1	v1	u2	v2	u3	v3	----			
					.	.	.	.		
Row 10:	u1	v1	u2	v2	u3	v3	u4	v4	u5	v5
	u6	v6	u7	v7	u8	v8	u9	v9	u10	v10
Row 1:	New Meteorological Period									
					.	.	.	.		

options, followed by a list of the source options and input. Next are the source data followed by a printout of meteorological conditions used in the execution of the model for the current simulation period. These are followed by information on how TRIAD simulates the release, including simulation period, simulation time, puff release rate, minimum source-receptor distance, and dispersion type. The next two output sections are optional. If LPIC = T, then intermediate concentrations are written every ISAMPL seconds. The time period for which the averages are appropriate is printed in the first line of the intermediate concentration output. A table of average concentrations is printed giving averages for each receptor for all meteorological periods. This output is repeated for all sources. Finally a table of average concentrations for all sources is provided.

If LPCC = T, then information on each puff is printed each ITIME in addition to average concentrations at each receptor. The information printed for each puff includes puff number and coordinates, time of puff release, total mass of the puff, sigmas and travel distance for the puff,

and its dispersion key. Because the puffs combine as they travel downwind, each puff's characteristics are adjusted each time it combines with another puff. All the parameters are affected by puff combinations except the dispersion key (KEYP). Puffs with different KEYP values do not combine.

TRIAD has three file output options on Unit 21, Unit 22, and Unit 25. These output files serve various purposes such as plotting, statistical analysis, and model evaluation, as discussed in Section II of this appendix.

For applications with chemical reactions, because the source strength (Q) on card 10 in the model input refers to the emission rate of the primary reactant (UF_6 in this case), the output gives the concentrations (in g/m^3) of this reactant species. The user can easily convert these values into the equivalent concentrations of the product species by multiplying with the ratios of the respective molecular weights and their stoichiometric constants. This is best explained using an example:

$$a.A + b.B \longrightarrow p.P + r.R$$

Here A and B are the reactant species, P and R are the product species, and a, b, p, and r are the respective stoichiometric constants. Given the concentration (g/m^3) of species A, then the corresponding concentrations of P and R are given as follows:

$$C_p = \left(\frac{p}{a}\right) \cdot \left(\frac{M_P}{M_A}\right) C_A$$

$$C_R = \left(\frac{r}{a}\right) \cdot \left(\frac{M_R}{M_A}\right) C_A$$

where M_i denotes the molecular weight (g/mole) of the species i. Applying these equations to Eq. (14), and noting that the molecular weights of UF_6, H_2O, UO_2F_2, and HF are, respectively, 352.025, 18, 308.025, and 20 g/mole, the concentrations of the product species can be easily obtained using the following relations:

$$C_{UO_2F_2} = 0.875\ C_{UF_6}$$

$$C_{HF} = 0.227\ C_{UF_6}$$

These calculations can be conveniently performed in the TRIAD program by utilizing the input option card 2A. For example, if the concentrations of HF are required, the user should specify 0.227 for CONVF and g/m^3 for CUNITS on card 2A. The title specified on card 1 may be used to identify the calculated concentrations as those of HF. The emission rate input on card 10 should be that of the primary reactant (UF_6 in this case), irrespective of whether the reactant or the product species concentrations are calculated in a run.

SENSITIVITY ANALYSIS

This section presents a simple sensitivity analysis designed to acquaint the user with the magnitude of changes expected in pollutant concentrations and CPU time when certain model inputs are varied. A near-surface release was used as a basis for this analysis.

Puff Combination -- SDCMBN

Integrated puff models are by their nature computationally time consuming. One means by which run time is reduced in TRIAD is by ignoring distant puffs when computing the concentration at a given receptor. A particularly effective technique is to combine or remove puffs under appropriate conditions. The parameter SDCMBN controls the rate of puff combinations. If the value of SDCMBN is 1, then the puffs combine when their centers are within one lateral standard deviation of each other.

As noted in Fig. A-11, CPU time increases rapidly as SDCMBN approaches zero due to the increased number of puffs. Execution time for SDCMBN equal to 0.2 is more than three times longer than for an SDCMBN of 1. CPU time levels off for SDCMBN greater than 1. Increasing SDCMBN from 1 to 3 results in only a 50% reduction in execution time.

The sensitivity of ground-level centerline concentrations to SDCMBN is shown in Table A-7. Varying SDCMBN from 0 to 3 has little effect on concentrations. However, shifting the wind direction can increase the percentage difference. This result, in conjunction with decreased computer costs with increasing SDCMBN (see Fig. A-11), suggests that SDCMBN equal to 1 is a reasonable value for puff combination.

Table A-7. Percent change in concentrations* using different SDCMBN values.

Downwind distance (km)	SDCMBN				
	0.4	0.6	1.0	2.0	3.0
0.5	0	0	0	+2	0
1.0	0	0	0	-2	0
2.0	0	0	0	0	+1
3.0	0	0	0	0	-1
5.0	0	0	0	0	0
10.0	0	0	0	0	0
20.0	0	0	0	0	+3
30.0	0	0	0	0	0
50.0	0	0	0	0	+2

* Concentrations were compared with those computed with SDCMBN = 0.2.

Size of Modeling Region

By defining the modeling region carefully, the user may save substantial computer costs as illustrated in Fig. A-12. For example, it makes little sense to extend the modeling region 50 km downstream of the source when all the receptors are within 5 km. TRIAD keeps track of all puffs in the modeling region regardless of their distance from a particular receptor. It might, nevertheless, be useful to have a large modeling region under some circumstances, such as in a dramatic wind shift situation that blows puffs back over the receptors.

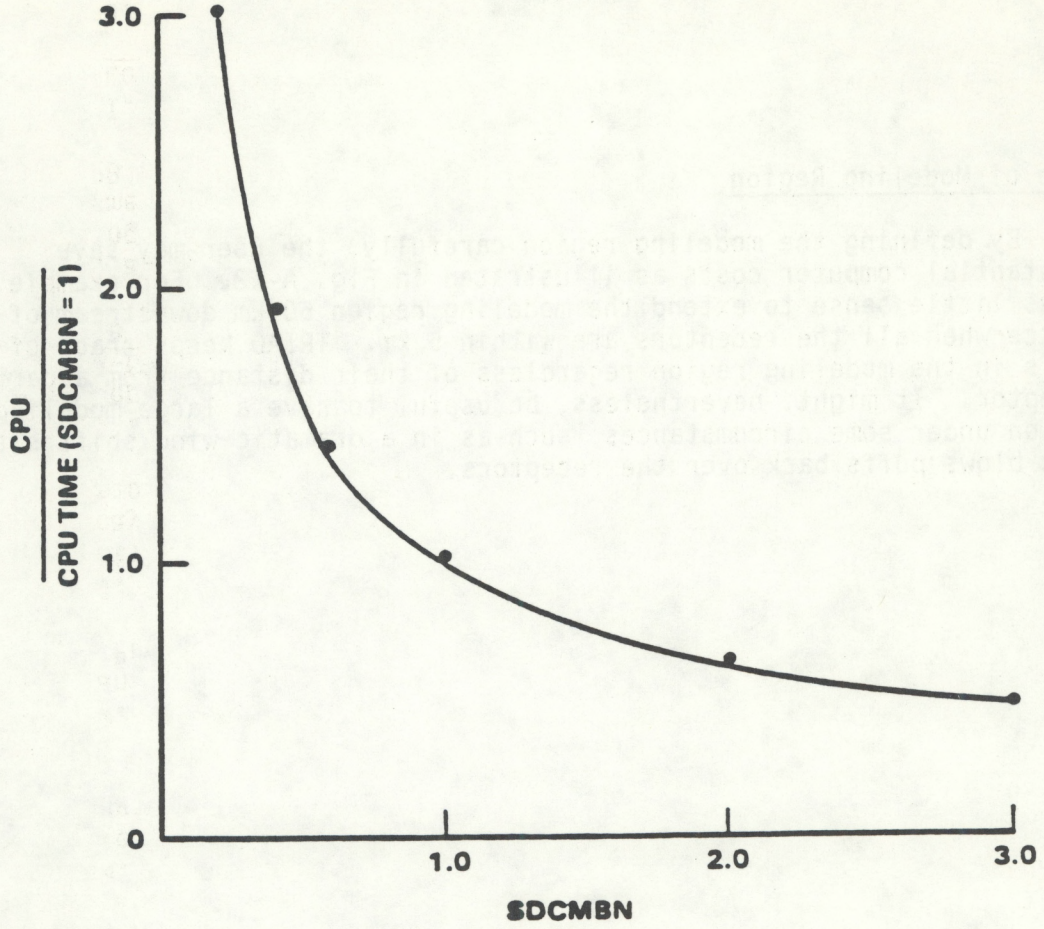

Figure A-11. Sensitivity of CPU time to the puff combination parameter SDCMBN.

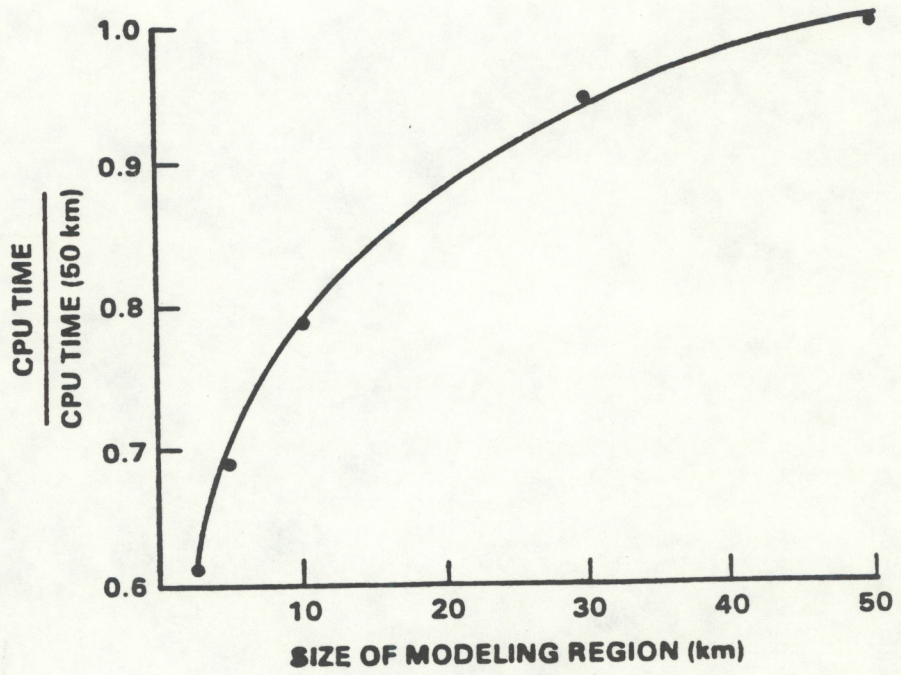

Figure A-12. Sensitivity of CPU time to size of modeling region.

REFERENCES

Batchelor, G. K., 1953: The Theory of Homogeneous Turbulence. Cambridge University Press, London.

Briggs, G. A., 1969: Plume Rise. USAEC Critical Review Series. TID-25075, National Technical Information Service, Springfield, VA, 81 pp.

Briggs, G. A., 1971: Some recent analyses of plume rise observation. In: Proceedings of the Second International Clean Air Congress, H. M. Englund and W. T. Beery, eds., Academic Press, New York, 1029-1032.

Briggs, G. A., 1973: Diffusion estimation for small emissions. NOAA Atmospheric Turbulence and Diffusion Laboratory, Contribution File No. 79. Oak Ridge, TN, 59 pp.

Briggs, G. A., 1975: Plume rise predictions. In: Lectures on Air Pollution and Environmental Impact Analysis, D. A. Haugen, ed., Am. Meteorol. Soc., Boston, MA, 59-111.

Cramer, H. E., 1976: Improved techniques for modeling the dispersion of tall stack plumes. In: Proceedings of the Seventh International Technical Meeting on Air Pollution Modeling and its Application, No. 51, NATO/CCMS, 731-780. (NTIS PB 270 799).

Draxler, R. R., 1976: Determination of atmospheric diffusion parameters, Atmos. Environ. 10, 99-105.

Gifford, F. A., 1976: Turbulence diffusion typing schemes: a review. Nuclear Safety 17, 68-86.

Hanna, S. R., G. A. Briggs, J. Deardorff, B. A. Egan, F. A. Gifford, and F. Pasquill, 1977: AMS workshop on stability classification schemes and sigma curves--summary of recommendations. Bull. Am. Meteorol. Soc. 58, 1305-1309.

Hanna, S. R., G. A. Briggs, and R. P. Hosker, 1982: Handbook on Atmospheric Diffusion. DOE/TIC-11223. Available as DE81009809 from NTIS, Springfield, VA, 102 pp.

Irwin, J. S., 1983: Estimating plume dispersion - a comparison of several sigma schemes. J. Clim. Appl. Meteorol. 22, 92-114.

Just, R. A., and W. R. Williams, 1986: A Computer Program for Simulating the Atmospheric Dispersion of UF_6 and other Reactive Gases having Positive, Neutral, or Negative Buoyancy. Martin Marietta Energy Systems Inc., Engineering Document K/D-5694, Oak Ridge, TN.

Panofsky, H. A., and J. A. Dutton, 1984: Atmospheric Turbulence: Models and Methods for Engineering Applications. John Wiley & Sons, New York, 397 pp.

Pasquill, F., 1961: The estimation of the dispersion of windborne material. Meteorol. Magazine 90, 33-49.

Pasquill, F., 1976: Atmospheric Dispersion Parameters in Gaussian Plume Modeling. Part II. Possible Requirements for Change in the Turner Workbook Values. EPA-600/4-76-030b, U.S. Environmental Protection Agency, Research Triangle Park, NC, 44 pp.

Petersen, W. B., J. A. Catalano, T. Chico, and T. S. Yuen, 1984: INPUFF - A Single Source Gaussian Puff Dispersion Algorithm. EPA-600/8-84-027, U.S. Environmental Protection Agency, Research Triangle Park, NC, 110 110 pp.

Petersen, W. B., and L. G. Lavdas, 1986: INPUFF 2.0 - A Multiple Source Gaussian Plume Dispersion Algorithm. EPA/600/8-86-011, U.S. Environmental Protection Agency, Research Triangle Park, NC, 105 pp.

Ramsdell, J. V., G. F. Athey and C. S. Glantz, 1983: MESOI Version 2.0: An Interactive Mesoscale Lagrangian Puff Dispersion Model with Deposition and Decay. NUREG/CR-3344 (PNL-4753), U.S. Nuclear Regulatory Commission, Washington, D.C.

Rao, K. S., 1982: Analytical Solutions of a Gradient-Transfer Model for Plume Deposition and Sedimentation. NOAA Tech. Memo. ERL ARL-109, 75 pp; EPA-600/3-82-079, U.S. Environmental Protection Agency, Research Triangle Park, NC. (NTIS PB 82-215 153).

Rao, K. S., and H. F. Snodgrass, 1982: PAL-DS Model: The PAL Model Including Deposition and Sedimentation. EPA-600/8-82-023, U. S. Environmental Protection Agency, Research Triangle Park, NC, 49 pp. (NTIS PB 83-117 739).

Taylor, G. I., 1921: Diffusion by continuous movements. In: Proceedings of the London Mathematical Society, 20, 196-212.

Turner, D. B., 1970: Workbook of Atmospheric Dispersion Estimates. Office of Air Programs Publication No. AP-26. U.S. Environmental Protection Agency, Research Triangle Park, NC, 84 pp. (NTIS PB 191 482).

APPENDIX B

TRIAD EXAMPLE PROBLEMS

by

Ronald J. Dobosy
Atmospheric Turbulence and Diffusion Division, NOAA
P.O. Box 2456, Oak Ridge, TN 37831

Two example runs are included, both considering hypothetical ground-level releases of pure gaseous uranium hexafluoride into the air. Example 1 considers a continuous source, with a small release rate of 1 kg/s for the duration of the simulation. Example 2 has the largest source release rate which the model is designed to handle, 20 kg/s. This source, which simulates the rupture of a shipping cylinder of uranium hexafluoride, is assumed to last 15 minutes, the duration of a typical accidental release of this magnitude. The computed plume rise of the reaction products is due entirely to the heat of reaction between uranium hexafluoride and the atmospheric water vapor. (Although the release typically occurs between 57 C and 120 C, the exit temperature is specified to be same as the ambient temperature. This assumption partly compensates for the effects of density on the plume rise). The buoyant plume rise due to fast exothermic reaction of the UF_6 is about 48 m in Example 1, and 436 m in Example 2.

Both runs use the same wind field, although differences in puff height result in somewhat different trajectories due to the power-law adjustment of the wind speeds. Figure B-1 shows the meteorological grid region used in these examples. Tables B-1 and B-2 give the input data file and the model output listing for Example 1. Figure B-2 shows the wind vectors and the puff trajectories for the sequential simulation periods for this example. Similar I/O listings and plots for Example 2 are shown in Tables B-3 and B-4, and Figure B-3, respectively.

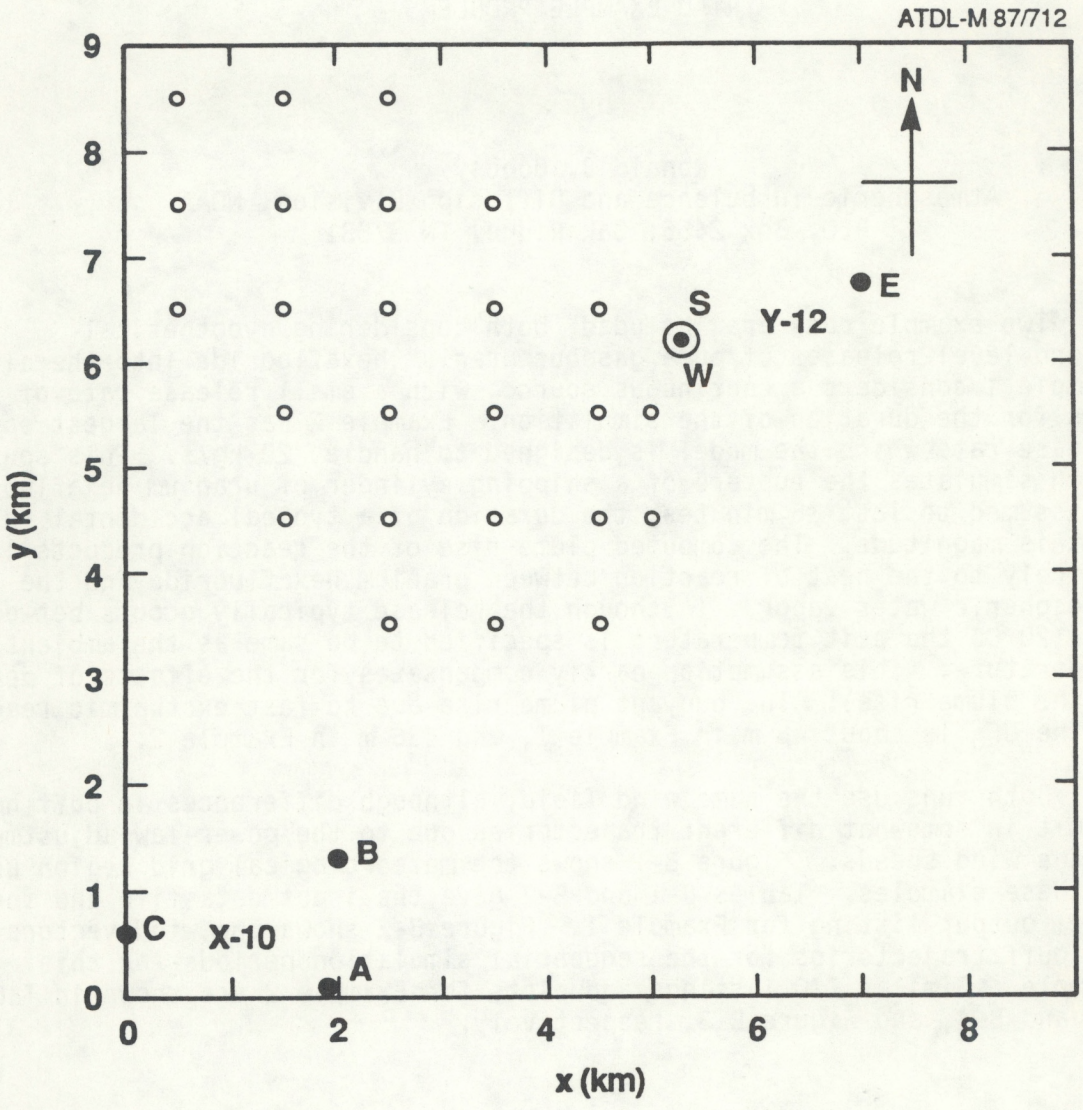

Figure B-1. Meteorological grid and model region for the two hypothetical examples presented in this appendix. The spots identified by letters are the anemometer locations. The source at anenometer site W is circled and marked by the letter S. Two industrial plants of the Oak Ridge complex are indicated by "X-10" and "Y-12". The open circles are receptors, at which concentrations are calculated by the model. These concentrations are included in the model output (Tables B-2 and B-4). The receptors are numbered from bottom to top starting at x = 0.5 km, y = 6.5 km.

Table B-1: Input data set for Example 1. Reference level is taken to be at the source elevation. All receptors and anemometer sites are assumed to have the same ground-level elevation as the source. Winds are measured at 10 m above the local ground level. Legends giving the card type are not part of the input data set, but are included for reference to Table 5. Input records normally start in column 1.

```
Card Type 1  UF6 DISPERSION IN OAK RIDGE,SOURCE 1KG/S,08-10HR,11/17/86

Card Type 2  6,T,F,2,1000.,F,F,F,F

Card Type 3  0.,0.,9.,9.

Card Type 4  9,900,1,25

Card Type 5  0.5,6.5,0.
             0.5,7.5,0.
             0.5,8.5,0.
             1.5,4.5,0.
             1.5,5.5,0.
    *        1.5,6.5,0.
             1.5,7.5,0.
             1.5,8.5,0.
             2.5,3.5,0.
             2.5,4.5,0.
             2.5,5.5,0.
             2.5,6.5,0.
    *        2.5,7.5,0.
             2.5,8.5,0.
             3.5,3.5,0.
             3.5,4.5,0.
             3.5,5.5,0.
             3.5,6.5,0.
             3.5,7.5,0.
    *        4.5,3.5,0.
             4.5,4.5,0.
             4.5,5.5,0.
             4.5,6.5,0.
             5.0,4.5,0.
             5.0,5.5,0.

Card Type 5a (10F7.2)

Card Type 5b 0.,0.,10,10,1.,1.,7

Card Type 5c 1.9 0.1 10 0. 0 'A'
             2.0 1.3 10 0. 0 'B'
    *        0.0 0.6 10 0. 0 'C'
    *        5.3 7.2 10 0. 0 'W'
    *        7.0 7.75 10 0. 0 'E'
             -5.1 1.5 10 0. 1 'K'
             -4.7 -3.7 10 0. 1 'BR'
```

Table B-1 (continued)

```
Card Type 5d 86 321 8 00 042010 040016 003010 061006 042011 999999 999999
             86 321 8 15 035009 043013 001008 006008 039014 999999 999999
    *        86 321 8 30 062009 057013 021009 060013 038016 999999 999999
    *        86 321 8 45 027010 029015 006010 114013 099015 999999 999999
    *        86 321 9 00 094010 086014 108013 114010 089012 999999 999999
             86 321 9 15 061011 044012 110009 120012 100013 999999 999999
             86 321 9 30 060012 061016 099011 112012 099019 999999 999999
             86 321 9 45 069010 053015 095015 097012 108019 999999 999999
             86 321 10 00 079012 078014 104017 132008 137015 999999 999999

Card Type 6  F,F,F,F,T,T

Card Type 7  30,900,0,1.,10.

Card Type 8  61. 0.6 250. 4 5.5 14.0 283.9 90. 1000. .5
             6. 0.8 275. 4 5.5 24.0 283.9 90. 1000. .5
    *        60. 1.3 300. 4 5.5 15.0 283.8 90. 1000. .5
    *        114. 1.3 325. 3 6.5 16.0 283.9 90. 1000. .5
    *        114. 1.0 350. 3 6.5 15.0 284.1 90. 1000. .5
             120. 1.2 375. 3 6.5 11.0 284.1 90. 1000. .5
             112. 1.2 400. 2 8.5 9.0 284.2 90. 1000. .5
             97. 1.2 425. 2 8.5 19.0 284.3 90. 1000. .5
             132. 0.8 450. 2 8.5 15.0 284.5 90. 1000. .5

Card Type 9  5.3,7.2,0.,1,-1,0.,0.

Card Type 10 1000.,0.,284.,1.,0.,0.,1.5,1.5,0.,0.
```

Table B-2: TRIAD model output for Example 1, the small source. The stated number of anemometer sites includes the five active sites along with two more sites (K and BR) which are off the meteorological grid.

```
MESOI ----> GRID INITIALIZATION


MESOI ----> STATION INITIALIZATION

 NUMBER OF ANEMOMETER SITES:          7

    THE CURRENT WIND GRID IS:  10 ROWS X  10 COLUMNS

   DX =       1.00,  DY =       1.00

THE GRID IS  10. M ABOVE THE REFERENCE LEVEL

ABSOLUTE COORDINATES OF THE SOUTHWEST GRID POINT ON THE METEOROLOGICAL GRID

   XSWC =      0.00   YSWC =      0.00

THERE ARE CURRENTLY  7 STATIONS WITH  2 DISABLED

 STA NAME      GRIDX     GRIDY    HEIGHT (M, AGL)    GROUND ELEV (M)    ISTAT
  1  A          1.90      0.10         10.                0.              0
  2  B          2.00      1.30         10.                0.              0
  3  C          0.00      0.60         10.                0.              0
  4  W          5.30      7.20         10.                0.              0
  5  E          7.00      7.75         10.                0.              0
  6  K         -5.10      1.50         10.                0.              1
  7  BR        -4.70     -3.70         10.                0.              1
NOTE:  GRIDX, GRIDY GIVE THE RELATIVE COORDINATES OF THE WIND SITES IN KILOMETERS
WITH RESPECT TO THE SOUTHWEST-CORNER POINT OF THE METEOROLOGICAL GRID
WHICH HAS ABSOLUTE COORDINATES XSWC, YSWC


**  END GRID INITIALIZATION **
```

Table B-2 (continued)

TRIAD 2.0 MULTIPLE SOURCE INTEGRATED PUFF MODEL (VERSION 88271)
AN ATMOSPHERIC TRANSPORT AND DISPERSION MODEL FOR UF6

UF6 DISPERSION IN OAK RIDGE,SOURCE 1KG/S,08-10HR,11/17/86

M O D E L O P T I O N S A "T" INDICATES THAT
THE OPTION HAS BEEN EXERCISED

USER SUPPLIED WIND FIELD	T
UNIT 22 OUTPUT OPTION	F
PRINT PUFF INFORMATION	F
INTERMEDIATE CONCENTRATIONS	F
CONVERT CONCENTRATION UNITS	F
CONCEN. OUTPUT ON UNIT 25	F

DISPERSION CALCULATED USING IRWIN, ET. AL. (TIME DEPENDENT) SIGMA CURVES,
WITH TRANSITION TO DRAXLER'S LONG RANGE TRANSPORT SIGMA-Y AT SYMAX = 1000.0 METERS.

B E G I N A N A L Y S I S O F S O U R C E N U M B E R 1

S O U R C E O P T I O N S A "T" INDICATES THAT
THE OPTION HAS BEEN EXERCISED

STACK DOWNWASH	F
BUOYANCY INDUCED DISPERSION	F
DEPOSITION AND SETTLING	F
USER PLUME RISE	F
PERFORM PUFF COMBINATIONS	T
INCLUDE EFFECTS OF REACTIONS	T

Table B-2 (continued)

I N P U T P A R A M E T E R S

SOURCE UPDATE INTERVAL = 8100 SECONDS. (-1 INDICATES NO UPDATE)
START CONCENTRATION CALCULATIONS AT TIME = 0 SECONDS.
ANEMOMETER HEIGHT = 10.0 METERS.

INPUT DATA CHECK WHILE READING SOURCE NUMBER 1, FOR SOURCE EMISSIONS PERIOD 2:
STACK HEIGHT WILL BE RESET TO 1.0 M.
HPP(IS) = 0.000000000E+00 M.

* * * I N F O R M A T I O N F O R S O U R C E N U M B E R 1 * * *

SOURCE STRENGTH (G/SEC)	STACK HEIGHT (M)	STACK TEMP. (DEG-K)	STACK GAS VELOCITY (M/SEC)	STACK DIAMETER (M)	VOLUME FLOW (M**3/SEC)	COORD. AT TIME 0 SECONDS EAST (KM)	NORTH (KM)	ELEV ABOVE REF LEVEL (M)
.100E+04	0.00	284.000	0.000	1.000	0.000	5.300	7.200	0.0

SOURCE SPEED (M/SEC)	SOURCE DIRECTION (DEG)	PLUME HEIGHT (M)	INITIAL SIGMAS (R) (M)	(Z) (M)	DEPOSITION VELOCITY (CM/SEC)	SETTLING VELOCITY (CM/SEC)
0.000	0.0	47.60	1.9	1.7	0.00	0.00

* * *
CONCENTRATIONS FROM INTERMEDIATE METEOROLOGICAL PERIODS
* * *
ARE OMITTED FROM THIS TABLE, BUT APPEAR IN OUTPUT.
* * *

Table B-2 (continued)

* * * M E T E O R O L O G Y * * *

WIND DIR. (DEG)	WIND SPD. (M/SEC)	MIXING HGT. (M)	PROF.EP (DIMEN)	STABILITY (CLASS)	U PLUME (M/SEC)	TEMP (K)	SIGMA TH. (DEG.)	SIGMA PH. (DEG.)
132.0	0.800	450.	0.070	2	0.800	284.5	15.000	8.500

SIMULATION PERIOD START (SEC)	SIMULATION PERIOD STOP (SEC)	SIMULATION TIME (SEC)	PUFF RELEASE RATE (SEC)	SOURCE RECEPTOR DISTANCE (KM)	PUFF COMB. CRITERION (SIGMA)
7200	8100	900	30.000	0.50	1.000

900 SEC AVG. CONCENTRATION AT RECEPTORS FOR SIMULATION PERIOD 7200 TO 8100 SECONDS
DUE TO SOURCE NUMBER 1

CONCENTRATION UNITS ARE G/M**3

RECEPTORS NO.	X (KM)	Y (KM)	Z (M)	CONCENTRATION
1	0.500	6.500	0.000	6.489E-09
2	0.500	7.500	0.000	5.014E-05
3	0.500	8.500	0.000	1.468E-03
4	1.500	4.500	0.000	0.000E+00
5	1.500	5.500	0.000	0.000E+00
6	1.500	6.500	0.000	1.144E-09
7	1.500	7.500	0.000	8.434E-05
8	1.500	8.500	0.000	2.177E-03

Table B-2 (continued)

9	2.500	3.500	0.000	0.000E+00
10	2.500	4.500	0.000	0.000E+00
11	2.500	5.500	0.000	0.000E+00
12	2.500	6.500	0.000	6.283E-10
13	2.500	7.500	0.000	3.111E-04
14	2.500	8.500	0.000	1.020E-03
15	3.500	3.500	0.000	0.000E+00
16	3.500	4.500	0.000	0.000E+00
17	3.500	5.500	0.000	0.000E+00
18	3.500	6.500	0.000	1.071E-08
19	3.500	7.500	0.000	2.184E-03
20	4.500	3.500	0.000	0.000E+00
21	4.500	4.500	0.000	0.000E+00
22	4.500	5.500	0.000	0.000E+00
23	4.500	6.500	0.000	6.435E-09
24	5.000	4.500	0.000	0.000E+00
25	5.000	5.500	0.000	0.000E+00

* *

2.25 HR AVG. CONCENTRATION AT RECEPTORS FOR ALL SIMULATION PERIODS
DUE TO SOURCE NUMBER 1

CONCENTRATION UNITS ARE G/M**3

	RECEPTORS			
NO.	X (KM)	Y (KM)	Z (M)	CONCENTRATION
1	0.500	6.500	0.000	1.587E-04
2	0.500	7.500	0.000	1.519E-04
3	0.500	8.500	0.000	3.351E-04
4	1.500	4.500	0.000	9.522E-05
5	1.500	5.500	0.000	2.416E-04
6	1.500	6.500	0.000	2.299E-04
7	1.500	7.500	0.000	2.049E-04
8	1.500	8.500	0.000	5.918E-04
9	2.500	3.500	0.000	9.046E-07
10	2.500	4.500	0.000	9.358E-05

Table B-2 (continued)

11	2.500	5.500	0.000	2.492E-04
12	2.500	6.500	0.000	2.320E-04
13	2.500	7.500	0.000	2.927E-04
14	2.500	8.500	0.000	4.623E-04
15	3.500	3.500	0.000	9.107E-08
16	3.500	4.500	0.000	4.708E-05
17	3.500	5.500	0.000	3.387E-04
18	3.500	6.500	0.000	2.501E-04
19	3.500	7.500	0.000	9.653E-04
20	4.500	3.500	0.000	3.361E-10
21	4.500	4.500	0.000	1.252E-06
22	4.500	5.500	0.000	2.841E-04
23	4.500	6.500	0.000	1.027E-03
24	5.000	4.500	0.000	2.348E-08
25	5.000	5.500	0.000	4.216E-05

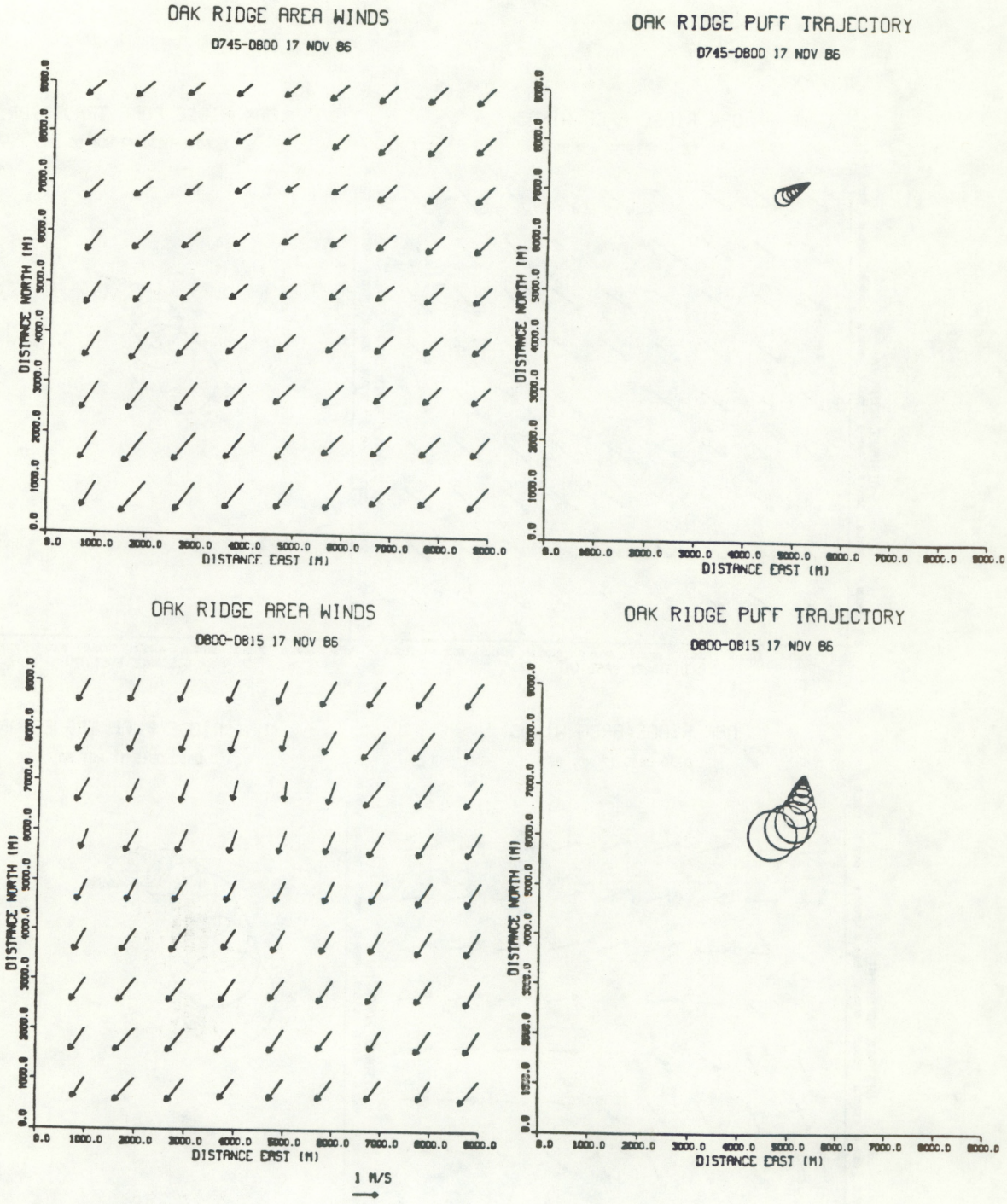

Figure B-2. Wind-field vectors and associated puff trajectories for Example 1, the model run with a small source emission of 1 kg/s uranium hexafluoride. The winds were 15-min average data from meteorological towers in the Oak Ridge area for nine sequential periods between 0745 and 1000 on 17 November, 1986. The wind speed, indicated by the length of the arrow, applies to the height to which the observed winds are interpolated. This height is 10 m above the source since the source, receptors, and towers are all assumed to be at the same elevation.

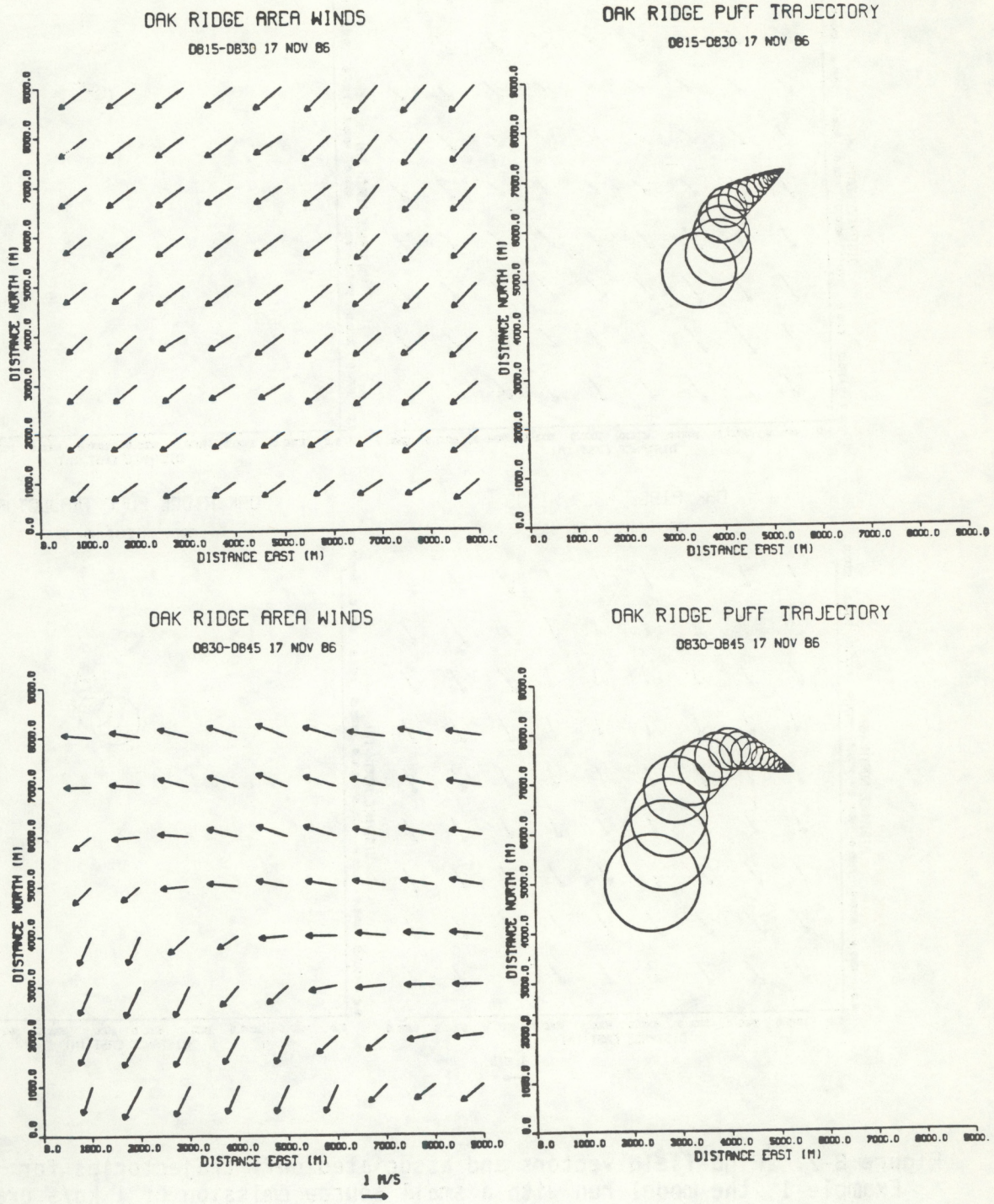

Figure B-2 (continued).

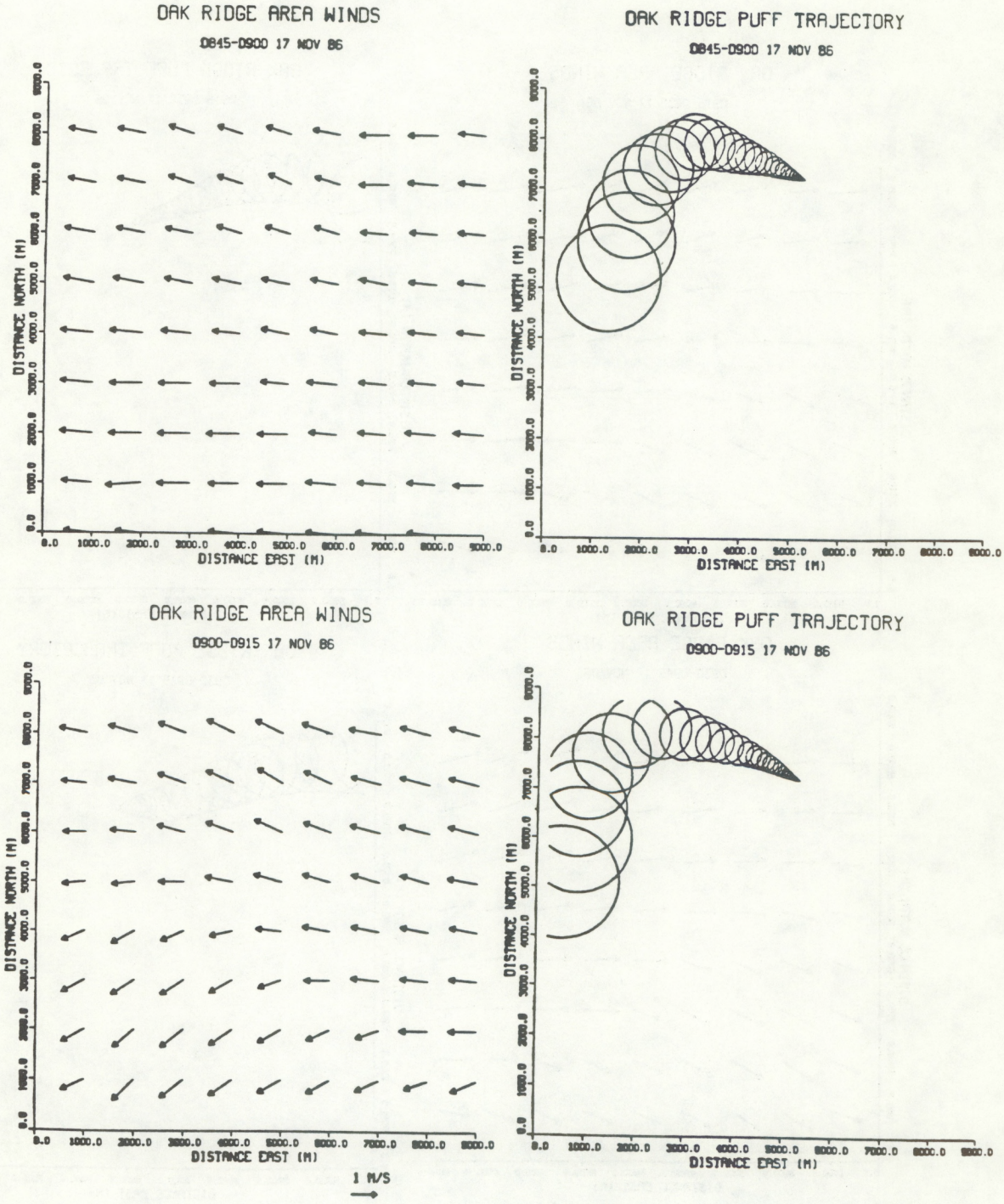

Figure B-2 (continued).

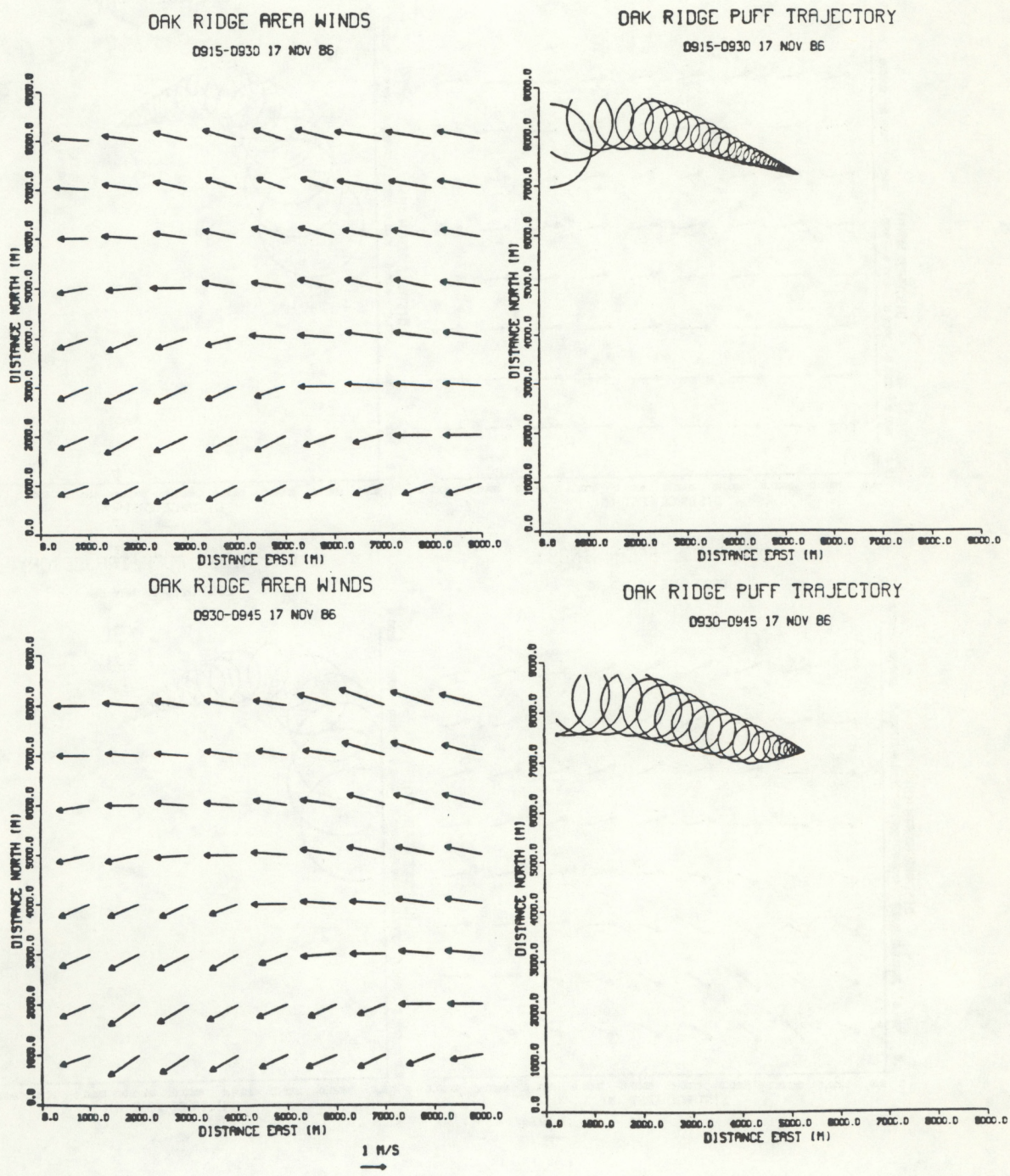

Figure B-2 (continued).

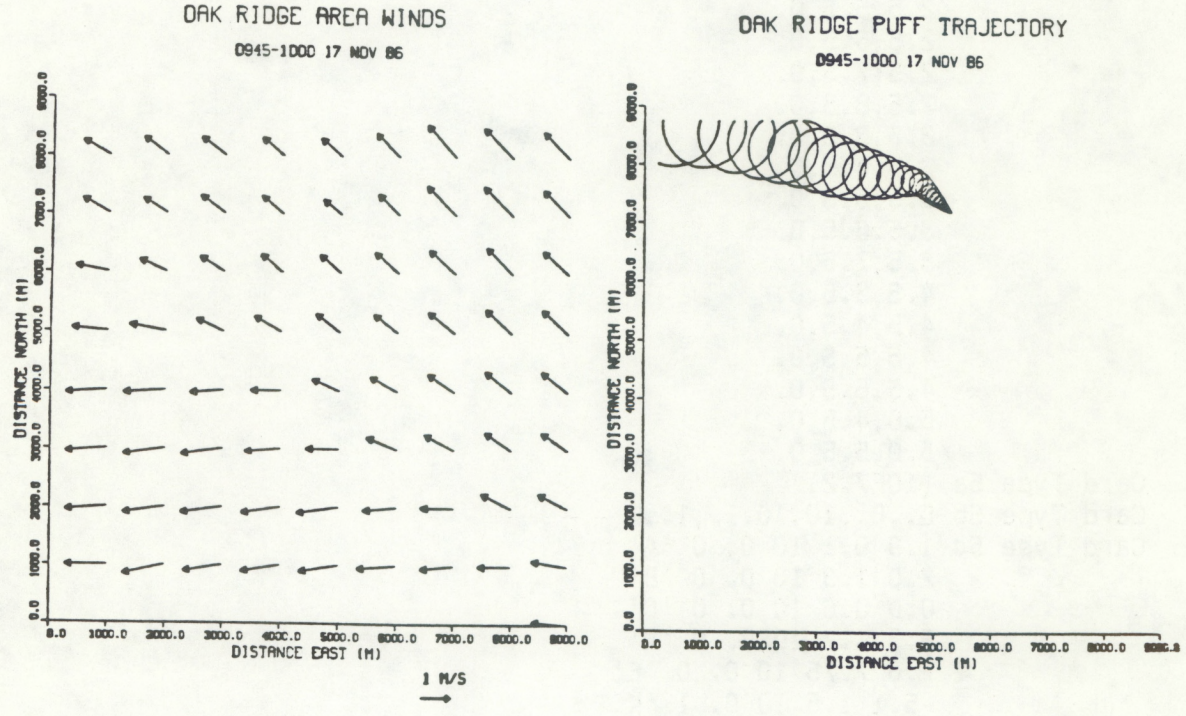

Figure B-2 (continued).

Table B-3: Input data set for Example 2. Elevation of the source, receptors and wind measurements above the reference level is the same as for Example 1.

```
Card Type 1  UF6 DISPERSION IN OAK RIDGE,SOURCE 20KG/S,08-10HR,11/17/86
Card Type 2  6,T,F,2,1000.,T,F,F,F
Card Type 3  0.,0.,9.,9.
Card Type 4  9,900,1,25
Card Type 5  0.5,6.5,0.
             0.5,7.5,0.
             0.5,8.5,0.
             1.5,4.5,0.
             1.5,5.5,0.
    *        1.5,6.5,0.
             1.5,7.5,0.
             1.5,8.5,0.
             2.5,3.5,0.
             2.5,4.5,0.
             2.5,5.5,0.
             2.5,6.5,0.
    *        2.5,7.5,0.
             2.5,8.5,0.
             3.5,3.5,0.
             3.5,4.5,0.
             3.5,5.5,0.
             3.5,6.5,0.
             3.5,7.5,0.
    *        4.5,3.5,0.
             4.5,4.5,0.
             4.5,5.5,0.
             4.5,6.5,0.
             5.0,4.5,0.
             5.0,5.5,0.
Card Type 5a (10F7.2)
Card Type 5b 0.,0.,10,10,1.,1.,7
Card Type 5c 1.9 0.1 10 0. 0 'A'
             2.0 1.3 10 0. 0 'B'
    *        0.0 0.6 10 0. 0 'C'
    *        5.3 7.2 10 0. 0 'W'
    *        7.0 7.75 10 0. 0 'E'
             -5.1 1.5 10 0. 1 'K'
             -4.7 -3.7 10 0. 1 'BR'
Card Type 5d 86 321 8 00 042010 040016 003010 061006 042011 999999 999999
             86 321 8 15 035009 043013 001008 006008 039014 999999 999999
    *        86 321 8 30 062009 057013 021009 060013 038016 999999 999999
    *        86 321 8 45 027010 029015 006010 114013 099015 999999 999999
    *        86 321 9 00 094010 086014 108013 114010 089012 999999 999999
             86 321 9 15 061011 044012 110009 120012 100013 999999 999999
             86 321 9 30 060012 061016 099011 112012 099019 999999 999999
             86 321 9 45 069010 053015 095015 097012 108019 999999 999999
             86 321 10 00 079012 078014 104017 132008 137015 999999 999999
```

Table B-3 (continued)

```
Card Type 6  F,F,F,F,T,T
Card Type 7  30,900,0,1.,10.
Card Type 8  61. 0.6 250. 4 5.5 14.0 283.9 90. 1000. .5
             6. 0.8 275. 4 5.5 24.0 283.9 90. 1000. .5
     *       60. 1.3 300. 4 5.5 15.0 283.8 90. 1000. .5
     *       114. 1.3 325. 3 6.5 16.0 283.9 90. 1000. .5
     *       114. 1.0 350. 3 6.5 15.0 284.1 90. 1000. .5
             120. 1.2 375. 3 6.5 11.0 284.1 90. 1000. .5
             112. 1.2 400. 2 8.5 9.0 284.2 90. 1000. .5
             97. 1.2 425. 2 8.5 19.0 284.3 90. 1000. .5
             132. 0.8 450. 2 8.5 15.0 284.5 90. 1000. .5
Card Type 9  5.3,7.2,0.,9,900,0.,0.
Card Type 10 20000.,0.,284.,1.,0.,0.,1.5,1.5,0.,0.
             0.,0.,284.,1.,0.,0.,1.5,1.5,0.,0.
     *       0.,0.,284.,1.,0.,0.,1.5,1.5,0.,0.
     *       0.,0.,284.,1.,0.,0.,1.5,1.5,0.,0.
     *       0.,0.,284.,1.,0.,0.,1.5,1.5,0.,0.
             0.,0.,284.,1.,0.,0.,1.5,1.5,0.,0.
             0.,0.,284.,1.,0.,0.,1.5,1.5,0.,0.
             0.,0.,284.,1.,0.,0.,1.5,1.5,0.,0.
             0.,0.,284.,1.,0.,0.,1.5,1.5,0.,0.
```

Table B-4: TRIAD model output for Example 2, the large source. The option to print puff information has been selected in this run. Puffs released at 30 s intervals will contain 600 kg of uranium hexafluoride at the emission rate specified. Puffs showing greater mass than this have been formed by puff combination, a model feature designed to reduce computation time. The times, sizes and elevations of the puffs are also adjusted during combination.

```
    MESOI ----> GRID INITIALIZATION


    MESOI ----> STATION INITIALIZATION

     NUMBER OF ANEMOMETER SITES:          7

        THE CURRENT WIND GRID IS:  10 ROWS X  10 COLUMNS

       DX =       1.00,  DY =       1.00

 THE GRID IS  10. M ABOVE THE REFERENCE LEVEL

 ABSOLUTE COORDINATES OF THE SOUTHWEST GRID POINT ON THE METEOROLOGICAL GRID

       XSWC =      0.00   YSWC =      0.00

    THERE ARE CURRENTLY  7 STATIONS WITH  2 DISABLED

     STA NAME      GRIDX     GRIDY    HEIGHT (M, AGL)    GROUND ELEV (M)    ISTAT
      1  A          1.90      0.10         10.                0.              0
      2  B          2.00      1.30         10.                0.              0
      3  C          0.00      0.60         10.                0.              0
      4  W          5.30      7.20         10.                0.              0
      5  E          7.00      7.75         10.                0.              0
      6  K         -5.10      1.50         10.                0.              1
      7  BR        -4.70     -3.70         10.                0.              1
    NOTE:  GRIDX, GRIDY GIVE THE RELATIVE COORDINATES OF THE WIND SITES IN KILOMETERS
    WITH RESPECT TO THE SOUTHWEST-CORNER POINT OF THE METEOROLOGICAL GRID
    WHICH HAS ABSOLUTE COORDINATES XSWC, YSWC

    **  END GRID INITIALIZATION **
```

Table B-4 (continued)

TRIAD 2.0 MULTIPLE SOURCE INTEGRATED PUFF MODEL (VERSION 88271)
AN ATMOSPHERIC TRANSPORT AND DISPERSION MODEL FOR UF6

UF6 DISPERSION IN OAK RIDGE,SOURCE 20KG/S,08-10HR,11/17/86

M O D E L O P T I O N S A "T" INDICATES THAT THE OPTION HAS BEEN EXERCISED

USER SUPPLIED WIND FIELD	T
UNIT 22 OUTPUT OPTION	F
PRINT PUFF INFORMATION	T
INTERMEDIATE CONCENTRATIONS	F
CONVERT CONCENTRATION UNITS	F
CONCEN. OUTPUT ON UNIT 25	F

DISPERSION CALCULATED USING IRWIN, ET. AL. (TIME DEPENDENT) SIGMA CURVES,
WITH TRANSITION TO DRAXLER'S LONG RANGE TRANSPORT SIGMA-Y AT SYMAX = 1000.0 METERS.

B E G I N A N A L Y S I S O F S O U R C E N U M B E R 1

S O U R C E O P T I O N S A "T" INDICATES THAT THE OPTION HAS BEEN EXERCISED

STACK DOWNWASH	F
BUOYANCY INDUCED DISPERSION	F
DEPOSITION AND SETTLING	F
USER PLUME RISE	F
PERFORM PUFF COMBINATIONS	T
INCLUDE EFFECTS OF REACTIONS	T

Table B-4 (continued)

I N P U T P A R A M E T E R S

SOURCE UPDATE INTERVAL = 900 SECONDS. (-1 INDICATES NO UPDATE)
START CONCENTRATION CALCULATIONS AT TIME = 0 SECONDS.
ANEMOMETER HEIGHT = 10.0 METERS.

INPUT DATA CHECK WHILE READING SOURCE NUMBER 1, FOR SOURCE EMISSIONS PERIOD 2:
STACK HEIGHT WILL BE RESET TO 1.0 M.
HPP(IS) = 0.000000000E+00 M.

* * * I N F O R M A T I O N F O R S O U R C E N U M B E R 1 * * *

SOURCE STRENGTH (G/SEC)	STACK HEIGHT (M)	STACK TEMP. (DEG-K)	STACK GAS VELOCITY (M/SEC)	STACK DIAMETER (M)	VOLUME FLOW (M**3/SEC)	COORD. AT TIME 0 SECONDS EAST (KM)	NORTH (KM)	ELEV ABOVE REF LEVEL (M)
.200E+05	0.00	284.000	0.000	1.000	0.000	5.300	7.200	0.0

SOURCE SPEED (M/SEC)	SOURCE DIRECTION (DEG)	PLUME HEIGHT (M)	INITIAL SIGMAS (R) (M)	(Z) (M)	DEPOSITION VELOCITY (CM/SEC)	SETTLING VELOCITY (CM/SEC)
0.000	0.0	435.95	3.4	2.3	0.00	0.00

Table B-4 (continued)

* * * M E T E O R O L O G Y * * *

WIND DIR. (DEG)	WIND SPD. (M/SEC)	MIXING HGT. (M)	PROF.EP (DIMEN)	STABILITY (CLASS)	U PLUME (M/SEC)	TEMP (K)	SIGMA TH. (DEG.)	SIGMA PH. (DEG.)
61.0	0.600	250.	0.150	4	0.940	283.9	14.000	5.500

SIMULATION PERIOD START (SEC)	SIMULATION PERIOD STOP (SEC)	SIMULATION TIME (SEC)	PUFF RELEASE RATE (SEC)	SOURCE RECEPTOR DISTANCE (KM)	PUFF COMB. CRITERION (SIGMAS)
0	900	900	30.000	0.50	1.000

PUFF#	X (KM)	Y (KM)	Z (M)	TIME (SEC)	TOTAL Q (GRAMS)	SY (M)	SZ (M)	TRAV. D. (KM)	KEYP
1	4.637	6.816	435.949	104	3600000.00	102.9	3.0	0.489	3
2	4.762	6.888	435.949	255	2400000.00	87.8	2.9	0.397	3
3	4.837	6.932	435.949	345	1200000.00	78.1	2.8	0.341	3
4	4.912	6.975	435.949	435	2400000.00	68.1	2.7	0.286	3
5	5.000	7.026	435.949	539	1800000.00	55.7	2.6	0.221	3
6	5.062	7.062	435.949	615	1200000.00	46.3	2.6	0.175	3
7	5.112	7.091	435.949	675	1200000.00	38.5	2.5	0.138	3
8	5.150	7.113	435.949	720	600000.00	32.3	2.5	0.111	3
9	5.175	7.128	435.949	750	600000.00	28.0	2.4	0.092	3
10	5.200	7.142	435.949	780	600000.00	23.5	2.4	0.074	3
11	5.225	7.157	435.949	810	600000.00	18.9	2.4	0.055	3
12	5.250	7.171	435.949	840	600000.00	14.1	2.3	0.037	3
13	5.275	7.186	435.949	870	600000.00	8.9	2.3	0.018	3
14	5.300	7.200	435.949	900	600000.00	3.4	2.3	0.000	3

* * *

* * * CONCENTRATIONS AND PUFF DATA FROM INTERMEDIATE METEOROLOGICAL PERIODS ARE OMITTED FROM THIS TABLE, BUT APPEAR IN THE OUTPUT.

* * *

Table B-4 (continued)

* * * M E T E O R O L O G Y * * *

WIND DIR. (DEG)	WIND SPD. (M/SEC)	MIXING HGT. (M)	PROF.EP (DIMEN)	STABILITY (CLASS)	U PLUME (M/SEC)	TEMP (K)	SIGMA TH. (DEG.)	SIGMA PH. (DEG.)
132.0	0.800	450.	0.070	2	0.800	284.5	15.000	8.500

SIMULATION PERIOD START (SEC)	SIMULATION PERIOD STOP (SEC)	SIMULATION TIME (SEC)	PUFF RELEASE RATE (SEC)	SOURCE RECEPTOR DISTANCE (KM)	PUFF COMB. CRITERION (SIGMAS)
7200	8100	900	30.000	0.50	1.000

PUFF#	X (KM)	Y (KM)	Z (M)	TIME (SEC)	TOTAL Q (GRAMS)	SY (M)	SZ (M)	TRAV. D. (KM)	KEYP
1	-2.234	6.046	435.949	704	8400000.00	628.1	113.2	8.407	1

900 SEC AVG. CONCENTRATION AT RECEPTORS FOR SIMULATION PERIOD 7200 TO 8100 SECONDS
DUE TO SOURCE NUMBER 1

CONCENTRATION UNITS ARE G/M**3

RECEPTORS NO.	X (KM)	Y (KM)	Z (M)	CONCENTRATION
1	0.500	6.500	0.000	9.599E-11
2	0.500	7.500	0.000	8.205E-12
3	0.500	8.500	0.000	5.500E-14
4	1.500	4.500	0.000	4.584E-18
5	1.500	5.500	0.000	2.093E-14

Table B-4 (continued)

6	1.500	6.500	0.000	3.029E-14
7	1.500	7.500	0.000	4.056E-18
8	1.500	8.500	0.000	0.000E+00
9	2.500	3.500	0.000	0.000E+00
10	2.500	4.500	0.000	0.000E+00
11	2.500	5.500	0.000	0.000E+00
12	2.500	6.500	0.000	0.000E+00
13	2.500	7.500	0.000	0.000E+00
14	2.500	8.500	0.000	0.000E+00
15	3.500	3.500	0.000	0.000E+00
16	3.500	4.500	0.000	0.000E+00
17	3.500	5.500	0.000	0.000E+00
18	3.500	6.500	0.000	0.000E+00
19	3.500	7.500	0.000	0.000E+00
20	4.500	3.500	0.000	0.000E+00
21	4.500	4.500	0.000	0.000E+00
22	4.500	5.500	0.000	0.000E+00
23	4.500	6.500	0.000	0.000E+00
24	5.000	4.500	0.000	0.000E+00
25	5.000	5.500	0.000	0.000E+00

* *

2.25 HR AVG. CONCENTRATION AT RECEPTORS FOR ALL SIMULATION PERIODS
DUE TO SOURCE NUMBER 1

CONCENTRATION UNITS ARE G/M**3

NO.	RECEPTORS X (KM)	Y (KM)	Z (M)	CONCENTRATION
1	0.500	6.500	0.000	1.067E-11
2	0.500	7.500	0.000	9.117E-13

Table B-4 (continued)

3	0.500	8.500	0.000	6.111E-15
4	1.500	4.500	0.000	5.094E-19
5	1.500	5.500	0.000	2.326E-15
6	1.500	6.500	0.000	3.365E-15
7	1.500	7.500	0.000	4.506E-19
8	1.500	8.500	0.000	0.000E+00
9	2.500	3.500	0.000	0.000E+00
10	2.500	4.500	0.000	0.000E+00
11	2.500	5.500	0.000	0.000E+00
12	2.500	6.500	0.000	0.000E+00
13	2.500	7.500	0.000	0.000E+00
14	2.500	8.500	0.000	0.000E+00
15	3.500	3.500	0.000	0.000E+00
16	3.500	4.500	0.000	0.000E+00
17	3.500	5.500	0.000	0.000E+00
18	3.500	6.500	0.000	0.000E+00
19	3.500	7.500	0.000	0.000E+00
20	4.500	3.500	0.000	0.000E+00
21	4.500	4.500	0.000	0.000E+00
22	4.500	5.500	0.000	0.000E+00
23	4.500	6.500	0.000	0.000E+00
24	5.000	4.500	0.000	0.000E+00
25	5.000	5.500	0.000	0.000E+00

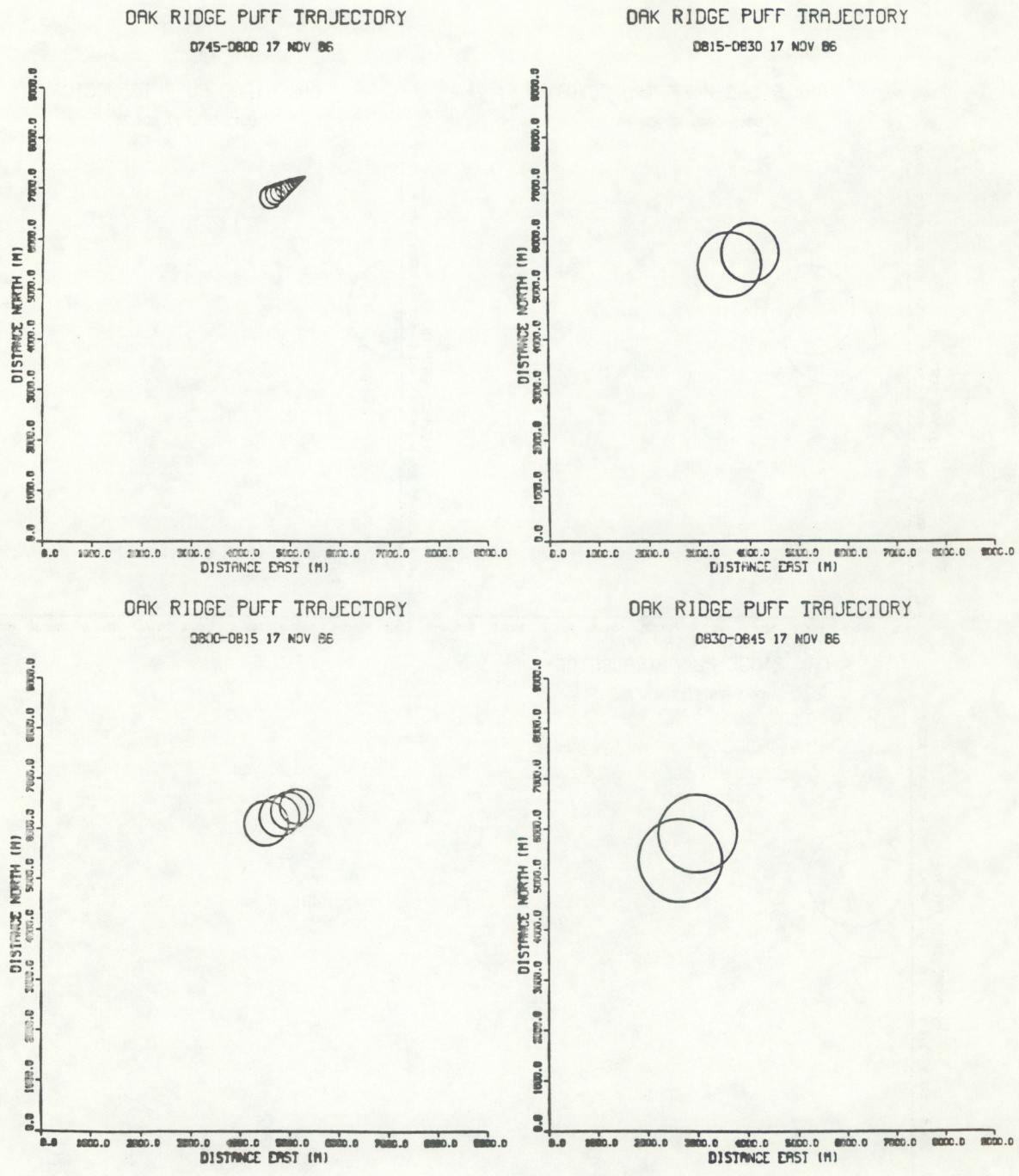

Figure B-3. Puff trajectories for Example 2, with the large source. The winds for the corresponding times are the same as shown for Example 1. This source lasts 15 minutes producing a plume segment which the model eventually combines into two puffs as the cloud spreads. The last two periods are not displayed since the puffs have been carried off the grid.

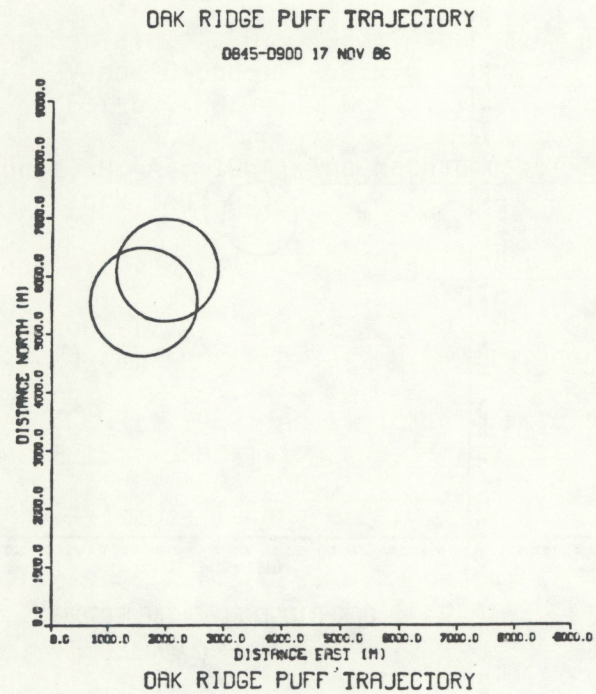

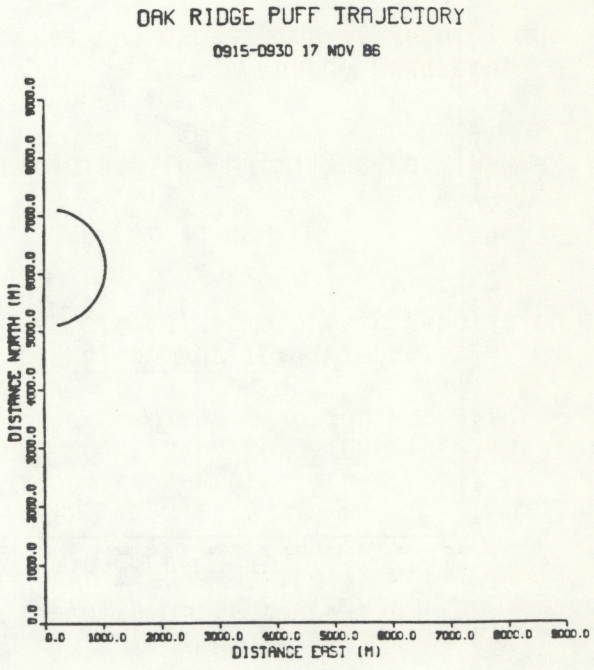

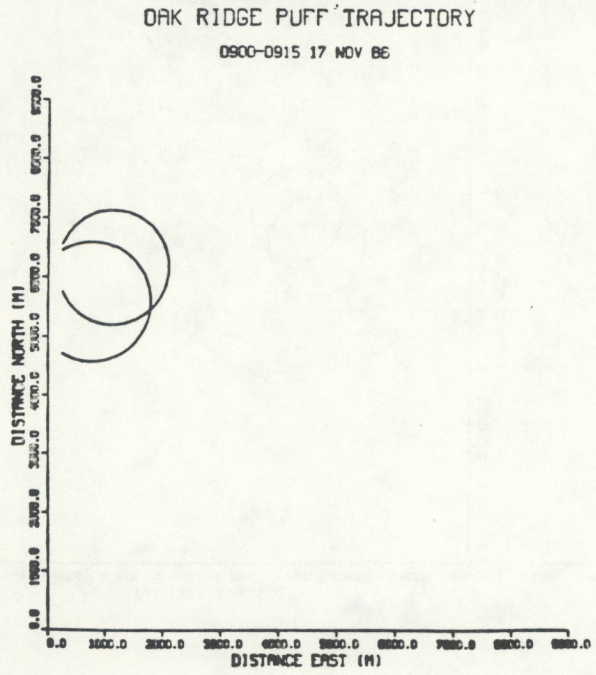

Figure B-3 (continued).

APPENDIX C

PLUME RISE

(This Appendix was adapted from Petersen and Lavdas (1986) by K. S. Rao, ATDD/NOAA)

The use of Briggs' equations to estimate plume rise and effective height of emission are discussed below. In all calculations, it is assumed that the actual or an estimated wind speed at stack top, u(h), is available.

STACK DOWNWASH

To account for stack downwash, the physical stack height is modified following Briggs (1973). The modified stack height h' is given by

$$h' = h + 2\{[v_s/u(h)] - 1.5\}d \quad \text{for } v_s < 1.5\ u(h), \qquad \text{(C-1)}$$

$$h' = h \quad \text{for } v_s \geq 1.5\ u(h),$$

where h is the physical stack height (meters), v_s is the stack gas exit vertical velocity (meters per second), and d is the stack-top inside diameter (meters). The h' is used throughout the plume height computation. If stack downwash is not considered, then h' = h is used in the following equations.

BUOYANCY FLUX

For most plume rise calculations, the value of the Briggs buoyancy flux parameter, F (m^4/s^3), is needed. Following Briggs (1975), this is given by

$$F = (g\ v_s\ d^2\ \Delta T)/(4\ T_s), \qquad \text{(C-2)}$$

where $\Delta T = T_s - T$, T_s is stack gas temperature (Kelvin), and T is ambient air temperature (Kelvin).

UNSTABLE OR NEUTRAL: CROSSOVER BETWEEN MOMENTUM AND BUOYANCY

For cases with effluent gas temperature greater than or equal to the ambient air temperature, it must be determined whether the plume rise is dominated by momentum or buoyancy. The crossover temperature difference $(\Delta T)_c$ is determined for (1) F less than 55 and (2) F greater than or equal to 55. If the difference between stack gas temperature and ambient air temperature, ΔT, exceeds or equals $(\Delta T)_c$, plume rise is assumed to be buoyancy dominated; if the difference is less than $(\Delta T)_c$, plume rise is assumed to be momentum dominated (see below).

The crossover temperature difference, for F < 55, is given by

$$(\Delta T)_c = 0.0297\ v_s^{1/3}\ T_s/d^{2/3}. \qquad \text{(C-3)}$$

For $F \geq 55$,

$$(\Delta T)_c = 0.00575\ v_s^{2/3}\ T_s/d^{1/3}. \qquad \text{(C-4)}$$

UNSTABLE OR NEUTRAL: BUOYANCY RISE

For situations where ΔT exceeds or is equal to $(\Delta T)_c$ as determined above, buoyancy is assumed to dominate. The distance to final rise x_f (in kilometers) is determined from Briggs'(1971) equations, given below. This distance is assumed to be 3.5 x*, where x* is the distance at which atmospheric turbulence begins to dominate entrainment. For $F < 55$,

$$x_f = 0.049\ F^{5/8}. \qquad \text{(C-5)}$$

For $F \geq 55$,

$$x_f = 0.119\ F^{2/5}. \qquad \text{(C-6)}$$

The effective plume height, H (in meters), is determined from the Briggs'(1971) equations, as follows. For $F < 55$,

$$H = h' + 21.4\ F^{3/4}/u(h), \qquad \text{(C-7)}$$

For F equal to or greater than 55,

$$H = h' + 38.7\ F^{3/5}/u(h). \qquad \text{(C-8)}$$

UNSTABLE OR NEUTRAL: MOMENTUM RISE

For situations where the effluent gas temperature is less than the ambient air temperature, it is assumed that the plume rise is dominated by momentum. Also, if ΔT is less than $(\Delta T)_c$ from Eq. C-3 or C-4, it is assumed that the plume rise is dominated by momentum. The plume height is calculated (Briggs, 1969) as follows:

$$H = h' + 3\ d\ v_s/u(h) \qquad \text{(C-9)}$$

Briggs (1969) suggests that this equation is most applicable when v_s/u is greater than 4. Since momentum rise occurs quite close to the point of release, the distance to final rise is set equal to zero.

STABILITY PARAMETER

For stable situations, the stability parameter s is calculated from the following equation (Briggs, 1971):

$$s = g(\partial\theta/\partial z)/T \qquad \text{(C-10)}$$

where g is the acceleration of gravity and θ is the potential temperature.

As an approximation, for stability class E, $\partial\theta/\partial z$ is taken as 0.02°K/m, and for stability class F, $\partial\theta/\partial z$ is taken as 0.035°K/m.

STABLE: CROSSOVER BETWEEN MOMENTUM AND BUOYANCY

For cases with effluent gas temperature greater than or equal to the ambient air temperature, it must be determined whether the plume rise is dominated by momentum or buoyancy. The crossover temperature difference $(\Delta T)_c$ for this case is determined from Briggs (1969, 1975) as

$$(\Delta T)_c = 0.0196 \quad v_s \; T \; s^{1/2} \qquad \text{(C-11)}$$

If the difference between effluent gas temperature and ambient air temperature (ΔT) exceeds or equals $(\Delta T)_c$, the plume rise is assumed to be buoyancy dominated; if ΔT is less than $(\Delta T)_c$, the plume rise is assumed to be momentum dominated.

STABLE: BUOYANCY RISE

For situations where ΔT is greater than or equal to $(\Delta T)_c$, buoyancy is assumed to dominate. The distance to final rise (in kilometers) is determined from Briggs (1975) as

$$x_f = 0.00207 \quad u(h) \; s^{-1/2} \qquad \text{(C-12)}$$

The effective plume height is then given by

$$H = h' + 2.6 \{F /[u(h) \; s]\}^{1/3} \qquad \text{(C-13)}$$

The stable buoyancy rise for calm conditions (Briggs, 1975) is also evaluated:

$$H = h' + 4 \; F^{1/4} \; s^{-3/8}. \qquad \text{(C-14)}$$

The lower of the two values obtained from Eqs. C-13 and C-14 is taken as the final effective height.

By setting Eqs. C-13 and C-14 equal to each other and solving for u(h), one can determine the wind speed that yields the same plume rise for the wind conditions (C-13) as does the equation for calm conditions (C-14). This wind speed is

$$u(h) = 0.275 \quad F^{1/4} \; s^{1/8}. \qquad \text{(C-15)}$$

For wind speed less than or equal to this value, Eq. C-14 should be used for plume rise; for wind speeds greater than this value, Eq. C-13 should be used.

STABLE: MOMENTUM RISE

When the effluent gas temperature is less than the ambient air temperature, it is assumed that the plume rise is dominated by momentum. If ΔT is less than $(\Delta T)_c$ as determined by Eq. C-11, it is also assumed that the plume rise is dominated by momentum. The effective plume height is calculated (Briggs, 1969) as

$$H = h' + 1.5 \{(v_s^2 d^2 T)/[4 T_s u(h)]\}^{1/3} s^{-1/6}. \qquad \text{(C-16)}$$

The equation for unstable or neutral momentum rise (C-9) is also evaluated. The lower result of these two equations is used as the resulting plume height.

REFERENCES

Briggs, G. A., 1969: Plume Rise. USAEC Critical Review Series. TID-25075, National Technical Information Service, Springfield, VA, 81 pp.

Briggs, G. A., 1971: Some recent analyses of plume rise observation. In: Proceedings of the Second International Clean Air Congress, H. M. Englund and W. T. Beery, eds., Academic Press, New York, 1029-1032.

Briggs, G. A., 1973: Diffusion estimation for small emissions. NOAA Atmos. Turb. and Diff. Lab., Contribution File No. 79, Oak Ridge, TN, 59 pp.

Briggs, G. A., 1975: Plume rise predictions. In: Lectures on Air Pollution and Environmental Impact Analysis, D. A. Haugen, ed., Am. Meteorol. Soc., Boston, MA, 59-111.

Petersen, W. B., and L. G. Lavdas, 1986: INPUFF 2.0 - A Multiple Source Gaussian Plume Dispersion Algorithm. EPA/600/8-86-024, U.S. Environmental Protection Agency, Research Triangle Park, NC, 105 pp.

APPENDIX D

SETTLING AND DEPOSITION VELOCITIES

by

K. Shankar Rao
Atmospheric Turbulence and Diffusion Division, NOAA
P.O. Box 2456, Oak Ridge, TN 37831

(This Appendix is reproduced and adapted from Rao (1982)).

For a monodisperse particulate cloud, the individual particles have a constant gravitational settling velocity. This terminal velocity is given by Stokes' equation (Fuchs, 1964):

$$W = \frac{d^2 g \rho}{18 \mu} \qquad \text{(D-1)}$$

where d is the diameter of the particle, g is acceleration due to gravity, ρ is the density of particles, and μ is the dynamic viscosity of air. For $d > 100$ μm, the terminal fall velocity is sufficiently great that turbulence in the wake of the particle cannot be neglected, and the drag force F_d on the particle is greater than given by Stokes' law, $F_d = 3\pi d\mu W$. For a particle with $d = 400$ μm, the actual value of W is about one-third the value given by Eq. (D-1). Stokes' expression for the drag force describes the effects of collisions between air molecules and a particle, assuming air to be a continuum. This assumption is not valid for very small particles, since the mean free path between molecular collisions is then comparable to the particle size; under these conditions "slippage" occurs, and the particles undergo Brownian motion and diffusion, which give a terminal velocity greater than that predicted by Eq. (D-1). A discussion of the slip correction factor for Stokes' equation can be found in Fuchs (1964) and Cadle (1975).

The values for the terminal gravitational settling velocities for different particulate materials were given in tabular form by Lapple (1961), based on particle diameter and Reynolds number. These values, which account for the deviations from Stokes' equation discussed above, were calculated for spherical particles with a specific gravity of 2.0 in air at 25 C and 1 atm. pressure. This table was reprinted in Sheehy et al. (1969) and Stern (1976).

The dry deposition pollutant removal mechanisms at the earth's surface include gravitational settling, turbulent and Brownian diffusion, chemical absorption, inertial impact and thermal and electrical effects. Some of the deposited particles may be re-released into the atmosphere by mechanical resuspension. Following the concept introduced by Chamberlain (1953), particle removal rates from a polluted atmosphere to the surface are usually described by dry deposition velocities which vary with particle size, surface properties (including surface roughness (z_0) and moisture), and meteorological conditions. The latter include wind speed and

direction, friction velocity (u_*), and thermal stratification of the atmosphere. Deposition velocities for a wide variety of substances and surface and atmospheric conditions may be obtained directly from the literature (e.g., McMahon and Denison, 1979; Sehmel, 1980). Sehmel and Hodgson (1974) gave plots relating deposition velocity (V_d) to d, z_o, u_*, and the Monin-Obukhov stability length.

Considerable care needs to be exercised in choosing a representative deposition velocity since it is a function of many factors and can vary by two orders of magnitude for particles. Generally, V_d should be defined relative to the height above the surface at which the concentration measurement is made. The particle deposition velocity is approximately a linear function of wind speed and friction velocity, and its minimum value occurs in the particle diameter range 0.1 - 1 μm.

In the trivial case of $W = V_d = 0$, settling and deposition effects are negligible. For very small particles ($d < 0.1$ μm), gravitational settling can be neglected, and dry deposition occurs primarily due to the nongravitational effects mentioned above. In this case, $W = 0$ and $V_d > 0$. For small particles ($d = 0.1 \sim 50$ μm), $0 < W < V_d$; deposition is enhanced here beyond that due to gravitational settling, primarily due to increased turbulent transfer resulting from surface roughness. For larger particles ($d > 50$ μm), it is generally assumed that $V_d = W > 0$, since gravitational settling is the dominant deposition mechanism. When $W > V_d > 0$, re-entrainment of the deposited particles from the surface back into the atmosphere is implied as, for example, in a dust storm. The first four sets of model parameters given above are widely used in atmospheric dispersion and deposition of particulate material. The deposition of gases is a special case of the particulate problem with $W = 0$. Thus, one has to carefully select the values of W and V_d for use in the model.

REFERENCES

Cadle, R. D., 1975: The Measurement of Airborne Particles. John Wiley & Sons, New York, 342 pp.

Chamberlain, A. C., 1953: Aspects of Travel and Deposition of Aerosol and Vapor Clouds. A.E.R.E. Report H.P.-1261, Atomic Energy Research Estab., Harwell, Berks., U.K., 32 pp.

Fuchs, N. A., 1964: The Mechanics of Aerosols. The Macmillan Co., New York, 408 pp.

Lapple, C. E., 1961: J. Stanford Res. Inst. 5, p. 95.

McMahon, T. A., and P. J. Denison, 1979: Empirical atmospheric deposition parameters - a survey. Atmospheric Environment 13, 571-585.

Rao, K. S., 1982: Analytical Solutions of a Gradient-Transfer Model for Plume Deposition and Sedimentation. NOAA Tech. Memo. ERL ARL-109, 75 pp; EPA-600/3-82-079, U.S. Environmental Protection Agency, Research Triangle Park, NC. (NTIS 82-215 153).

Sehmel, G. A., and W. H. Hodgson, 1974: Predicted dry deposition velocities. In: Atmosphere-Surface Exchange of Particulate and Gaseous Pollutants. Available as CONF-740921 from NTIS, Springfield, VA, 399-423.

Sehmel, G. A., 1980: Particle and gas dry deposition: a review. Atmospheric Environment 14, 983-1011.

Sheehy, J. P., W. C. Achinger, and R. A. Simon, 1969: Handbook of Air Pollution. Public Health Service Publication No. 999-AP-44, U.S. EPA, Research Triangle Park, NC.

Stern, A. C., 1976: Air Pollution. Academic Press, New York, Vol. I, 3rd ed., 715 pp.

APPENDIX E

GRAPHICS SOFTWARE

by

Ronald J. Dobosy
Atmospheric Turbulence and Diffusion Division, NOAA
P.O. Box 2456, Oak Ridge, TN 37831

A plotting subroutine is not included as part of the TRIAD model because of the lack of standardization of plotting facilities from one computer center to another. In this section we discuss a plotting scheme applicable to the IBM 3033 computer at Oak Ridge National Laboratory (ORNL). We have the benefit of DISSPLA, a commercially available high-level graphics package. Those users who have such a system at their computer center should be readily able to apply this example. For others, we illustrate the necessary input data and the types of plots which may be obtained.

ORNL's IBM 3033 computer uses the Multiple Virtual System (MVS) job control language. Job-control statements are included with the program listings to illustrate the necessary input/output files. If the codes are run interactively, the Unit 5 data are most easily read from the keyboard.

The program uses FORTRAN-invocable subroutines from the DISSPLA package, version 9.2. They should work correctly on version 10 except for the way in which plot files are handled. Reference should be made to the appropriate DISSPLA manuals for further information.

There are two separate programs used to plot output from TRIAD. The first, called WNDPLT, plots the winds interpolated to the meteorological grid at the standard elevation (HGTMET). These data are taken directly from the Unit 21 output of TRIAD. The program does not adjust wind speed to the puff height before plotting. The winds are shown as vectors with tails at the grid points. The length of the vector is proportional to the wind speed. A sample of the resulting plots was shown in Appendix B.

Control data entered on Unit 5 include the meteorological grid spacing, the number of grid points in each direction, the number of meteorological periods to be plotted and the scale length for the vectors, in centimeters, which represents 1 m/s of wind speed. The scale length for the vectors is chosen so that the vectors are long enough to be readily seen, but short enough not to foul against each other. A sample vector is provided in the lower right-hand corner to show the length selected by the user to correspond to 1 m/s.

Additional control information entered from Unit 5 to the wind-plotting program includes the format with which Unit 21 of TRIAD was written (TRIAD-input card type 5a), the date to which the meteorological periods apply and the times of the meteorological periods. The date and times are used in the titles of the plots. Only one date may be entered in any one run. Also no more than nine meteorological periods may be plotted in any one run. These limits can be extended by adjusting the code.

Table E-1 is a listing of the FORTRAN code and MVS job control language for WNDPLT. Explanatory comment statements are provided.

The second plotting program is called PUFPLT. This code plots locations and sizes of the individual puffs defined to the system at each meteorological period. The puffs are plotted as circles with center at the puff location and radius equal to one standard deviation of the Gaussian distribution of concentration in the horizontal. Puff data are read from the Unit 22 output from TRIAD. Samples of the results of PUFPLT were shown in Appendix B, Figures B-1 and B-2.

Control data entered from Unit 5 include the meteorological grid spacing and the coordinates of the southwest corner point of the meteorological grid, in kilometers. These data are used to define the domain of the plot and to relate the TRIAD-specified puff locations to positions within the plot domain. The number of grid points in the x and y directions are also specified to determine the size of the domain. As with WNDPLT, time and date information are also read from Unit 5. PUFPLT will handle one calendar date and nine meteorological periods. Since Unit 22 is unformatted, it is necessary to run PUFPLT on the same machine as that on which TRIAD was run. Otherwise the Unit-22 data will be unintelligible.

Table E-2 is a listing of the FORTRAN and MVS job control language for the program PUFPLT. Explanatory comment statements are provided.

Table E-1: Listing of FORTRAN code and job control language for the wind plotting program, WNDPLT.

```
//RQDWNPT JOB (nnnnn,IO4),' NOAA/ATDL  DOBOSY',TIME=(0,15),
//  MSGCLASS=T,NOTIFY=RQD
//*  SCRATCH ANY EXISTING COPY OF THE OUTPUT DATA SET.
//SCRATCH EXEC SPDASCR
//SYSIN DD *
  METAFILE.WN15PLOT
/*
//PLOT EXEC FORTVCLG,PLOT=DISOLDV
//FORT.SYSIN DD *
      PROGRAM WNDPLT
C  THIS PROGRAM READS WIND DATA FROM INPUFF INPUT FILE AND PLOTS
C  VECTORS FOR EACH GRID POINT SHOWING DIRECTION AND SPEED.
      DIMENSION USCL(1000),VSCL(1000)
      CHARACTER CHOLD(9)*10,CDATE*9,CTIME*20,SNDLN*20,FRMATR*72
C  GRID SPACING, DGX,DGY IN X AND Y DIRECTIONS ARE IN KM.
C  NTIME IS THE NUMBER OF PERIODS TO BE PLOTTED.
```

Table E-1 (continued)

```
C  NUMX,NUMY ARE THE NUMBER OF GRID POINTS IN THE X AND Y DIRECTIONS.
C  FRMATR IS THE INPUT FORMAT FOR THE WIND DATA TO BE PLOTTED.
C  USCALE IS THE NUMBER OF CM REPRESENTING 1 M/S IN THE WIND VECTOR.
      READ(5,*) DGX,DGY,NUMX,NUMY,NTIME,USCALE
      NUMT=NUMY*NUMX
      READ(5,*) FRMATR
      READ(5,25) CDATE
      READ(5,50) CHOLD
   25 FORMAT(A9)
   37 FORMAT(A20)
   50 FORMAT(6A10/3A10)
C  OUTPUT WILL BE TO A DISSPLA COMPRESSED DATA SET FOR POST-
C  PROCESSING.
      CALL COMPRS
C  SET THE PLOTTING UNITS TO CENTIMETERS.
      CALL UNITS('CM')
      DO 500 IT=1,NTIME
C  READ IN THE WIND DATA IN U,V PAIRS STARTING WITH THE SOUTHWEST
C  CORNER AND PROCEEDING EASTWARD AND NORTHWARD IN THAT ORDER.
      READ(1,FRMATR) (USCL(IJ),VSCL(IJ),IJ=1,NUMT)
      DO 300 J=1,NUMY
      DO 200 I=1,NUMX
      IJ=(J-1)*NUMX+I
      USCL(IJ)=USCL(IJ)*USCALE
      VSCL(IJ)=VSCL(IJ)*USCALE
  200 CONTINUE
  300 CONTINUE
C  SET UP THE SUBPLOT AREA BY DEFINING THE AXES.
      WX=(NUMX-1)*DGX
      WY=(NUMY-1)*DGY
C SCALE IS THE RATIO, ACTUAL TO PLOTTED GRID, SUCH THAT THE LONGEST
C  AXIS IS EXACTLY 18CM LONG.
      SCALE=AMAX1(WX,WY)/.18
C  DEFINE THE AXIS LENGTHS IX,IY.
      IF(AMAX1(WX,WY).EQ.WX) THEN
        IX=18
        IY=WY/WX*IX
      ELSE
        IY=18
        IX=WY/WX*IY
      END IF
C  SET LOCATION OF PHYSICAL ORIGIN IN CM FROM LWR LH CORNER OF PAGE.
      CALL PHYSOR(2.43,2.0)
      CALL AREA2D(IX,4.)
      CALL VECTOR(13.,0.,13+USCALE,0,3101)
      CALL MESSAG('1 M/S',5,13.,0.5)
C  END THE CURRENT SUBPLOT AND SET UP FOR THE MAIN VECTOR PLOT.
      CALL ENDGR(IT)
C  LOCATE THE PHYSICAL ORIGIN OF THE PLOT 2.5 CM ABOVE THE PREVIOUS.
      CALL OREL(0.,2.5)
C  SUBROUTINE AREA2D DEFINES THE AXIS LENGTHS AND SETS UP THE SUBPLOT.
      CALL AREA2D(IX,IY)
```

Table E-1 (continued)

```
C  DEFINE THE AXIS LABELS.
      CALL XNAME('DISTANCE EAST (M)',17)
      CALL YNAME('DISTANCE NORTH (M)',18)
      CTIME=' '//CHOLD(IT)//CDATE
C  SPECIFY A TITLE FOR THE PLOT.  EACH CALL WRITES A NEW LINE.
C  20 IS THE NUMBER OF CHARACTERS IN THE FIRST LINE.
C  3 IS THE FACTOR TO MULTIPLY THE STANDARD LETTER HEIGHT.  THE FIRST
C  LINE IS THREE TIMES NORMAL SIZE OF 0.14 INCHES.
C  2 IS THE TOTAL NUMBER OF CALLS TO HEADIN FOR THIS TITLE.
      CALL HEADIN('OAK RIDGE AREA WINDS',20,3,2)
      CALL HEADIN(CTIME,20,2,2)
C  SUBROUTINE GRAF(XORIG,XSTP,XMAX,YORIG,YSTP,YMAX) SETS UP THE AXES.
      CALL GRAF(0.,DGX,DGX*(NUMX-1),0.,DGY,DGY*(NUMY-1))
C  SUBROUTINE VECTOR PLOTS THE ACTUAL VECTORS.  THEY WILL COME EVERY
C  TWO CENTIMETERS ON THIS PLOT.
      DO 400 I=1,NUMX
      DO 400 J=1,NUMY
      IJ=(J-1)*NUMX+I
      XI=2.*FLOAT(I-1)
      YI=2.*FLOAT(J-1)
      USCL(IJ)=USCL(IJ)+XI
      VSCL(IJ)=VSCL(IJ)+YI
      IF(USCL(IJ).LE.0..OR.VSCL(IJ).LE.0..OR.USCL(IJ).GE.18.
     1.OR.VSCL(IJ).GE.18.) GO TO 400
      CALL VECTOR(XI,YI,USCL(IJ),VSCL(IJ),3101)
  400 CONTINUE
      CALL ENDPL(IT)
  500 CONTINUE
      CALL DONEPL
      STOP
      END
//*  INPUT FILE FROM TRIAD UNIT 21
//GO.FT01F001 DD DSN=TRIAD.UNIT21,DISP=SHR,LABEL=(,,,IN)
//*
//*  THE TIMES AND DATE BELOW ARE FOR A 15-MINUTE-AVERAGE DATA SET.
//*
//GO.FT05F001 DD *
1000. 1000. 10 10 9 1.
'(10F7.2)'
17 NOV 86
0745-0800 0800-0815 0815-0830 0830-0845 0845-0900 0900-0915
0915-0930 0930-0945 0945-1000
//*
//*  THE TIMES AND DATE BELOW ARE FOR AN HOUR-AVERAGE DATA SET.
//*
//*GO.FT05F001 DD *
//*2000. 2000. 10 10 9 1.
//*'(10F7.1)'
//*30 AUG 85
//*0300-0400 0400-0500 0500-0600 0600-0700 0700-0800 0800-0900
//*0900-1000 1000-1100 1100-1200
//GO.FT18F001 DD UNIT=SPDA,SPACE=(TRK,(10,5),RLSE),
//  DSN=METAFILE.WN15PLOT,DISP=(NEW,CATLG),
//  DCB=SYS2.DCB.DMF
/*
//
```

Table E-2: Listing of FORTRAN code and job control language for the puff-trajectory plotting program, PUFPLT.

```
//RQDPFPT JOB (nnnnn,IO4),' NOAA/ATDL  DOBOSY',TIME=(0,20),
//  MSGCLASS=T,NOTIFY=RQD
//*  SCRATCH ANY EXISTING COPY OF THE OUTPUT DATA SET
//SCRATCH EXEC SPDASCR
//SYSIN DD *
    METAFILE.PUFFPLOT
/*
//PLOT EXEC FORTVCLG,PLOT=DISOLDV
//FORT.SYSIN DD *
      PROGRAM PUFPLT
C  THIS PROGRAM READS INPUFF OUTPUT FROM UNIT 22 AND PLOTS
C  THE PUFF LOCATION AND SIZE AS A CIRCLE, ONE FOR EACH PUFF
C  DEFINED TO THE SYSTEM AT THE END OF THE GIVEN METEOROLOGICAL PERIOD.
C  PUFF COORDINATES AND SIGMAS ARE ASSUMED TO BE IN METERS.  IF
C  INPUFF GIVES THEM IN KILOMETERS IT WILL BE IMMEDIATELY APPARENT IN
C  THE PLOTS AND THE MULTIPLICATION BY 1000 CAN BE REMOVED FROM THIS
C  PROGRAM.
      DIMENSION XPUFF(600),YPUFF(600),ZPUFF(600),SY(600),SZ(600)
      DIMENSION XREC(100),YREC(100),ZREC(100),CONC(100)
      DIMENSION XTEMP(158),YTEMP(158)
      CHARACTER CHOLD*10(9),CDATE*9,CTIME*20,SNDLN*24
C  READ THE GRID SPACING (DGX, DGY), THE NUMBER OF GRID
C  POINTS IN THE METEOROLOGICAL GRID IN THE X AND Y DIRECTIONS AND THE
C  LOCATION OF THE GRID POINT (1,1) ON THE SOUTHWEST CORNER OF THE GRID.
C  DGX, DGY, XSWC,YSWC ARE IN KILOMETERS.
      READ(5,*) DGX,DGY,NUMX,NUMY,XSWC,YSWC
      READ(5,150) CDATE
      READ(5,100) CHOLD
  100 FORMAT(6A10/3A10)
  125 FORMAT(A24)
  150 FORMAT(A9)
C  CONVERT TO METERS.
      XSWC=XSWC*1000.
      YSWC=YSWC*1000.
      DGX=DGX*1000.
      DGY=DGY*1000.
      WX=DGX*(NUMX-1)
      WY=DGY*(NUMY-1)
      AMX=AMAX1(WX,WY)
C  SET THE LONGEST PLOT AXIS TO 18 CM.
      IF(AMX.EQ.WX) THEN
        IX=18
        IY=WY/WX*IX
      ELSE
        IY=18
        IX=WX/WY*IY
      END IF
C  COMPUTE THE SCALE FACTOR FOR THE PLOT. UNITS [M/CM].
      SCALE=AMX/18.
C  INITIALIZE THE PROPER DEVICE FOR PLOTTED OUTPUT.
C  FOR COMPRESSED DATA SET FOR POST PROCESSING CALL COMPRS.
      CALL COMPRS
```

Table E-2 (continued)

```
C  SET THE PLOTTING UNITS TO CENTIMETERS.
      CALL UNITS('CM')
C  SET THE MARGIN TO BE .5 CM INSIDE THE SUBPLOT AREA.
C  KEEPS PLOTTED CURVES FROM CROSSING THE AXES.
      CALL GRACE(-0.5)
      READ(22)NTIME,ITIME,NREC,NSOURC
      WRITE(6,200) NTIME,ITIME,NREC,NSOURC
  200 FORMAT(' NUMBER OF METEOROLOGICAL PERIODS',I3,' LENGTH'
     +,' OF METEOROLOGICAL PERIOD',I5,' SECONDS'/' NUMBER OF',
     +' RECEPTORS',I4,' NUMBER OF SOURCES',I3)
      DO 300 IREC=1,NREC
  300 READ(22)XREC(IREC),YREC(IREC),ZREC(IREC)
      READ(22) ISRCNO
      WRITE(6,400) ISRCNO
  400 FORMAT(' USING SOURCE NUMBER',I3)
      DO 1000 IT=1,NTIME
      READ(22) IIT,MSTEP
      IF(IT.EQ.IIT) GO TO 600
      WRITE(6,500) IT,IIT,MSTEP
  500 FORMAT(' METEOROLOGICAL LOOP INDICES DO NOT MATCH, IT,IIT,MSTEP'
     +,2I3,I10)
      CALL EXIT
C  CONCENTRATIONS AT THE RECEPTOR SITES APPEAR IN THIS PART OF THE
C  FILE ON UNIT 22.  SINCE THEY ARE NOT NEEDED IN THESE PLOTS, ONLY THE
C  TIME TO WHICH THE CONCENTRATIONS APPLY IS READ  (MSTM).  MSTM IS
C  TESTED TO FIND WHEN ALL CONCENTRATION DATA FOR THE CURRENT
C  METEOROLOGICAL PERIOD HAVE BEEN SKIPPED.
  600 READ(22) MST
      IF(MSTM.LT.1000*IT*ITIME) GO TO 600
C  START READING PUFF DATA FOR PLOTTING.
      READ(22) NPUFF
      WRITE(6,700) NPUFF,IT
  700 FORMAT(' THERE ARE',I4,' PUFFS DEFINED IN METEOROLOGICAL',
     +' PERIOD',I3)
      DO 800 IPF=1,NPUFF
  800 READ(22)XPUFF(IPF),YPUFF(IPF),ZPUFF(IPF),SY(IPF),SZ(IPF)
C  DEFINE THE SUBPLOT AREA FOR THIS METEOROLOGICAL PERIOD.
C  ARGUMENTS TO AREA2D ARE AXIS LENGTHS IN CENTIMETERS.
C  SUBROUTINES XNAME, YNAME PUT LABELS ON THE AXES.
      CALL AREA2D(IX,IY)
      CALL XNAME('DISTANCE EAST (M)',17)
      CALL YNAME('DISTANCE NORTH (M)',18)
      CTIME=CHOLD(IT)//CDATE
C  SPECIFY THE TITLE FOR THE PLOT.  EACH CALL WRITES A NEW LINE.
C  25 IS THE NUMBER OF CHARACTERS IN THE FIRST LINE.
C  3 IS THE FACTOR TO MULTIPLY THE STANDARD LETTER HEIGHT.  THE FIRST
C  LINE IS THREE TIMES NORMAL SIZE OF 0.14 INCHES.
C  2 IS THE TOTAL NUMBER OF CALLS TO HEADIN FOR THIS TITLE.
      CALL HEADIN('OAK RIDGE PUFF TRAJECTORY',25,3,2)
      CALL HEADIN(CTIME,20,2,2)
C  SUBROUTINE GRAF(XORIG,XSTP,XMAX,YORIG,YSTP,YMAX) SETS UP THE AXES.
      CALL GRAF(0.,DGX,WX,0.,DGY,WY)
```

Table E-2 (continued)

```
      DO 900 IPF=1,NPUFF
      XCNTR=(XPUFF(IPF)-XSWC)
      YCNTR=(YPUFF(IPF)-YSWC)
      SYRAD=2.*SY(IPF)
C  PLOTTED PUFF RADIUS WILL BE 2*SY.
C  SUBROUTINE CIRC(XCNTR,YCNTR,RAD,PCT,XTEMP,YTEMP,NT) IS A
C  LOCALLY-WRITTEN SUBROUTINE TO PLOT CIRCLES WITH CENTER AT
C  (XCNTR,YCNTR) AND RADIUS RAD.  PCT IS THE % ERROR OF THE
C  POLYGON APPROXIMATION TO A CIRCLE.  PCT=.02 USES 158
C  SEGMENTS IN THE POLYGON REQUIRING UTILITY ARRAYS XTEMP,
C  YTEMP OF SIZE NT=158.
      WRITE(6,850) XCNTR,XPUFF(IPF),SCALE,SYRAD,YCNTR
  850 FORMAT(' XCNTR,XPUFF,SCALE,SYRAD,YCNTR',5F10.3)
      CALL CIRC(XCNTR,YCNTR,SYRAD,.02,XTEMP,YTEMP,158)
      WRITE(6,*) ' AFTER CIRC CALL'
  900 CONTINUE
      CALL ENDPL(IT)
 1000 CONTINUE
      CALL DONEPL
      STOP
      END
      SUBROUTINE CIRC(XC,YC,R,PCT,XT,YT,NT)
C
C  AUTHOR:  C. W. NESTOR, JR.,
C           COMPUTER SCIENCE
C           X-10,  DATE UNKNOWN
C
C  USES DISSPLA SUBROUTINE CURVE TO PLOT A REGULAR
C  POLYGON APPROXIMATING A CIRCLE OF RADIUS R WITH
C  CENTER AT XC,YC (ALL IN USER'S UNITS).  PCT IS A
C  PERCENTAGE ERROR TO BE SPECIFIED BY THE USER.  A
C  VALUE OF .02 TO .01 USUALLY GIVES AN ACCEPTABLE
C  ILLUSION OF ROUNDNESS.  THE ARRAYS XT AND YT WITH
C  DIMENSION NT ARE USED FOR TEMPORARY STORAGE OF THE
C  COORDINATE PAIRS DEFINING THE VERTICES OF THE
C  APPROXIMATING POLYGON.
C
      DIMENSION XT(NT),YT(NT)
      DATA TWOPI/6.2831853/
      DT=SQRT(.08*PCT)
      DT=DT+DT
      NN=TWOPI/DT
      DT=TWOPI/FLOAT(NN)
      CDT=COS(DT)
      SDT=SIN(DT)
      XT(1)=XC+R
      YT(1)=YC
      CTH=1.
      STH=0.
      KT=1
      DO 100 N=1,NN
```

Table E-2 (continued)

```
C
C  GENERATE COORDINATES OF NEXT VERTEX.
C
      T=CTH*CDT-STH*SDT
      STH=STH*CDT+CTH*SDT
      CTH=T
      FACT=2./(1.+CTH*CTH+STH*STH)
      CTH=CTH*FACT
      STH=STH*FACT
      X=XC+R*CTH
      Y=YC+R*STH
      IF(KT.LT.NT) GO TO 90
C
C  IF THE ARRAYS ARE FULL, PLOT THE POINTS AND SET
C  UP FOR THE NEXT PASS.
C
      CALL CURVE(XT,YT,KT,0)
      XT(1)=XT(KT)
      YT(1)=YT(KT)
      KT=1
C
   90 KT=KT+1
      XT(KT)=X
      YT(KT)=Y
  100 CONTINUE
      IF(KT.LT.2) RETURN
C
C  IF ANY POINTS REMAIN, PLOT THEM.
C
      CALL CURVE(XT,YT,KT,0)
      RETURN
      END
//GO.FT22F001 DD DSN=TRIADPUF.DATA,DISP=SHR
//*
//*  THE TIMES AND DATE BELOW ARE FOR AN HOUR-AVERAGE DATA SET.
//*
//*GO.FT05F001 DD *
//*2. 2. 10 10 0. 0.
//*30 AUG 85
//*0300-0400 0400-0500 0500-0600 0600-0700 0700-0800 0800-0900
//*0900-1000 1000-1100 1100-1200
//*
//* THE TIMES AND DATE BELOW ARE FOR A 15-MINUTE-AVERAGE DATA SET.
//*
//GO.FT05F001 DD *
1. 1. 10 10 0. 0.
17 NOV 86
0745-0800 0800-0815 0815-0830 0830-0845 0845-0900 0900-0915
0915-0930 0930-0945 0945-1000
//GO.FT18F001 DD DISP=(NEW,CATLG),UNIT=SPDA,SPACE=(TRK,(5,5),RLSE),
//  DSN=METAFILE.PUFFPLOT,DCB=SYS2.DCB.DMF
/*
//
```

* U. S. GOVERNMENT PRINTING OFFICE: 1989 -656-483/ 80172